



AFRPL TR-85-066

AD:

20000801158

Non-Reacting Turbulent Mixing Experiments

Final Report
for the period
November 1979 to
August 1985

PLEASE REPLACE THE FRONT COVER AND DD 1473 OF AFRPL-TR-85-066 WITH THE
ATTACHED REVISION.

September 1985

Author:
C. Padova

Calspan Advanced Technology Ctr
P.O. Box 400
Buffalo, New York 14225

6632-A-Rev. 1
F04611-80-C-0011

Approved for Public Release

Distribution is unlimited. The AFRPL Technical Services Office has reviewed this report, and it is releasable to the National Technical Information Service, where it will be available to the general public, including foreign nationals.

prepared for the:

**Air Force
Rocket Propulsion
Laboratory**

Air Force Space Technology Center
Space Division, Air Force Systems Command
Edwards Air Force Base,
California 93523-5000

**Reproduced From
Best Available Copy**

NOTICE

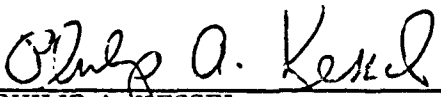
When U.S. Government drawings, specifications, or other data are used for any purpose other than a definitely related Government procurement operation, the Government thereby incurs no responsibility nor any obligation whatsoever, and the fact that the Government may have formulated, furnished, or in any way supplied the said drawings, specifications, or other data is not to be regarded by implication or otherwise, or in any manner licensing the holder or any other person or corporation, or conveying any rights or permission to manufacture, use or sell any patented invention that may in any way be related hereto.


FOREWORD

The Air Force Rocket Propulsion Laboratory is pleased to publish this report for contract F04611-80-C-0011 for use by its contractors and other workers studying the turbulent mixing of supersonic co-flowing jets. The data presented here are unique in terms of the range of test variables and spatial extent. Prior to publication, these data were analyzed for consistency by a member of the AFRPL advisory panel, Mr. R. Rhodes (CPIA Publication 384, Vol. II, p. 157+). It was found that the velocity and concentration profiles deduced from this data are reasonably consistent; however, the variation of the derived centerline properties such as velocity are not as well behaved as we would like them to be. This behavior of the derived quantities is thought to be at least partially an artifact of the data interpolation techniques used to estimate the value of the measured variables on a common computational grid. Another source of apparent scatter is the boundary layer behavior of the experimental device. Pergament (SAIC/PR TM-26, June 1984) found that the data correlation markedly improved when a proper description of the nozzle boundary layers was used as input in his finite difference modeling code. Unfortunately, a formal error analysis is not included in this report due to fiscal and contractor personnel availability limitations. We regret this omission and caution the serious user to peruse these two referenced reports to get an indication of the consistency of the data. These cautionary comments are made to encourage potential users of this data to perform as thorough an analysis of the data as the complexity of the experiment configuration requires.


We wish to thank the principle investigator, Dr. Corso Padova of the Arvin Calspan Corporation, for his dedication and diligence. This report literally could not have been written without his insight into the experimental program and his extra personal effort to produce a quality final report.

This technical report has been reviewed and is approved for publication and distribution in accordance with the distribution statement on the cover and on the DD Form 1473.


PHILIP A. WESSEL
Project Manager


L. KEVIN SLIMAK
Chief, Interdisciplinary Space
Technology Branch

FOR THE DIRECTOR


HOMER M. PRESSLEY JR., Lt Col, USAF
Chief, Propulsion Analysis Division

REPORT DOCUMENTATION PAGE

1a. REPORT SECURITY CLASSIFICATION UNCLASSIFIED		1b. RESTRICTIVE MARKINGS	
2a. SECURITY CLASSIFICATION AUTHORITY		3. DISTRIBUTION/AVAILABILITY OF REPORT Approved for Public Release; Distribution is unlimited.	
2b. DECLASSIFICATION/DOWNGRADING SCHEDULE			
4. PERFORMING ORGANIZATION REPORT NUMBER(S) 6632-A-3-Rev. 1		5. MONITORING ORGANIZATION REPORT NUMBER(S) AFRPL-TR-85-066	
6a. NAME OF PERFORMING ORGANIZATION Calspan Advanced Technology Center	6b. OFFICE SYMBOL (If applicable)	7a. NAME OF MONITORING ORGANIZATION Air Force Rocket Propulsion Laboratory	
6c. ADDRESS (City, State and ZIP Code) P.O. Box 400 Buffalo NY 14225		7b. ADDRESS (City, State and ZIP Code) AFRPL/DYSO (Stop 24) Edwards AFB CA 93523-5000	
8a. NAME OF FUNDING/SPONSORING ORGANIZATION AFRPL	8b. OFFICE SYMBOL (If applicable) DYSO	9. PROCUREMENT INSTRUMENT IDENTIFICATION NUMBER F04611-80-C-0011	
8c. ADDRESS (City, State and ZIP Code) Stop 24 Edwards AFB CA 93523-5000		10. SOURCE OF FUNDING NOS.	
		PROGRAM ELEMENT NO. 62302F	TASK NO. 10
		PROJECT NO. 3058	WORK UNIT NO. VK
11. TITLE (Include Security Classification) Non-Reacting Turbulent Mixing Experiments (U)			
12. PERSONAL AUTHOR(S) Padova, Corso			
13a. TYPE OF REPORT Final	13b. TIME COVERED FROM 79/11 TO 85/08	14. DATE OF REPORT (Yr., Mo., Day) 85/9	15. PAGE COUNT 166
16. SUPPLEMENTARY NOTATION Additional Cosati code 21 08			
17. COSATI CODES		18. SUBJECT TERMS (Continue on reverse if necessary and identify by block number)	
FIELD	GROUP	SUB. GR.	
17	05		
16	04		
		turbulent mixing, axisymmetric jets, co-flowing jets, supersonic jets, turbulence modeling, rocket exhaust plumes	
19. ABSTRACT (Continue on reverse if necessary and identify by block number) Detailed measurements of pressure, temperature and gas composition in coflowing streams have been obtained for a variety of relative Mach numbers and density ratios. These measurements were aimed to provide a comprehensive data base from which compressibility corrections can be calculated for the turbulence models used in the JANNAF Standard Plume Flowfield Model (SPF). Using a short-duration testing technique, low altitude non-reacting plume flowfields were simulated in which compressible turbulent mixing of coaxial supersonic jets occurred in a preevacuated altitude chamber. A ratio of the mixing jet diameters of 13:1 was obtained using an apparatus consisting of a 3-inch exit diameter nozzle/supply within the large-scale Calspan Ludwig Tube. The outer jet had a Mach number of 2 and a total temperature of 470°R. Inner jet Mach numbers of 2, 3 and 4 were obtained with interchangeable nozzles. Molecular weight and temperature of the inner jet streams were varied to provide ambient-to-jet density ratios from 0.6 to 10 using hydrogen-nitrogen mixtures heated up to 750°R. Tests discharging into a quiescent ambient were measured for reference; selected measure-			
20. DISTRIBUTION/AVAILABILITY OF ABSTRACT UNCLASSIFIED/UNLIMITED <input checked="" type="checkbox"/> SAME AS RPT. <input type="checkbox"/> DTIC USERS <input type="checkbox"/>		21. ABSTRACT SECURITY CLASSIFICATION UNCLASSIFIED	
22a. NAME OF RESPONSIBLE INDIVIDUAL Dr. Philip A. Kessel		22b. TELEPHONE NUMBER (Include Area Code) (805) 277-5591	22c. OFFICE SYMBOL AFRPL/DYSO

Section 19: Abstract (continued)

ments of the boundary layers at the mixing origin were also recorded. In addition to rapidly responding pressure and temperature probes, small-scale gas sampling probes with collection times of approximately 40 ms were used. After each test, the H_2 fraction of the samples was analyzed by measuring the thermal conductivity of the gas using the Pirani and Baratron gauge reading comparisons. Radial profiles of both velocity and H_2 mole-fraction were determined.

In the report, the operation and performance of the innovative jet apparatus and diagnostics, and the flow initiation, jet synchronization and operational envelope using various gas mixtures are summarized. Pressure and temperature histories identify features of the starting and terminating transients and the characteristics of the quasi-steady flow used for testing. Samples of pressure, temperature and species concentration distributions at various axial distances from the exhaust plane illustrate the data obtained during the experiments. The measurements obtained during the experiments are discussed from the point of view that identifiable trends emerge in the supersonic mixing behavior when jet density and Mach number are varied. Accordingly, the results have been divided into three major groups which describe the influence: (a) density variations on the mixing of $M_j = 4$ into the outer stream, (b) density variations on the mixing of $M_j = 3$ jets into still ambient, and (c) Mach number variations on the mixing of high and low density jets.

FOREWORD

Calspan has conducted a series of non-reacting turbulent jet mixing experiments utilizing innovative short-duration test techniques and fast-acting diagnostics. This program, under the sponsorship of the Air Force Rocket Propulsion Laboratory (AFRPL), covered a 36 month period from 1979 to 1982.

The experiments were conducted in separate phases that furnished the Air Force with milestones and decision gates before each succeeding phase. A very close liaison with the Air Force technical monitors, T. Dwayne McCay, A. Kawasaki and P. Kessel, existed throughout the program. In addition, frequent technical-direction meetings were held with the RPL Advisory panel consisting of T.D. McCay (RPL and later NASA Marshall), H. Pergament (SAI), B. Walker (Army Missile Command), G. Brown (Cal Tech), A. Roshko (Cal Tech), and R. Rhodes (ARO, AEDC).

The technical activity was detailed in monthly progress reports in addition to the Technical Direction meetings. Several reports were published during the program in which experimental data were submitted to AFRPL on a timely basis.

The program was conducted by the Aerodynamic Research Department at Calspan, utilizing a number of key technical people as part of the experimental team. The effort was initially led by C. E. Wittliff. Subsequent phases of the program were completed under the direction of C. Padova. Additional contributors were W. Wurster and D. Boyer in the areas of fast-acting diagnostics, data analysis and experimental techniques, and P. Marrone in data analysis and program direction. The efforts of R. Bergman, S. Sweet, M. Urso, C. Bardo, F. Urso and R. Hiemenz were also central to the success of the program.

The reports which were released as part of this effort are listed below:

1. Non-Reacting Turbulent Mixing Experiments CDRL Item 1, 8 January 1980, "Program Plan" Submitted by C. E. Wittliff.
2. Calspan Report No. 6632-A-1, 25 July 1980, "Phase 1 Test Report" Submitted by C. E. Wittliff.

3. Non-Reacting Turbulent Mixing Experiments, August 1981, "Phase 0 Test Report" Submitted by C. Padova and W. H. Wurster.
4. Tubulent Mixing Experiments, 18 November 1981, "Illustrative Raw Data from Phase 1/81 Tests" Submitted by C. Padova.
5. Non-Reacting Turbulent Mixing Experiments, 20 November and 3 December 1981, "Phase 1/81 Data Package (and Supplementary D.P.)" Submitted by C. Padova.
6. Calspan Report No. 6632-A-2, August 1982, "Phase II - Test Engineering Report" Submitted by C. Padova.
7. Calspan Report No. 6632-A-2, September 1982, "Phase II - Test Engineering Report. Supplement No. 1 - Data Plots" Submitted by C. Padova.

TABLE OF CONTENTS

<u>Section</u>	<u>Page</u>
1. INTRODUCTION	1
2. EXPERIMENTAL APPROACH AND APPARATUS	4
2.1 EXPERIMENT DESCRIPTION	4
2.2 TEST FACILITY	5
2.3 TEST ARTICLE	6
2.4 INSTRUMENTATION	8
3. PROCEDURES AND APPARATUS PERFORMANCE	13
3.1 CALIBRATIONS	13
3.2 DATA ACQUISITION	16
3.3 JET/STREAM CHARACTERISTICS	22
3.4 DATA REDUCTION	30
4. RESULTS AND DISCUSSION	34
4.1 MIXING MEASUREMENTS	34
4.2 BOUNDARY LAYER MEASUREMENTS	37
4.3 INFLUENCE OF DENSITY ON THE MIXING OF $M_\infty = 4$ JETS INTO $M_\infty = 2$ AMBIENT	37
4.4 INFLUENCE OF DENSITY ON THE MIXING OF $M_\infty = 3$ JETS INTO STILL AMBIENT	42
4.5 INFLUENCE OF MACH NUMBER ON THE MIXING OF JETS AT HIGH DENSITY AND AT LOW DENSITY	43
5. CONCLUSIONS	45
REFERENCES	47
APPENDIX I: MIXING MEASUREMENTS	104
APPENDIX II: BOUNDARY LAYER MEASUREMENTS	144

LIST OF FIGURES

<u>Figure</u>		<u>Page</u>
1	Calspan Ludwig Tube Wind Tunnel.....	57
2	Schematic of Jet Mixing Experiment	58
3	Ludwig Tube Facility Configuration for Turbulent Mixing Experiments	59
4	Schematic of Jet System	60
5	Views of the Apparatus	61
6	Nozzle Contours	62
7	View of the Instrumented Rake for Mixing Surveys	63
8	View of the Probes for Gasdynamic Measurements	64
9	Schematic of Heat Conductivity Gas Sampler System	66
10	View of the Probes for Gas Sampling	67
11	Response to Water Immersion of a Temperature Probe	68
12	Response of the Temperature Probes in the Jets at Various Compositions and Levels of Dynamic Pressure	69
13	Influence of Gas Composition on the Measurement of Pressure Using Pirani and Baratron Gauges	71
14	Gas Sampler Calibration	72
15	Pre-test Monitoring of Reference Temperatures	73
16	Histories of Flow Variables Measured in the Mixing Region	74
17	Sample of Averaged Data from the DDAS	75
18	Histories of Flow Variables Illustrating the Jet/Stream Characteristics	77
19	Synchronization of the CLT and Jet Discharges	78
20	Histories of Plenum Pressure for $M_j = 4, 3, 2$ Jets	79
21	Histories of Jet Variables in a Heated-Jet Test Case	80
22	Radial Variation of the Measurements in a Typical No-Wind Test Case	81

LIST OF FIGURES (Cont'd)

<u>Figure</u>		<u>Page</u>
23	Radial Variation of the Measurements in a Typical Wind-On Test Case	86
24	Reproducibility of the Data	92
25	Comparison of Radial Pitot Pressures with and without CLT Nozzle Extension	93
26	Illustrative Test Run Summary	94
27	Illustrative Calculation of Radial Velocity Profile	95
28	Variation of Jet Composition from Near to Far Field. $M_j = 4$ Jet Discharging into the Supersonic Stream With Density Matched	96
29	Variation of Pitot Pressure from Near to Far Field. $M_j = 4$ Jet Discharging into the Supersonic Stream With Density Matched	97
30	Velocity Variations from Near to Mid Field. $M_j = 4$; $M_\infty = 2$; Density Matched	98
31	Influence of Density Variations on Velocity Surveys at $40 R_j$. $M_j = 4$, $M_\infty = 2$	99
32	Axial Decay of Jet Core Composition	100
33	Influence of Density Variations on Core Length $M_j = 4$, $M_\infty = 2$	101
34	Pitot Pressure and Composition Profiles in the Mixing Jet at $20 R_j$. $M_j = 3$ Jet Discharging into Still Ambient with ρ_j Density Matched	102
35	Composition Profile in the Mixing Jet at $20 R_j$. $M_j = 2$ Jet Discharging into Still Ambient with $\rho_\infty/\rho_j = 0.6$	103

LIST OF TABLES

<u>Table</u>		<u>Page</u>
I	Nozzle Coordinates	48
II	Specifications for Hydrogen/Nitrogen Gas Mixtures.....	49
III	Matrix of Test Cases	50
IV	Completed Data Points	51
V	Data Points Surveying the Nozzle Boundary Layers	52
VI	Measured Nozzle Parameters	53
VII	Initial and Reference Parameters for the Mixing Measurements	54
VIII	Initial Velocities and Actual Density Ratios for the Mixing Measurements	56

LIST OF SYMBOLS

BL, GP, S T, RC, TR	Designation code for the diagnostic probes (as identified in the text at page 19)
M	Mach number
MW	Molecular weight
P	Static pressure in the flow field
P_i	Initial (pre-test) pressure in the charge tube of the jet or outer stream (CLT)
P_o	Stagnation pressure
P_o'	Pitot pressure
R	Universal gas constant
R_j	Radius at the exit plane of the jet
T_i	Initial (pre-test) temperature in the charge tube of the jet or outer stream (CLT)
T_o	Stagnation temperature
U	Axial component of velocity
X	Axial distance measured from the jet exit plane
X_{H_2}, X_{N_2}	Mole fractions of Hydrogen and Nitrogen
Y, Z	Horizontal and vertical reference axes with origin at the center of the cruciform probe holder

ρ Local gas density

γ Ratio of specific heats

SUBSCRIPTS

c at centerline in the mixing region

CO core of the jet

ct in jet charge tube, upstream of venturi throat

ref ambient level in the test chamber prior to jet initiation

j relative to the jet

∞ relative to the ambient surrounding the jet

COMPUTER SYMBOLS USED IN THE TABULATIONS OF APPENDIX I

MA, MJ, MWJ, PO, P, R, RHA/RHJ, U, X/RJ, XH_2
 All as identified in the text at page 30

Section 1

INTRODUCTION

Research on supersonic jet mixing, especially in the area of low-altitude rocket exhaust-plume technology, has been a critical part of the Air Force Rocket Propulsion Laboratory (AFRPL) program for several years. A major objective has been the development of computer codes for the prediction of plume observables, such as the radiation signature. These codes model complex physical and chemically-reactive flowfields. In the gasdynamic computations, modeling the turbulent transport processes remains as a major obstacle to a useful and widely applicable analysis of free turbulent flow phenomena. Work on this aspect is actively in progress. Advances in computational fluid dynamics have essentially offset the theoretical difficulties which constrained the complexity of the modeling approach up to the mid 1960s. These methods have been exercised on complex problems by using exact implementations of classical turbulence models and by developing new models to improve predictive power. In the course of this process, not surprisingly, a renewed need for experimental data has emerged to be used in the evaluation of the computational alternatives.

A case in point is the JANNAF-sponsored effort to develop an industry-standard gasdynamic model for low-altitude plumes. The turbulence module of the JANNAF Standard Plume Flow-Field (SPF) code¹ has five alternate turbulence models to predict the mixing phenomena that influences the development of exhaust plumes. They range from the simple traditional algebraic models to the advanced two-equation models, and they can be used in compressibility-corrected versions of the code that should improve the calculations of flow fields containing large density gradients.

In support of low-altitude plume research, AFRPL-sponsored experimental programs have been performed at AEDC and Calspan ATC. In general, the experiments were designed primarily to investigate the structure of the plume and its emitted radiation, often for particular propellant combinations, motor configurations and ambient conditions (i.e., Mach number and altitude).

Detailed information on the turbulent mixing phenomena is not readily discernible from these test data because of the complicating factors of the "real" plume. Recently, in response to the projected need to corroborate the SPF code, Calspan has defined a different experimental approach. The key concept of the approach is to use a unique short duration technique that is flexible enough to sequentially investigate, in a building block fashion, several of the physical and chemical complexities of low altitude plumes. Specifically, the technique would first be used to measure parameters such as density, Mach number and exit pressure in non-reacting jets over a broad range of gasdynamic conditions. Then the technique would be extended to mixing jets with "real" plume features also using basically the same controlled laboratory situation. These measurements would include having either or both jets laden with solid particulates and reacting mixtures combined with substantially an unaltered capability to control the gasdynamic parameters.

This report describes the results of the Calspan experimental program, sponsored by AFRPL, to investigate the supersonic mixing phenomena in the fundamental non-reacting jets case. The short duration approach outlined above was developed and applied to obtain these results. A primary objective of this experimental study was to generate a firm and comprehensive data base from which to select and establish compressibility corrections for the turbulence models of the JANNAF SPF. Within this framework, the needs for a fundamental description of the supersonic mixing phenomena were re-examined in the initial discussions with AFRPL. The influence of Mach number and density ratios were identified as the foremost gap to be filled. Fundamental measurements of turbulent mixing go back many years, and comprehensive reviews of experimental data are available.^{2,3} However, previous studies are scarce and most concentrate on specific and unrelated cases, especially in the range of Mach numbers above 2 and plume densities well below or well above ambient. Thus, experiments with non-reacting jets at Mach numbers of 2, 3 and 4 and ambient-to-jet density ratios from 0.6 to 10 were identified as having the highest potential of yielding the data needed to support the use and future development

of the SPF. Experiments with jets discharging both in a Mach 2 outer stream and in a quiescent ambient were judged important for their applications and for correlations with existing data. Mixing measurements over the above range of conditions were completed recently and are presented in this report.

Following this introduction, Section 2 briefly describes the Calspan test facility used. In the same section, the jet apparatus and the fast-response diagnostics which were designed especially for the experiments are reviewed in some detail. The procedures to obtain these mixing data are presented in Section 3 with a general description of the measured characteristics of the jets and outer stream. In Section 4, the extensive measurements of pressure, temperature, and gas species which describe the mixing of the jets are discussed. The mean velocities computed from the measurements are also presented to indicate how the Mach number and density variations influence the mixing process. The actual measurements are tabulated in Appendix I; plots of the measurements were published earlier (Reference 4).

Section 5 presents a précis of the main observations derived from the experimental investigation. They support these overall conclusions:

- well resolved measurements of gas species and velocity profiles have been obtained for a variety of Mach numbers and density ratios;
- these measurements expand the data base needed to support the ongoing turbulence modeling effort; and
- the short duration technique developed for the measurements represents a valuable tool for investigating fundamental plume phenomena over a broad range of experimental conditions.

Section 2

EXPERIMENTAL APPROACH AND APPARATUS

2.1 EXPERIMENT DESCRIPTION

A unique short-duration testing technique^{5,6} was developed at Calspan to study the supersonic mixing phenomena. The approach is especially suited to the broad range of test conditions of interest and for its application to reacting plume measurements. The technique is based on the capabilities of the large-scale Calspan Ludwig Tube (CLT) wind tunnel, depicted in Figure 1. Using this facility, an experiment was configured as sketched in Figure 2. A jet of arbitrary gas composition, a few inches in diameter at its origin, was exhausted into an essentially unconfined ambient which could simulate a wide range of altitude conditions. The ambient surrounding the jet was either still or moving at supersonic speed. A key operating characteristic of the CLT is permitted control of gas species in both the jet and the freestream flow to meet the demanding experimental requirements. Specific combinations of various gases were used to achieve a broad range of density ratios. In addition, for flow diagnosis, freestream and jet gases with the same composition were tagged with a trace amount of suitable gas additive. For each of the mixing flow fields that were generated, the measurements consisted of radial surveys of the jet plume at selected axial stations downstream of the exit plane. Because of the large scale of the jets, their mixing could be probed in detail with diagnostics simultaneously measuring pitot and static pressures, temperature, and gas species.

The flexibility of the short-duration testing approach for supersonic mixing measurements is apparent from the experimental conditions used in the Calspan investigation. Their range is indicated in Figure 2. The conditions were selected to separately evaluate the effects of freestream-to-jet density ratio, jet Mach number and freestream Mach number. The three jet Mach numbers, M_j , of 2, 3, and 4 were produced by interchangeable nozzles. The molecular weight, mw_j , and stagnation temperature, T_{0j} , of the jets were varied to span values of the ambient-to-jet density ratio, ρ_∞/ρ_j , from 0.6 to 10. This was achieved by using hydrogen-nitrogen mixtures heated as high as 800°R. The ambient, in which the

jet discharged was either quiescent (no-wind cases) or flowing at $M_{\infty} = 2$ (wind-on cases), had a stagnation temperature, $T_{0\infty}$, at or below ambient as determined by the operating characteristics of the CLT. In keeping with the overall purpose of generating a fundamental data base, complicating factors which characterize "real" low altitude plumes, such as a repetitive shock structure or significant base flows, were avoided. In all cases, the jet nozzles were contoured to provide a uniform, parallel flow at the exit. The bluntness at the exit of the nozzles was minimal, with a difference between inner and outer diameters of only 0.125 inches. The pressure of the freestream and jet at the exit plane were very closely matched. The locations in the CLT at which the mixing flowfield could be surveyed varied over a broad range, and the diagnostics were designed to cover radial locations from the jet axis to fifteen times the exit radius, R_j , in the outer region. The axial location of the surveys could be chosen arbitrarily between zero and $100 R_j$ downstream of the exit plane. In this study, however, a given number of tests were allocated to seven axial survey locations selected optimally with respect to a twofold criteria. For comparison with calculations used for turbulence model selection, the survey locations should provide radial velocity profiles from close field to far field in each experimental condition. For establishing trends of dependence on density ratio and Mach number, independent of the calculations, the survey locations should provide the minimum number of data points needed to describe important global mixing characteristics such as core length, centerline velocity decay, and spreading rate.

2.2 TEST FACILITY

The Calspan Ludwig Tube^{7,8} is a large scale, upstream diaphragm tube wind tunnel which operates on the non-steady gasdynamic principles.⁹ Figure 1 depicts the facility and identifies its main components. The supply tube is 60 ft long and has an inner diameter of 42 inches. Between the supply tube and the receiver tank nozzle the diaphragm station houses a mylar diaphragm and a quick release cutter bar. One of four interchangeable nozzles, a conical $M = 2$ nozzle with an included angle of 6° and an exit diameter of 42 inches, was used in the mixing experiments. The nozzle discharged into the receiver tank which is 8 ft in

diameter and 60 ft long. For a typical mixing test in these investigations, the supply tube was pressurized with nitrogen and the tank was evacuated and filled to a predetermined pressure with nitrogen. Flow was initiated by rupturing the diaphragm with the cutter simultaneously with jet plume initiation. After a brief initial transient, an expansion wave propagated upstream in the tube at acoustic speed and accelerated the test gas to a steady velocity. The gas expanded through the nozzle into the low pressure receiver tank. The nozzle supply conditions remained constant while the wave traveled up the supply, reflected from the end wall and returned to the nozzle. Currently, the CLT provides 95 ms of useful test time. The gas expanding through the nozzle provided the supersonic freestream into which the plume exhausted. During a test, the endwall of the receiver tank reflected a weak compression which propagated upstream and ultimately perturbed the test conditions established by the nozzle. The useful test time elapsed before this perturbation reached the test section was essentially equal to that provided by the supply tube.

2.3 TEST ARTICLE

Figure 3 depicts the nozzle/gas-supply assembly designed to generate the test plumes. Most of this assembly is contained within the CLT sting. The principal components of the assembly are three interchangeable nozzles and the jet gas supply. The latter consists of three main units: (a) 160 ft of 1 inch i.d. high pressure tubing, (b) a pneumatically operated quick opening ball valve (action time of about 10 ms), and (c) a venturi metering nozzle which distributes the supply gas to the large cross section of the nozzle settling chamber. The arrangement of these units is shown schematically in Figure 4.

Jets having Mach numbers of 2, 3, and 4 were generated with three contoured nozzles designed to provide parallel exit flow. The nozzles attach to the CLT sting via a conical adapter. The outside of each nozzle is also conical so that the sting can gradually taper down to the diameter of the nozzle exit. This satisfied the modeling requirements of a clean, non-bluff base region. Figure 5a offers a close-up of a portion of the jet supply which shows the quick valve actuator in the foreground. Figure 5b gives a view of the test assembly from the jet exit.

In several respects, the jet apparatus operates using the same non-steady gasdynamic process as the CLT. The length of the supply tube is dictated by the test time requirement and the acoustic speed of the gas. The length was chosen to provide a useful test time, at least equal as the CLT's, when using heated, pure hydrogen as the charge gas. The tube is considerably longer than can be contained in the CLT sting and is routed outside the facility through the cutter housing strut supports. The gas supply and CLT sting form an integral system to which the interchangeable jet nozzles are attached and offer a clean aerodynamic shape to the outer stream. For tests which require a heated jet gas mixture, 35 ft. of the gas supply tube is wrapped with heating tape. Heating of a limited segment of the tubing is sufficient, since only this fraction of the gas in the supply is required in a test. The heated segment of the supply is coiled inside the CLT sting. The temperature of the jet gas is monitored by thermocouples placed along the tube length.

The jet apparatus operates differently than the CLT in one important respect. The test gas accelerating to a steady velocity in the supply tube is expanded twice to supersonic velocities before it leaves the nozzle. After the first expansion, which takes place in the venturi, the gas goes through a stationary shock that results in an increase in critical cross-section and a decrease in total stream pressure. By this process, nozzles with throat diameters larger than the diameter of the supply tube can be operated under steady conditions. The stationary shock is established and maintained automatically by the equal mass flow rates required at the venturi and the nozzle throats. Relevant characteristic dimensions are indicated in Figure 4.

The internal contours of the nozzles are based on available designs from two different sources. The coordinates for the $M = 2$ and 3 nozzles were calculated using a modified version of the NASA program of Ref. 10 at Calspan. The coordinates for the $M = 4$ nozzle, listed in Table I, were obtained from ARO/AEDC. All nozzles have exit diameters of 3 inch and use a 3 inch diameter settling chamber. The settling chamber length varies with the Mach number in order to compensate for the fact that nozzle length increases with increasing

Mach number. Figure 6 illustrates the nozzle contours and gives the throat diameters and other important dimensions.

2.4 INSTRUMENTATION

Mean velocity profiles at various radial points in the mixing flowfield were the primary data obtained from these experiments. To generate these profiles from the isobaric mixture of gases having different compositions, surveys of pitot pressure and of gas species concentrations were required. In addition, total temperature surveys were needed for the heated jet test cases. In Calspan's experiments, temperature measurements were also used to obtain accurate velocity profiles in the cold jet test cases where deviations from strictly isothermal mixing occurred because the two streams were accelerated differently by expanding from similar initial ambient conditions. In all experiments, isobaric mixing was obtained by controlling the initial pressure of the jets. However, small deviations from the isobaric conditions were expected that could significantly affect the determination of local Mach number. Surveys of static pressure were also used to obtain accurate velocity profiles.

The instrumentation consisted of four sets of single probes, three for the measurement of gasdynamic quantities, one for gas sampling, and two rakes for closely spaced pitot measurements. To survey the flowfield at selected axial positions downstream of the jet nozzle exit, these instruments were mounted on a cruciform holder which was anchored to the walls of the receiver tank. The vertical and horizontal diameters of the holder were designed so that individual probes or rakes could be mounted on one-inch spacings from the centerline to 15 jet radii, R_j , outboard. For more closely packed measurements, the horizontal arm had 1/2" spacings on a segment $\pm 4 R_j$ around the centerline.

Pitot measurements were taken using rakes which closely space the measurement points. The rake arrangement is simple and flexible: when regions of large gradients are surveyed, the probes can be packed in as in Figure 7; to accommodate jet spreading, the probes can be relocated with greater spacing increments.

Besides surveying the mixing flow field, ten quantities were monitored during each test to document actual experimental conditions. Total pressures and temperatures were taken (a) in the gas supply, (b) in the nozzle settling chamber, and (c) in the CLT settling chamber. One pitot and two static pressures were taken at the nozzle exit plane. Times of mixing flowfield gas sample were also recorded in each test.

Gasdynamic Diagnostics

The gasdynamic diagnostics were of conventional design. Individual probes are shown in Figure 1. The total temperature probes were small shielded thermocouples, patterned after designs presented in Ref. 11, with thermocouple junctions of Chromel-Alumel or Chromel-Constantan wires (thickness 0.001 in) butt-welded and protruding into the shield vane from a ceramic insulator. The pitot probes consisted of a single stem which held a slender 0.125 inch diameter transducer directly facing the flow. This arrangement eliminated any influence on the probe response derived from the impedance of the tubing connecting the pitot mouth to the transducer location. The static probes were made up of 0.065 inch o.d. hypodermic tubing with a conical tip of 20° included angle. Four pressure sensing holes, 0.008 inch in diameter were drilled in the tubing 12 diameters downstream of the tip and 20 diameters upstream of the probe body which contained a piezoelectric sensing transducer.

The rake, shown in Figure 8b, permitted pitot measurement at locations 0.250 inch apart. It consisted of ten 0.096 inch o.d. tubes each leading to a 0.37 inch diameter pressure transducer housed in the probe body. It was intended primarily for measurements in the mixing region, however, since its design minimizes the effects of mutual interference, it was also used to probe the initial wake region of the nozzles. To define the inside and outside boundary layers of the nozzles at the exit plane, the rake in Figure 8c was used. Its design allowed a close spacing of the pitot probes in the boundary layer without

interference from the transducer assembly, and the nonlinear displacement of the probes permitted close probe spacing in the region of large gradients near the wall. The individual probes were 0.032 inch o.d. hypodermic tubing with substantially increased base size to increase their strength.

All of the transducers used in the gasdynamic diagnostics were available from the Calspan stock of fast response pressure transducers. Some had been developed in-house, others were commercially produced. Generally, the transducers employ a lead zirconium titanate piezoelectric ceramic as a pressure sensitive energy source and field effect transistors as power amplifiers. Each transducer is compensated internally to minimize acceleration effects. A line-of-sight heat shield is used where required to minimize heat transfer effects. Their linearity, sensitivity and broad dynamic response are fully documented and periodically checked using in-house calibration facilities. The combined pressure range of the transducer used in these experiments goes from 0.005 psia to several hundred psia.

Gas Species Diagnostics

The gas sampling and analysis system developed for these experiments was based on similar experience with gas sampling in other short-duration facilities. The system relies on a capture technique applicable to the steady-state test time in the CLT and on post-test analysis of the captured samples. In principle, there are different techniques that could be used to conduct post-test measurements of species concentrations; in these experiments, the captured samples were individually expanded to a manifold and analysis station outside the facility after each test. The highly different heat conductivity values of H_2 and N_2 were used for the analysis. The pressure of the expanded gas sample was measured simultaneously with an Autovac Pirani gauge and with a Baratron gauge. The first operates by measuring the rate of heat transfer between a heated wire and its surroundings and its calibration is dependent on the nature of the gas. The latter utilizes diaphragm flexure and provides accurate pressure data independent of gaseous species. By exploiting the calibration corrections

that were required for the Pirani tube indications, the hydrogen concentration of the samples was obtained.

Figure 9 schematically identifies the components and layout of the heat conductivity gas sampler system (HCGS). Ten separate probes were used for sample capture; each a pencil-shaped 0.25 inch o.d. tube with a 30° conical tip with a 1 mm diameter orifice sealed by a molded valve seat. For sample capture, the seat-stem assembly located inside the probe tube retracts 3 mm in less than 4 ms and can be programmed to remain open up to 50 ms to obtain a sample volume of about 10 cm^3 . Key elements of the seat-stem actuator system are shown in Figure 10 and include small thin-walled nickel bellows sealed to a long stem on one end and to a solenoid armature sling on the other, the solenoid used to open the probes, and the probe housing into which the whole assembly is inserted. Actuation is achieved by an impulse discharge from a capacitor through the solenoid coil. A photograph of the assembled probes prior to installation in the cruciform holder is shown in Figure 10b. The probe array is seen (Figure 10a) protruding from an aluminum support bar that simulates the holder. Below the holder, the capture sample section and the valves that seal it for subsequent analysis can be seen. In the schematic of Figure 9 these valves are labeled, V_1 and V_2 . The sample was expanded into a low volume sampling manifold through the lower valve which led to the Pirani tube, the Baratron gauge and, through two controllable valves, to a larger throughput purge line. Vacuum sources, supporting electronics for the pressure gauges, and plumbing to a battery of calibration gases completed the system.

A brief description of the HCGS operation as used in this program follows. Prior to the test, the entire system up to the stem seal was evacuated to about 10^{-3} torr with a refrigerated-trapped forepump. Valves V_1 , V_2 and the purge valve were open. About one minute before the test, V_2 was closed and the actuating capacitor charged. A trigger signal synchronized the stem opening time with the test gas flow events, permitting the sample collection during about 40 ms of stem-open time. Immediately following the test, all ten V_1 valves were closed, isolating the captured samples for sequential analysis. Each sample was analyzed by closing the purge valve and opening valve V_2 . This permitted the

captured sample to expand into the manifold and analysis line. The sample pressure was then brought to a preselected value indicated on the Baratron gauge bleeding gas into the purge line. After waiting approximately two minutes for equilibration, the corresponding reading from the Pirani was recorded. Then the sample was bled to a lower Baratron pressure and the Pirani reading repeated. From the Pirani readings, the partial pressures which constitute the desired data were directly derived using previously established calibration curves, such as those discussed in Section 3.1. This was done to ensure an analysis at a lower pressure for cases where the only data available was from probes exposed to a low dynamic pressure. In the system, calibration data could be repeated at any time by admitting a sample of premixed H_2/N_2 mixtures to the analysis station. This feature was used to ascertain the reproducibility of the measurements and to correct them for small temperature influences.

Section 3

PROCEDURES AND APPARATUS PERFORMANCE

3.1 CALIBRATIONS

The critical components and subsystems of the apparatus prepared for these mixing experiments were calibrated either individually by bench testing or as assembled in the operational system. In the latter cases, functional tests especially designed for calibration purposes were employed. The procedures and results from the calibration of the temperature probes and the HCGS analysis instrumentation are briefly reported in this section. In calibrating these parts of the apparatus and others such as the gas samplers, the pneumatic actuator, and the quick valve, the aim was either to empirically establish their behavior or to verify that their characteristics conformed to known levels.

The temperature probes were calibrated for sensitivity and response to recovery temperature. The electromotive force generated at the thermocouple junction was detected and directly reduced to a temperature reading by using the known sensitivity. In a few of the probes, the measuring junction was referenced to an electronic cold junction. In the remaining probes, the reference was provided by a constant temperature block which was monitored and held constant during the measurements. The two calibration techniques resulted in identical measurements when the probes were exposed to the same temperature.

The ability of the temperature probes to equilibrate promptly to the local flow conditions also had to be verified. A preliminary evaluation of thermocouples of different materials, wire thicknesses, and junction geometries was conducted by simpl. water immersion tests. For a prescribed water temperature, the quick immersion of a temperature probe provided an oscilloscope trace, as shown in Figure 11, to identify the response time. The absolute value of the response time obtained under such conditions cannot be related simply to that which occurs during operation in a gas moving at high speed, but it is useful in a relative comparison among probes. For example, the figure shows that the butt-welded junctions of Chromel-Constantan wire having a 0.003 inch thickness responds beyond 95% of the final level in about 7 ms. In contrast, vendor's thermocouples of the same wire with junctions in the

shape of a 0.005 inch diameter ball were found to require 14 ms and for 0.002 inch wire with butt-welded junctions, about 3 ms.

In the demanding environment of the short duration tunnel the thermocouples must be robust for durability as well as fast in response. This calls for the selection of the thickest wire with adequate response. Initially, considerations of durability and of the results from the bench evaluation resulted in the use of the 0.003 inch wire probes with butt-welded junctions. They were later found to respond well in some but not all of the gas stream conditions for which accurate temperatures were desired. In the mixing experiments the probes must operate satisfactorily from cases where they suddenly heat up from ambient temperature to about 250°F to cases where they suddenly cool down from ambient to -60°F. Depending on the local dynamic pressure and temperature, the 0.003 inch wire probes were found to respond too slowly when measuring gas streams cooler than ambient. The importance of tip geometry (inlet length, venthole size, etc.) was quickly ruled out as a factor by trying probes with modified tips. Adequate response was finally obtained by relaxing the durability requirement and using 0.001 inch butt-welded wire in the probes. Figure 12 documents the ability of the 0.001 inch wire temperature probes below or above ambient in a variety of gas stream conditions. In all cases shown, the static pressure was about 1.7 psia; the local dynamic pressure is indicated in each case. The residual temporal variations that were present in the heated cases correspond to actual jet conditions and are discussed in Section 3.4.

The major calibration required for the HCGS consisted of the empirical determination of the relation between gas composition and pressure differences indicated by the Pirani and Baratron gauges. This calibration was carried out with the whole system ready for final operation. In an early feasibility phase, seven gas mixtures of known composition were prepared in-house for calibration purposes.

In the calibration procedure a sample of a known gas mixture at a preselected pressure was admitted into the capture portion of the sampling probes. This duplicated the post-test condition which followed a mixing survey. The captured samples were then released into the analysis manifold. At several pressure levels the Pirani and Baratron outputs were recorded. These readings were found to be related as shown in the solid curves of Figure 13. As expected, the Pirani readings decreased monotonically and non-linearly with decreasing pressure. At any H_2/N_2 mixture ratio the Pirani reading rate of decrease increased as pressure decreased. For a gas sample of given pressure, the Pirani reading was highest at the highest H_2 concentration. The pressure differences indicated by the Pirani and the Baratron gauges were used to calculate the gas sample composition. Figure 13 presents measurements of a representative test run in which ten samples, identified by different symbols, were collected and analyzed. The initial pressure in each sample depends on its location in the flowfield. Each sample was expanded sequentially 3 or 4 times for analysis, obtaining the H_2/N_2 pairs plotted in the figure. From a best fit of these data relative to the calibration curves, an accurate definition of the gas composition of each sample was obtained. For instance, sample No. 1 was evaluated to contain 10% H_2 . The advantage associated with samples of higher initial pressure is also apparent from the figure. For routine measurements, however, practical consideration suggests that a simpler procedure be used to obtain the composition using the known Pirani/Baratron relation. In the simpler procedure, two analysis pressure levels are selected and the measurements are compared to the calibrations only at these levels. The expected initial sample pressures, the known expansion ratios between capture volume and the analysis manifold, and the limitations in the Pirani range of operation determined the selection of 3 and 1 torr as the analysis pressure levels. Crossplots of the Pirani readings versus gas composition show a very nearly linear relationship as illustrated by the solid lines in Figure 14. At 3 torr the sensitivity is about + 0.03 mV for a 1% increase of the H_2 fraction. At 1 torr this sensitivity is decreased by a factor of 2 (0.015 mV). The sensitivity of the Pirani is unaltered by temperature changes, however, they do affect the level of the Pirani output. This effect was empirically evaluated at $\pm 4\%$ of the H_2 fraction for a

+ 3°F variation in Pirani temperature. In the actual operation of the HCGS system, the temperature influence was eliminated by using a constant temperature bath.

As mentioned earlier, the calibration curves established during the HCGS feasibility study used gas mixtures prepared in house with seven different levels of H_2 content. Later, the calibration was repeated with samples of the gases used to generate the jets. These gases were prepared and certified by the vendor according to specific tolerances which are given in Table II. The symbols in Figure 14 identify both the preliminary and final calibration points; only negligible differences were found.

3.2 DATA ACQUISITION

The overall objective of obtaining turbulent mixing data for non-reacting supersonic flows over a range of Mach numbers and density ratios was achieved by completing a matrix of thirteen test conditions. In the experiments, the jet mixing region was measured at various axial locations downstream of the jet exit plane. In addition, a number of surveys at the exit plane of the jets were taken to measure the boundary layers that influence the mixing phenomena.

The typical test sequence and data acquisition for each experiment included the following:

- model (jet nozzle) preparation, and probes and survey rake positioning;
- Ludwig Tube Test chamber, jet charge tube and heat conductivity gas sampling (HCGS) system evaluation to ensure removal of trace gases; and
- N_2 loading in the test chamber at a preselected ambient pressure level, P_{ref} .

From this point the preparations differed according to the test conditions.

In the simplest case, a jet at ambient temperature discharging into the quiescent ambient, the following steps were taken:

- The charge tube jet gas was loaded from cylinders of the pre-mixed H_2/N_2 . The charge tube was set at a pressure selected so that the pressure at the exit of the jet matched the pressure of the test chamber (receiver tank). The temperature, T_{ij} , of the charge tube was monitored during loading to ascertain deviations from the ambient resulting from compression.
- All initial conditions and initiation of the jets (test run) were recorded.
- The gasdynamic measurements, high speed digital sampling (each channel sampled every 250 μs), and the data channels recording was triggered automatically by run initiation. For each data record, pre-triggering base-lines were also recorded by the Calspan Digital Data Acquisition System (DDAS).
- Gas samples were collected and trapped in the probes' reservoirs over a preselected time interval during the test. The samples were analyzed sequentially after the test.

For a jet at ambient temperature discharging into the outer stream, two additional steps were required.

- A variable delay between the trigger signals that initiate the jet and the Ludwig tube flows was set.
- The CLT supply was loaded with N_2 . The CLT pressure was set so that the pressure at the exit of the CLT nozzle matched the

pressure of the test chamber. The CLT temperature was ascertained to have quickly returned to ambient following loading.

When the jet gas supply required heating prior to discharge, the loading sequence consisted of successive pressure increases and heating of the charge gas. The pretest temperature variations in the charge tube were monitored at four locations along the tube. The temperature records of a typical loading and heating sequence are shown in Figure 15. The lower trace is the measurement of the jet supply a short distance upstream of the quick opening valve. The sensor's reading deviates sharply from the initial ambient level as the supply was filled to 600 psia. Quick equilibration to the original level followed. Then the heating was applied for about 15 minutes. Successive gas loadings, as heating continued, are indicated by the spikes at 15, 16, 22 and 28 minutes. Once the desired temperature was reached, three controllers maintained it for a period of time sufficient for equilibration. Firing followed as indicated in the trace. The temporal variations of temperature in the test chamber and plenum of the CLT nozzle are also documented in Figure 15. As indicated earlier, their deviations from ambient are negligible.

For any of the experimental conditions, the histories of all gasdynamic measurements were promptly available for inspection from the DDAS following the test run. In a few minutes the data could also be filtered (if required), reduced to engineering data units, and averaged over selected time intervals. Analysis of the gas samples required a longer time. After a test run, raw measurements related to gas composition were available in the form of manually recorded voltages from the Pirani gauge. These raw measurements were converted to H_2 fraction values by using the predetermined calibration curve that relates the two quantities.

The essential features of recorded flow variable histories measured in the experiments are illustrated in Figure 16. The initial transient associated with jet initiation lasted less than 20 ms. Steady flow conditions followed for a 50 to 90 ms period depending on test conditions. Over a substantial fraction of this time the data records were averaged to derive values of pitot pressure,

static pressure, and recovery temperature at each probe location. In the figure, the data for the pitot probe at the radial location 1 inch from the jet axis closely follows the temporal behavior of the stagnation pressure in the jet plenum. As shown, the steady flow conditions were terminated by the expansion wave that traveled upstream and reflected back into the supply. A detailed description of the jet/stream characteristics is given in Section 3.4.

All the flow variable histories were saved on magnetic tapes creating an extensive data bank from the experiments. For the immediate analysis of the data, the averages of the measurements during the steady flow were utilized. An example of the DDAS averaging format for a typical 40 msec time interval is given in Figure 17. All data channels were averaged during this time interval. Referring to Figure 17, all jet pitot measurement channels are labelled T, TR, or BL; all jet static pressure measurement channels are labelled S (static); and jet temperature measurements are labelled TC (thermocouple). The remaining channels are jet nozzle and ambient measurements. The gas sampling measurements, labelled GP, have been added at the end of the table since they were manually entered into the data following the analysis after each test. These data create a permanent file suitable for automatic data reduction. The gas sampling open gate time was set to occur during steady test conditions by adjusting a variable delay between jet initiation and GSP plunger triggering. The data averaging interval was matched to the gas capture time shown in Figure 16 by the gas samplers open-time trace. In this trace, the opening of the probes is marked by the step up and the end of the capture interval corresponds to the step down. In bench tests the measured open gate time for all ten probes was nearly equal.

The averaging time interval given in the example is typical of the interval used in all experiments. Minor variations did occur which were determined by differences in the test conditions, and for a selected number of tests, the flow variables were averaged over time intervals occurring earlier or later during steady state or with time intervals having different durations. In all cases the deviations in the values of pressure and temperature were found to be insignificant in relation to the characterization of mixing phenomena.

Table III lists the thirteen test conditions for the turbulent mixing experiments. Values of the ambient-to-jet density ratio (ρ_∞ / ρ_j) from 0.6 to 10 were obtained by using pure hydrogen and H_2/N_2 mixtures with molecular weights (MW_j) up to 26. As originally planned, experiments were conducted with quiescent ($M_\infty = 0$) and supersonic ($M_\infty = 2$) outer ambients. The test cases covered a broad range of ambient-to-jet velocity ratios. Later it is shown that values of velocity ratio from 0.164 to 0.643 were obtained with the jets discharging in the supersonic outer stream (wind-on cases). These wind-on experiments simulated plumes from rockets at altitudes of about 50,000 ft flying at speeds of about 1600 fts^{-1} . Including the quiescent ambient cases, the jet velocities ranged from 1600 to 9940 fts^{-1} .

The different density ratios were obtained by changing the jet gas composition and its initial temperature. Diatomic jet gases were used in all cases. Their molecular weights and compositions in percent mole fraction are listed in Table III. The use of diatomic gases offered two advantages. It eliminated the specific heat ratio of the jet and free stream flow as an additional variable in the matrix, and permitted the use of a single contoured nozzle to generate the jet Mach numbers needed. With nitrogen for the outer ambient and H_2 in the jets as a tracer the density ratios of the tests had a lower bound of 0.6. Except for two of the cases with high density ratios, the jet total temperatures (T_{oj}) corresponded to the jet supply system which was room temperature ($528^\circ R$ nominally) prior to testing. The high density ratios of 10 for $M_j = 4$, and 7 for $M_j = 3$ were obtained by designing the apparatus to heat the gas charge to just above $800^\circ R$. Originally, the $M_j = 2$ jet was to be used to investigate the range of ρ_∞ / ρ_j from 0.6 to 10 with $M_\infty = 0$. Difficulties with the operation of the $M_j = 2$ jet, however, resulted in the use of the $M_j = 3$ jet instead. For the $M_j = 3$ jet, the heating limit prevented obtaining $\rho_\infty / \rho_j = 10$; a value of 7 was the upper limit.

As stated earlier, the experiments probed the jet mixing region at axial locations between 10 and 100 jet radii downstream of the jet exit plane. More than 80 test runs were performed during the course of the entire experimental program in order to collect mixing measurements with more velocity and

species surveys conducted at $M_\infty = 2$ than at $M_\infty = 0$. From these runs, the tests that yielded the primary results of the program are listed in Table IV and V. For each test case and survey location listed, the applicable test run is identified. The test runs are numbered to indicate the phase and test within the phase. The test phase is indicated by the codes 01 (for Phase I/80) and 1 and 2 (for Phase I/81 and Phase II) which appear before the period of the test number. The run number within each phase follows the period.

The mixing region of the jets was surveyed at one to four axial locations as indicated in Table IV. More than fifty percent of the test cases were surveyed at four axial locations in the near through far field. Emphasis was placed on the cases with $M_j = 4$; 16 of the 20 tests devoted to this case were in the wind-on condition. Approximately an equal number of tests investigated the effect of Mach number at $M_j = 3$ and $= 2$ in cases with low and high density plumes. Overall, the survey locations chosen provide an optimal distribution among the given number of tests with respect to the twofold objectives for the measurements. For comparisons with calculations for turbulence model selection, they provide velocity profiles in the close field, mid field, and far field of the mixing regions. For establishing mixing behavior trends independently of the calculations when density ratio and Mach number are varied, they provide sufficient data points to describe core length, centerline velocity decay, mixing width, and the like in nearly all test cases.

The nozzle internal and external boundary layers were surveyed for each of the jets at low and high plume densities during the tests listed in Table V. In some cases these measurements were taken simultaneously.

The total number of test runs performed during the experimental program exceeds the number indicated in Tables IV and V for two reasons. First, a number of tests investigated specific facets of the testing technique such as data reproducibility, effect of pressure disturbances at the exit of the outer nozzle, and jet alignment. Results from some of these tests are reported in Section 3.4. Second, not all tests were fully successful and some measurements at selected conditions were repeated. The measurements from a number

of these duplicated tests contain data valuable for appraising the core data base. These data are in the form of repetitive measurements of pressure, temperature, or gas composition, and of measurements of the sensitivity to perturbations in jet-to-ambient pressure ratio. The measurements that constitute the core data base are tabulated in Appendices I and II of this report.

3.3 JET/STREAM CHARACTERISTICS

An illustrative overview of the key features of the test jets, the outer stream, and the mixing region is presented in this subsection with the aid of typical measurement histories. Both quiescent and wind-on cases are discussed. Data from all the tests closely resemble the traces shown in this section, with particular differences due to different mixtures and initial test conditions.

Figure 18 presents flow variable histories of a jet discharging into a wind-on and still ambient and schematically shows the points of measurement. The jet behavior is shown in Figure 18a. The measurements of stagnation pressure, P_{oj} , in the nozzle plenum present the expected characteristics of an initial sudden rise in pressure followed by a constant plateau. The initial transient lasted no more than 25 ms. The plateau corresponds to the steady supply conditions that existed in the charge tube behind the expansion fan travelling upstream. In the case shown this is of the order of 150 ms. Viscous effects in the long, small diameter tube were responsible for the slight steady decline in pressure. The jet duration varies inversely with the speed of sound, hence it was shorter at the lower molecular weight of the gas mixtures and at the higher charge temperatures. Although the jet duration is independent of the nozzle used, the highest charge temperatures with pure H_2 were used in $M_j = 4$ tests resulting in the shortest jet duration. The test plateau in this latter case lasted at least 50 ms.

The recovery temperature trace, T_{oj} , in the nozzle plenum also shows the initial transient phenomena followed by the steady flow period. The apparent long duration of the transient resulted from the response lag of the probe. The initial overshoot in temperature is associated with the passage of the starting shock, soon followed by the cooler expanded gas from the charge tube.

In Figure 18b pressure and temperature measurements in the supply tube upstream of the metering venturi are shown. These measurements helped to monitor the performance of the jet apparatus. As expected, their behavior corresponded closely to those of P_{oj} and T_{oj} . A notable difference is the immediate cooling at flow initiation since, at this position, only the expansion fan travelling upstream sweeps the probe.

Representative pressure conditions at the exit plane of the jet are shown in Figure 18c. The P_j probe measured the static pressure of the jet and the P_∞ probe the static pressure of the ambient in which the jet discharged. The ambient pressure was only slightly disturbed by the jet initiation and remained close to the initial level during the steady test time. As desired, during this later time interval, the jet and ambient pressure were very nearly equal to each other. To maintain this, small adjustments in the pressure level of the test section (P_{ref}) were necessary, depending on the nozzle and the gas mixture used.

The test jets discharged in the $M_\infty = 2$ nitrogen stream in the wind-on mixing experiments. Initially all chambers were filled with nitrogen at ambient temperature. The CLT driver pressure was set so that the static pressure at the exit of its supersonic nozzle matched the pressure of the jet and the ambient during the test. The CLT supersonic stream was initiated simultaneously with the jet by rupturing the mylar diaphragm that separated the high pressure driver from the low pressure tank. Using matched pressure, only weak waves may have been present in the test flow although none were identified in the flowfield surveys.

Pressure and temperature measurements in the plenum and at the exit of the $M = 2$ nozzle to verify CLT operation were taken, and they are presented in Figure 18d, e. The CLT plenum stagnation pressure, $P_{0\infty}$, rose sharply to a well defined plateau of about 80 ms duration (Figure 18d). Correspondingly, the recording of the recovery temperature, $T_{0\infty}$, reports cooling to the level predicted by performance calculations. The stagnation pressure was monitored again in the $M = 2$ stream at the exit plane of the conical nozzle. It was obtained from the pitot measurement, $P_{0\infty}$ of Figure 18e. After the initial starting transient (cutting of diaphragm, passage of starting shock), the flow shows an extremely uniform plateau during which the jet mixing was initiated. The static pressure, P_{∞} , in the $M = 2$ stream maintained a behavior substantially similar to the one described in quiescent tests.

Synchronization of the jet and outer-stream constitutes an important aspect of the short-duration testing technique. The objective is to time the firing sequence so that the steady-state jet discharge optimally coincides with the steady flow available from each component of the apparatus. Figure 19 shows that firing the jet 3 ms after the outer stream achieved the objective. In this case, no adverse effects caused by mutual interference during the starting process were found. In fact, mutual interference effects were proven to be very modest over a range of sequences going from cases in which the jet was initiated 20 ms before the CLT stream to cases in which the jet was initiated 10 ms after the CLT.

The jet stagnation pressures were different for each nozzle as determined by the gas expansion to the selected ambient pressure. Figure 20 shows traces illustrative of the $M_j = 4, 3$ and 2 nozzle performance. The corresponding static pressures at the exit plane are included. In each of these cases the jet duration extended beyond the 200 ms time mark because of the high nitrogen content (more than 30%) of the gas mixture used. Gas mixture differences also slightly influence the rate of pressure drop during steady flow because

of the viscosity effects in the charge tube. The requirement that P_{oj} could not be reduced by more than 5% in any test during the 50 ms test interval was met in the experiments. For each of the nozzles, the measured ratio of static-to-total pressure (P_o/P_{oj}) was used to establish the actual Mach number of the jets. The average values and standard deviations computed from a number of tests having the same nominal conditions are presented in Table VI.

A difficulty was encountered in the operation of the $M_j = 2$ nozzle. Under some combinations of charge pressure and gas mixture, it was not possible to establish nozzle flow into the usual ambient pressure. This was traced to an unsteady viscous-inviscid interaction phenomena caused in the venturi by the strength of the throttling shock. The $M_j = 2$ experimental results were obtained in test cases where the jet unsteadiness either did not occur naturally, or was prevented by altering the test procedure. In the latter case the jet was initiated into the CLT tank pressurized at a very low level. Quickly thereafter, mixing at the desired ambient pressure was established by initiating the CLT stream at the usual flow level. Based on the diagnostics available, the $M_j = 2$ results appear fully valid, however anomalies in the mixing measurements (discussed later) were later detected. It is possible that these anomalies are associated with larger fluctuations upstream of the nozzle throat.

Two of the test conditions selected for the mixing experiments required the use of heated jets. In Figure 21 the jet characteristics of these cases are illustrated with reference to the $M_j = 4$ nozzle. The total temperature, T_{oj} , of the jet increased undesirably during the test time. There are two possible causes for the temperature variations. Residual longitudinal temperature variations in the charge gas may have been present after heating and equilibration. As the gas is expelled through the nozzle these appeared as temporal variations. Transversal variations in the temperature of the charge gas were present as it flowed to the nozzle plenum because the boundary layer became heated inside the charge tube. As the expansion fan progressed upstream in the tube, more of the boundary layer flow contributed to the gas in the

plenum of the nozzle. This may have caused the temporal temperature variations observed. In any case the impact of this observed temperature behavior on the mixing measurement was assessed and found to be acceptable within the scope of these experiments. The measured change in T_{oj} during the test time could only cause a percentual deviation in the initial velocity of the jet less than $\pm 2\%$ of the computed value.

Representative measurements in the jet mixing region for a no-wind case are shown in Figure 22 and for a wind-on case in Figure 23. In the figures, the flowfields are described by their measured radial distributions of pitot pressure and selected local histories for each gasdynamic measurement. Surveys at two axial stations are also presented. Radial pitot probe data at the $X/R_j = 20$ axial station (30 inches downstream of jet exit nozzle) are given in Figure 22a. The close-in probe data shown by 3L 1 closely follows the P_{oj} temporal behavior discussed above. This correspondence decreased steadily at larger radial locations until the T8 probe, located 9 inches off-axis, essentially recorded the ambient tank pressure.

Radial static probe data at $X/R_j = 20$ are given in Figure 22b. The innermost probe (S4 at 0.5") indicated that after the initial transient the static pressure dropped about 0.15 psi below the ambient tank level and remained at that level for the test duration. Farther off-axis (probe S3 at 7"), the recorded pressure equalled that of the ambient tank. Its temporal behavior can be directly compared with the pressures shown in Figure 18c, which gives the test chamber pressure history. The P_{∞} probe in Figure 18c is located at the exit of the CLT nozzle, which for the quiescent tests represents an integral part of the test section volume. The direct correspondence among the records is readily observed. The pressure data presented in Figure 22 show that the available test time was terminated by the appearance of the wave reflected from the tank endwall. This occurred approximately 100 msec after the jet ball valve was opened.

Radial temperature probe data at the $X/R_j = 20$ station are given in Figure 22c. The close-in probe, TC12, remained at ambient temperature for the

entire duration of the test. Farther off-axis probe LTTO recorded a negligible temperature rise.

Similar pitot and static probe data are presented for $X/R_j = 100$ in the remainder of Figure 22. The predicted behavior of the measurements associated with the jet velocity decaying axially and spreading radially is apparent. Notable here is the progression in the level of fluctuations at selected locations in the mixing region and the degree of uniformity indicated by the measurements of the static pressure.

The flowfield of a jet mixing into an outer stream is described with the aid of Figure 23 using the same approach used for Figure 22. Radial pitot probe data at the $X/R_j = 20$ axial station are given in Figure 23a, b, c. Again the close-in probe data shown in Figure 23a closely follows the temporal behavior of the jet pitot; the level decreasing steadily, and moving off-axis, and approaching the level measured in the outer stream (probe T8 at 9").

Radial static probe data at $X/R_j = 20$ are given in Figure 23b. At the 0.5" and 2.5" locations the probes indicated that, after the initial transient, the static pressure dropped slightly below the ambient tank level and remained at that level for the full test duration. Farther off-axis (probe S3 at 7") the pressure, after the initial transient, returned essentially to the initial ambient level. This transitory behavior can be compared directly with that shown in Figure 18e (which gives the outer stream pressure history). Here again, the direct correspondence among the records is readily observed.

Radial temperature probe data at the $X/R_j = 20$ station are given in Figure 23c. The close-in probe, TC13, started at ambient temperature (shown as 0°F on the scale), increased as the starting shock traversed the probe, and then decreased as the actual jet gas flow passed it. The steady flow level corresponded closely to that measured in the plenum of the jet. The farthest-out probe, TC12, located outside of the jet mixing region and thus encountering only

the $M_\infty = 2$ ambient flow, behaved quite differently. A starting transient was still present but cooling followed and continued to the level measured in the CLT plenum. As expected, the behavior of probes situated in-between TC-13 and TC-12 showed similarities in temporal variation and level that progressively shift from duplicating the jet to duplicating the outer stream.

Also illustrating the wind-on mixing case, measurements of pitot, static, and temperature at $X/R_j = 100$ are presented in the remainder of Figure 23. The decreased rate of decay in the jet velocity along the axis and the change in the spreading rate are apparent even in these illustrative comparisons. However, density differences are also of significance here as discussed in Section 4.

Because of the innovative nature of the short-duration jet apparatus used to obtain the mixing measurements in the Calspan experiments, the early series of tests^{12,13} were mainly to verify the performance of the apparatus and the validity of the technique. Generally, the initial tests involved three types of experiments: (1) check out experiments to document the duration of the steady test time, the quick valve operation repeatability, the GSP timing, and the jet/CLT synchronization, (2) technique validation experiments to establish the reproducibility of the data, the validity of assuming the jet alignment known, and the influence of the expansion waves from the lip of the CLT nozzles on turbulent mixing and (3) initial turbulent mixing experiments to observe the data character for exemplary test cases ranging over a number of survey locations and test conditions. Results from the checkout experiments were reviewed earlier in this section. Results from the technique validation experiments are briefly reviewed here. Section 4 presents all results from turbulent mixing experiments.

Reproducibility of the data in the context of the short-duration experimental technique implies both the ability to reset identical test

conditions from test run to test run, as the flowfield is surveyed at different locations, and the repeatability of the data in identical tests. Reproducibility of test conditions in the CLT have been documented in a variety of studies and specifically in several investigations of fundamental flowfield phenomena. The whole apparatus used in the turbulent mixing experiments operates essentially like the CLT facility, and the previous experience is directly applicable. Nevertheless, this conclusion was checked in a few tests. In Figure 24, the repeatability of the data is shown for a survey of radial pressures close to the exit plane of the $M_j = 4$ nozzle. The excellent agreement obtained in the two independent sets of measurements is representative of the repeatability expected under nearly identical test conditions. The ability to control test conditions to be very nearly the same while mapping the flowfield in separate tests is documented in the jet/stream performance measurements given in Appendix I.

Concern that flow disturbances strong enough to disturb the test region may originate at the lip of the CLT nozzle arose because the nozzle is conical. It generates a slightly diverging flow that is turned in the receiver tank. To resolve this concern, measurements were made at a fixed axial location with and without a CLT nozzle extension of 3 feet. If disturbances had been present, pressure distribution differences arising from the formation of a definite test rombus delineated by weak waves would have resulted. None were detected as is indicated in Figure 25 and in the corresponding static pressure surveys.

Several tests were undertaken to measure the jet boundary layer near the exit plane of the jet nozzles. These tests used the boundary-layer probe array installed at the exit plane (Figure 2). The influence of the boundary layers on the mixing phenomena investigated in these experiments is presented in Section 4.

3.4 DATA REDUCTION

Section 3.2 explained how the primary measurements were obtained and filed in two basic formats: 1) histories of pressure and temperature and 2) composition values from the analysis of the captured gas samples. The initial step in the data reduction, which was also described in Section 3.2, was the averaging of the gasdynamic probe data records over the 40 ms time interval of steady test flow matching the gas capture interval. From this point to the computation of radial velocity profiles in the mixing flow, a combination of special purpose software, implemented on the DDAS computer, and mainframe programs were utilized. The DDAS data handling package can automatically execute the entire data reduction procedure transforming the primary measurements into radial velocity profiles. The code starts with a table of averaged measurements, such as the one given in Figure 17, and combines each probe value with a file of probe locations. At this stage a tabulation that summarizes all the results obtained during a test run can be generated. Alternatively, a tabulated summary could also be obtained from punched or magnetic data records transferred to the mainframe computer. An example of a test run summary of this type is given in Figure 26.

In Figure 26, the mixing measurements from test run 2.16 (Run No. 16 from the experiments of Phase II) are listed. They are used in the following discussion to illustrate the remaining data reduction steps to obtain velocity profiles. The table first lists the test conditions of the experiment: Mach numbers of the jet (MJ) and ambient (MA), density ratio ($RHA/RHJ = \rho_{\infty}/\rho_j$), and the survey location (x/RJ). Jet and ambient parameters are listed next and include gas composition (XH2) and molecular weight (MWJ), initial total temperatures (TO), initial total and static pressures (PO and P) and initial velocities (U). The measurements taken in the mixing region are listed under the heading "mixing survey". Four listings present the measurements of pitot and static pressure, composition of gas samples, and recovery temperature versus their radial location. The latter is indicated in two ways. The values of the coordinates Y and Z represent the location of the measurements

in the cartesian frame of reference having its origin at the center of the cruciform holding the probes, the Z axis vertical and the Y axis horizontal. A value of zero indicates the origin or center of the particular plane. The value of the coordinate R gives the radial distance of each measurement from the actual axis of symmetry of the jet. The location of this axis was determined by reflection of diametrically opposed measurements as explained below.

The actual axis of the jet was located by reflecting diametrically opposed measurements of pitot pressure (in the vertical plane) and of H_2 mole fractions (in the horizontal plane). Next, the radial distances of each probe from the jet axis were computed. In test run 2.16, the jet axis was found to be displaced 0.15 in the positive Y direction and 0.20 in the negative Z direction. Probe coordinates were computed with respect to a reference frame with the origin on the jet axis, and the value of R listed in the table was recomputed accordingly. In general, the jet axis adjustment was found to be on the order of ± 0.25 in, with variations introduced by rake positioning and nozzle changes made without moving the survey rake. When the correction for jet misalignment was completed, the results provided the final radial profiles of gas mixture, pitot and static pressures, and temperatures. Plots of the data in this format for all the test runs are available in Reference 4.

In the next data reduction step, the radial distributions of the mixing variables were fitted with cubic spline lines. Computation of velocity values requires interpolation of the measurements; this can be done in any number of ways once the primary data is properly fitted. Initially, in these experiments, the approach was to interpolate at a dense set of radial positions obtained by using all of the available data of pitot pressure and gas composition. For each of these radial positions the remaining three distributions were interpolated so that a set of mixed measured-interpolated values were obtained to generate velocity data. This was accomplished as follows. Ratios of static pressure to pitot pressure, P/p_0 were computed at each radial

location. From these ratios, the radial distribution of Mach number was derived using the isentropic flow relationship in subsonic flow regions ($P/p'_0 > 0.5283$) and by using the Rayleigh pitot formula where the flow was supersonic. In all computations, a γ value of 1.4 that applies to these diatomic gas mixtures was used.

The gas sampler probe data was then used to obtain the molecular weight of the gas mixture at the selected radial locations using

$$\begin{aligned} MW_{\text{mix}} &= 28.02 X_{N_2} + 2.016 X_{H_2} \\ &= 28.0 - 26.0 X_{H_2} \end{aligned}$$

where X_{N_2} and X_{H_2} are the mole fractions of N_2 and H_2 .

The gas mixture constant, R , is directly proportional to the molecular weight. The relation used here was

$$R_{\text{mixture}} = \frac{49740}{MW_{\text{mix}}}$$

Finally, velocities were computed using the relationship

$$U = M \sqrt{\frac{\gamma R_{\text{mix}} T_0}{1 + \frac{\gamma-1}{2} M^2}}$$

where the T_0 values were obtained by direct measurement.

The computed velocity distribution for Run 2.16 is shown in Figure 27. The figure shows that the velocity data points were calculated only at fairly sparse but regularly placed radial intervals. Because the effort required to collect the measurements was larger than anticipated, the data reduction effort had to be streamlined. One of the steps taken was to calculate velocity profiles at fewer, regularly spaced interpolated points. The resulting velocity profiles do not retain the information or the scatter of the original measurements, but this information is still available from the measurements listed in Appendix I.

Once the detailed mapping of the mixing flowfield was completed, in terms of velocity profiles and individual primary measurements, the analysis of the results began. In accordance with the initial aim of the investigation, the results are to be a) compared directly with existing computations, such as those from the SPF and b) applied, after cross correlation and interpretation, to establish trends in global mixing characteristics based on density ratio and Mach number. In connection with the latter objective, one observation is pertinent. To describe mixing characteristics such as core length, centerline velocity decay, and spreading rate, the velocities at the jet axis in the mixing region and in the surrounding ambient must be known. In these experiments the primary measurements extended sufficiently off-axis so that the velocity outside the jet was firmly established. The velocity at the jet centerline, however, was usually not directly available because only one probe could be located there, and preference was given to gas sampling. The velocities in the jet axis had to be obtained by either of two methods: a) for profiles in the core they were obtained by linear fitting of the available data points collected off-axis and b) for other profiles a circle was drawn through the data point closest to the jet axis tangent to a line between the last two data points (as shown in Figure 27). Where appropriate, the max core velocity limit was not surpassed.

The results of the experiment are presented and interpreted in the next section to establish an initial description of the mixing characteristics.

Section 4

RESULTS AND DISCUSSION

This section contains the mixing measurements obtained during the test runs listed in Tables IV and V. In addition, typical test data were selected to illustrate several key features and characteristics of the measurements, their effect on final test results, and the process used to generate the description of mixing from the velocity profiles. The results are presented in tabular form together with data summaries for clarification and then are briefly discussed in relation to the objectives of the experiments.

The experiments are discussed from the point of view of identifying the trends that emerge in the supersonic mixing behavior when jet densities and Mach number are varied. Accordingly, the results of the experiments have been divided into three major parts:

- a) influence of density on the mixing of $M_j = 3$ jets into still ambient,
- b) influence of density on the mixing of $M_j = 4$ jets into $M_\infty = 2$ ambient, and
- c) influence of Mach number on the mixing of high and low density jets.

4.1 MIXING MEASUREMENTS

The mixing measurements obtained during the test runs listed in Table III are contained in Appendix I ordered by the test conditions shown in Table III. Jet (MJ) and ambient (MA) Mach numbers, density ratio ($RHA/RHJ = \rho_a/\rho_j$), and survey location (x/RJ) are included, and are followed by jet and ambient parameters, including gas composition (XH2) and molecular weight (MWJ), initial total temperatures (TO), initial

total and static pressures (P_0 and P), and initial velocities (U). The measurements taken in the mixing region are listed with their axial locations under the heading "mixing survey." In most cases, four listings present the measurements of pitot and static pressure, gas samples composition and recovery temperature, all versus their radial location. As indicated earlier, the latter is indicated in two ways. The values of the coordinates Y and Z (or only one when the other is equal to zero) represent the location of the measurements in the cartesian frame of reference having its origin at the center of the cruciform holding the probes, the Z axis vertical and the Y axis horizontal. The value of the coordinate R is the radial distance of each measurement from the jet's actual axis of symmetry. Where applicable, the location of this axis was determined by reflection of diametrically opposed measurements.

A few of the tests listed in Appendix I do not show recovery temperature measurements. This is due to the fact that, under some testing conditions, the temperature probes used in the early tests responded unsatisfactorily to the temperature changes measured. Accordingly these early measurements have been deleted.

Table VI summarizes the values of the initial and reference parameters that define each test run. The Ludwig Tube test chamber pressure (P_{ref}) and temperature (T_{ref}) were recorded just prior to jet initiation.

The reference pressure was varied from run to run to obtain the desired match between jet and ambient pressures at the jet nozzle exit plane. In the ideal inviscid case, the jet pressure at the nozzle exit depends only on the jet supply pressure, and this was estimated prior to each test run. In practice, adjustments were necessary depending on the gas jet supply and on the nozzle used and necessitated by viscous effects, such as charge tube blockage and throttling shock displacement, which influence the performance of the double expansion Ludwig Tube jet supply. With the exception of two test cases using the $M_j = 2$ nozzle, reference pressure values between 1.5 and 2.0 psia were used. As discussed earlier, the Mach 2 nozzle, when used to generate low density jets, could not be started into an ambient having an equal pressure level.

Actual reference temperature values were recorded at the time of the tests. Their variation from test to test is negligible and the average value of 528°R was used in reducing the measurements. The actual jet composition (x_{H_2}) in units of mole fraction of hydrogen are indicated in column 3 of Table VII. The molecular weights in column 4 were computed from the known gas compositions.

The remaining columns of Table VII present actual run information. The values are averages taken over a specific time interval as indicated previously. The jet total temperature (T_{oj}) and pressure (P_{oj}) were measured in the nozzle plenum. Most of the experiments were made with the jet supply at ambient temperature prior to run commencement. For these, the T_{oj} indicated are at or near reference levels. In five cases the gas charge was heated, resulting in T_{oj} values from 650 to 750°R. The three levels of P_{oj} (approximately 260, 90 and 20 psi) indicated in column 6 of the table correspond to the three jet Mach numbers all having nearly the same exit pressures. The ambient or outer stream temperature (T_{oo}) and pressure (P_{oo}) were measured in the plenum of the CLT. The two levels discernible correspond to wind-on and no-wind test cases. The static pressures in the jet (P_j) and outer ambient (P_{oo}) were measured at the jet exit plane.

In Table VIII the values of the initial velocities of the jet (U_j) and the outer ambient (U_{oo}) are listed together with actual density ratios. All values in the table were computed from the nominal jet and ambient Mach numbers and the gas temperatures and compositions listed in Table VII using the relationships:

$$u = M \sqrt{\frac{\gamma R T_o}{1 + \frac{\gamma - 1}{2} M^2}} \quad (1)$$

$$\frac{p_{\infty}}{p_j} = \frac{MW_{\infty}}{MW_j} \frac{T_{oj}}{T_{o\infty}} \frac{1 + \frac{\gamma - 1}{2} M_{\infty}^2}{1 + \frac{\gamma - 1}{2} M_j^2} \quad (2)$$

4.2 BOUNDARY LAYER MEASUREMENTS

Different boundary layers developed on the internal surface of each of the nozzles used to generate the mixing jets. For each nozzle, differences were expected in the velocity profile of the boundary layer for low and high jet densities. In wind-on test cases, a boundary layer also develops on the external surface of the nozzles. These layers merge at the origin of the mixing region and influence its downstream development. The eight tests listed in Table V were selected to define the magnitudes and profiles of the boundary layers which affect the mixing measurements reported in the previous section. The surveys of pitot pressure that constitute the results of those tests are collected in Appendix II.

4.3 INFLUENCE OF DENSITY ON THE MIXING OF $M_j = 4$ JETS INTO $M_{\infty} = 2$ AMBIENT

When studying jet mixing, it is common to use the mean velocity profiles for a synthetic description of the flow behavior. However, in these experiments much relevant information was contained in the behavior of the primary flow variables themselves. Accordingly, the discussion here will cover the principal features of pitot pressure, composition or velocity observed in the surveys.

The radial distribution of gas composition for a case in which the jet and the outer stream had the same density is shown in Figure 28 at axial distances of 10 to 100 times the initial radius of the jet (run

numbers 1.8, 1.5 and 1.10). Good resolution of the regions of largest gradient were obtained together with measurements extending well into the outer nitrogen region. The jet had an initial composition of 61% hydrogen; a residual core is indicated at the 10 radii location. At $40 R_j$, the core has just ended. Downstream the maximum concentration on the axis did not decay very rapidly. At a location 60 radii from the nozzle (not shown in the figure) about 75% of the initial level was measured; at 100 radii it had decreased to 65% of the initial level. Spreading in the radial direction, as indicated by the point where essentially no hydrogen was measured, is seen to have moved from about 1.7 jet radii at the first axial survey to 2.7 jet radii at $40 R_j$ and to 4 jet radii at the last survey location.

A comparison of the data of figures 28 and 29 shows that the estimated centerline pitot pressure decays at a faster rate than the corresponding centerline H_2 fraction. The centerline pitot pressure and H_2 mole fraction decrease to 36% and 66% of the initial values, respectively, at a distance of 100 jet radii downstream of the nozzle exit plane. The radial profile of measured pitot pressure shows a distinct change in the way the pitot pressure varies between the centerline and external stream as a function of the proximity to the nozzle exit plane. At 10 nozzle radii downstream the pitot pressure profile shows a local minimum at 1.6 jet radii off-axis. This corresponds to the radial position of the theoretical slipline between the jet and external stream which also corresponds somewhat to the steep gradient in H_2 mole fraction shown in figure 28. The region of low pitot pressure shifts outward radially at the same rate that the jet spreads. The value of minimum pitot pressure increases as the flow proceeds downstream until the deficit disappears at about the 60 nozzle radii axial position.

Static pressure profiles and a temperature survey associated with this flowfield are listed in the appendix. The static pressure remained fairly constant throughout the flow region, but some moderate deviations were concentrated near the jet axis. The temperature behavior measured in test run 2.37

is typical of that expected in all wind-on tests with the jet discharging from initial ambient temperature. The jet recovery temperature on its axis is about 60°F above that of the outer stream. The difference occurs because in the supply tube of the outer stream the gas is expanded and accelerated to a higher velocity from the same initial temperature. The outer stream supply operates at a Mach number of 0.35, while the jet supply operates at a Mach number of 0.07. In accordance with the theoretical relationships¹⁴ which describe the Ludwig Tube operation, a lower total temperature is obtained for the supply gas flowing at higher Mach number. A consequence of the recovery temperature difference between jet and outer stream is that a radial survey in the mixing region shows a gradual decrease of temperature off-axis approaching the constant level of the outer stream.

How these measurements are combined into velocity variations describing the near field to far field mixing is shown in Figure 30. At the axial location of $10 R_j$, the core velocity of 3400 fps was constant for just under one jet radius. Approximately 0.7 radii further off-axis the velocity had dropped to a minimum, 16% below the level of the outer stream. The level of the outer stream was reached at about four radii off-axis. At the $40 R_j$ axial location the centerline velocity was 200 fps below the core level and dropped to the level of the outer stream in a distance of about two radii. A residual velocity defect of about 5% below the outer stream occurred at 2.1 radii off-axis.

Between the $60 R_j$ and the $100 R_j$ locations the velocity at the jet centerline decayed more gradually. At $60 R_j$, the velocity defect is barely detectable at about three radii off-axis. At the $100 R_j$ location the velocity decreased monotonically from the centerline value of 2500 fps to the level of the outer stream. The behavior of the velocities shown in Figure 30 corresponds qualitatively to the expectations for mixing jets. The velocity defect, found in the data of Figure 30 as well as in the data from other test conditions, is attributed to the persisting effect of the boundary layers which develop on the internal and external surfaces of the jet nozzle. The observed values of

minimum velocity and their location in the mixing region are consistent with the indications obtained from simple calculations based on an estimate of the initial boundary layers.

The above case with its uniform density is an appropriate baseline against which the influence of density variations can be determined. This was done, for example, in Figure 31 where radial velocity distributions at axial location $40 R_j$ are compared for ρ_∞/ρ_j values of 0.6, 1.0, 3.0 and 9. Best fit lines through the data points are used for clarity in the figure. The observations that follow, however, are firmly based on the actual measurements tabulated in the appendix. Starting with the higher jet density ($\rho_\infty/\rho_j = 0.6$), the velocity distribution retains all the characteristics of the uniform density case. In particular, the outer stream level was reached essentially at the same off-axis location and with a velocity defect present, although the velocity defect extended further off-axis. The initial velocity of the jet was 26% lower than the uniform density case, thus a more gradual drop in the radial direction characterizes this velocity profile.

The two jets with density lower than the outer stream ($\rho_\infty/\rho_j = 3.0$ and 9) displayed characteristics which were different than those of the uniform density case. In both, a region of constant core velocity extending a half radius appears to have been present. In the jet having $\rho_\infty/\rho_j = 3$, the velocity defect has been washed out completely. This may be attributed to the large difference in velocity between the jet axis and the outer stream. The inner stream reached the velocity of the outer ($M_\infty = 2$) stream at about three radii off-axis. The velocity defect was also absent in the case of the jet having $\rho_\infty/\rho_j = 9$. In addition, the inner stream reached the outer stream velocity further off-axis, about 3.5 radii from the centerline.

The relationship of pitot pressure and gas composition to the velocity differences evident in Figure 31 is quite interesting. The data in the appendix indicate that there are moderate differences in the radial distribution of pitot pressure among jets of different densities and, in fact,

such differences are opposite to those present in the velocities. This means that at a fixed radial location, a lower pitot pressure is associated with the $\rho_\infty/\rho_j = 9$ case and a higher one with the $\rho_\infty/\rho_j = 0.6$ case. As a consequence, the velocity is directly related to the local jet composition. In the cases of interest here, the density of the jets was controlled by varying the initial H_2 fraction from about 20% to 100%. However, this initial difference in composition did not alone account for the higher velocities off-axis. For example, at 3 inches from the jet axis the ratio of local-to-core H_2 fraction was zero for the $\rho_\infty/\rho_j = 0.6$ case but about 40% for the $\rho_\infty/\rho_j = 9$ case. Higher velocities occurred in the latter case as a consequence. Thus, at a fixed number of radii downstream from their origin, the less dense jets penetrated farther into the outer stream. This indicates that a greater level of turbulent mixing is associated with the lower density jet.

The influence of density of $M_j = 4$ jet cases is summarized by the measured axial decays of centerline jet composition presented in Figure 32. At each axial station shown, the centerline H_2 fraction, $(X_{H_2})_C$, was normalized by the initial level in the core, $(X_{H_2})_{CO}$, and plotted against axial distance on a logarithmic scale. In this format the variation of centerline jet composition is approximated well by straight lines through the data points. The figure shows that the decay slope does not differ significantly among different jet densities. Figure 33 presents core lengths estimated from the foregoing data by extrapolating the slope of the decay to the measured core composition for each test case. The somewhat surprising result that core length is nearly independent of density ratio is indicated in the figure. A core length markedly increasing with decreasing ambient-to-jet density ratio was expected based on the qualitative consideration that denser jets would be able to penetrate farther into the surrounding ambient. These expectations were quantitatively supported by pretest calculations. Uncertainties have been estimated for each data point, but their magnitude does not alter the basic conclusion drawn from the results.

4.4 INFLUENCE OF DENSITY ON THE MIXING OF $M_j = 3$ JETS INTO STILL AMBIENT

As in the case of $M_j = 4$ jets discharging into the $M_\infty = 2$ outer stream, a baseline description of the flowfield was established for $M_j = 3$ jets discharging into the still ambient by surveying one test case at four axial locations downstream of the nozzle exit plane. Here again the case of a jet matching the ambient density was selected as the baseline. Only surveys at axial station $60 R_j$ were possible within the scope of the program to characterize the effects of variations in the value of ρ_a/ρ_j . As a consequence, the final interpretation of the measurements for this no-wind set of test cases must rely on theoretical calculations to bridge the gaps in the available data. However, three main observations are warranted at the present stage.

First, the sequence of surveys taken for the uniform density case in test runs 2.33, 2.19, 2.34 and 2.6 provided data for an estimate of the core length. This was done using the procedure based on the known core level and the measured rate of axial decay. For these test runs, a core length extending about $17 R_j$ downstream of the nozzle was obtained. Thus, the first axial station ($x = 20 R_j$) where a radial survey of the flow variables could be made was outside the core. The measurements are shown in Figure 34. The jet width, based on the pitot pressure measurements, is about 4 inches; however traces of H_2 appear to have diffused 1.5 inch farther and into the surrounding nitrogen. Corresponding measurements at $x = 60 R_j$ indicated that the jet extended about 10 inches off-axis at that point, and the H_2 fraction on the jet axis had dropped to 53% of the core level while the maximum pitot pressure was about one third of the core level.

Second, the same sequence of surveys indicated that the axial rate of decay of jet core composition was only moderately steeper than in the case of a $M_j = 4$ jet discharging in the $M_\infty = 2$ outer stream with density matched (Section 4.3).

Third, the measurements at $x = 60 R_j$ for jets having ρ_a/ρ_j values of 0.6, 2 and 6 provided an estimate of the influence of jet density on core length. (Test run 2.53, 2.51 and 2.52 data in Appendix I contain these

measurements). The estimate was based on the assumption that under these conditions the axial rate of core decay was again negligibly affected by density variations. Core lengths that increase as the jet densities decrease were found. At $\rho_\infty/\rho_j = 6$ this effect resulted in a core length more than 50% longer than in the uniform density case.

4.5 INFLUENCE OF MACH NUMBER ON THE MIXING OF HIGH DENSITY AND OF LOW DENSITY JETS

Data for high density jets ($\rho_\infty/\rho_j = 0.6$) discharging into a still ambient were collected at three different Mach numbers in eight tests: for the $M_j = 4$ jet, surveys were taken at axial distances of 60 and 80 radii in test runs 2.54 and 2.47; for the $M_j = 3$ jet, at the same axial distances in test runs 2.53 and 2.50; and in the case of the $M_j = 2$ jet, at four axial distances from 20 to 100 radii downstream of the nozzle in test runs 2.4, 2.41, 2.21 and 2.28. These data are sufficient for (a) comparing jet spreading at mid and far field, (b) comparing core decay rates, and (c) estimating core lengths. Only observations relative to the last two will be made here.

The above data at different Mach number and fixed ambient-to-jet density ratio were first utilized to determine and compare the rates of decay in the centerline hydrogen content from the initial core value. At each axial station surveyed the centerline value of X_{H_2} was taken, normalized by the core value, and plotted against axial distance using semi-logarithmic scales as done earlier in Figure 32. In this format the axial decay of the maximum hydrogen content in the mixing jets is well represented by a straight line through the data points. Comparing the slope of these axial decay lines it is found that their value is similar in the case of Mach 4 and 3 jets, but that in the Mach 2 case the slope is steeper. The Mach 2 slope is based on the combined data at $X = 20, 40$ and $60 R_j$. A second anomaly in the $M_j = 2$ results is that the gas sampling at $X = 100 R_j$ indicated a level of H_2 content that is unchanged from the level measured at the preceding station ($60 R_j$). Since a well defined radial profile is present in the data, this last anomaly may be explained by uncertainty in the absolute level. This may be caused by the very low values of H_2 measured.

To determine the influence of Mach numbers on core lengths, their values were estimated by extrapolating the H_2 decay lines to the known initial jet composition. The data at Mach 4 and 3 verify the expected result of a longer core length for the jet having higher velocity. Specifically the core length of the $M_j = 4$ jet is found to be 21 jet radii long. The core length of the $M_j = 4$ jet extends $38 R_j$. The data at the Mach number of 2 are again anomalous. Figure 35 shows the radial distribution of H_2 at the axial station $x = 20 R_j$. A residual core is clearly indicated. The data are extremely well behaved and delineate a well defined radial profile even at these low H_2 concentrations. However, the core length indicated in the figure is inconsistent with the one measured for the $M_j = 3$ case because the initial velocity of the $M_j = 3$ jet is 60% higher than that of $M_j = 2$ jet.

Data for low density jets ($P_0/p_i = 10$) discharging into a $M_\infty = 2$ outer stream were collected at three different Mach numbers in eleven tests: for the $M_j = 4$ jet, surveys were taken at axial distances of 20, 40, 60 and 100 radii; for the $M_j = 3$ jet, at the same axial distances; and for the $M_j = 2$ jet, at 4, 80 and 100 radii downstream of the nozzle. The measurements provided a fairly complete data set which, for the purpose of this report, was examined to determine core length and rate of core decay.

The data collected at Mach numbers of 4 and 3 again show similar rates of axial decay in centerline jet composition. The core length of the $M_j = 3$ jet was estimated to be 30 jet radii long while the $M_j = 4$ jet, which had an initial velocity 26% higher, penetrated farther into the outer flow with a core that extended about 45 radii. The $M_j = 2$ data offered ambiguous results that have not been resolved.

The tests completed in these experiments include other cases whose data could be applied in an investigation of the influences of Mach number on the mixing. For example, two rather complete surveys of uniform density were completed for no-wind cases with jet Mach numbers of 4 and 3. Other comparisons could be made with the aid of calculations to bridge differences in the location of survey positions or jet density. These investigations could not be accommodated within the practical constraints imposed by the original program scope and by the larger than anticipated development difficulties. However, the results are fully documented and available for further analysis by the author or other investigators.

Section 5

CONCLUSIONS

In support of AFRPL-sponsored low-altitude plume research, the turbulent mixing of supersonic jets has been experimentally investigated at jet Mach numbers of 4, 3 and 2, and with six values of the ambient-to-jet density ratio in the range of 0.6 to 10. A comprehensive data base has been created that encompasses thirteen test conditions and detailed radial surveys of pressure, temperature and gas composition taken at axial locations within 0 to 100 jet radii downstream of the exit plane. The data base will be useful in the selection and validation of turbulence model compressibility corrections to be used in the JANNAF Standard Plume Flowfield Model (SPF). In addition, the data indicates important trends in the mixing characteristics as jet density and Mach number are varied.

For pressure ranges from 50 to 2 psia, temperature ranges from 700 to 470°R, and H_2/N_2 gas mixtures from 100% H_2 to a few percent H_2 , well resolved measurements of radial profiles of pitot and static pressure, recovery temperature and gas composition have been obtained. Velocity profiles can be calculated from this data and a few examples are presented. Data scatter and uncertainties are, in general, well below the uncertainty level needed to provide a definitive determination of the desired mixing characteristics. However, the data obtained with the $M_j = 2$ jets are less satisfactory in this respect. A few unresolved anomalies are present in these test cases and use of their data should be approached with caution.

The analysis of the data leads to several significant results:

(A) With regard to the influence of density on the mixing of $M_j = 4$ jets into the $M_\infty = 2$ outer stream:

1. The region of the mixing jet where a core is present is only weakly dependent on the ambient-to-jet density ratio. The core length is nearly constant and extends over a distance of about 40 jet radii.

2. Well defined regions of velocity defect are present when the jet's density is below or equal to the level of the surrounding ambient. This feature of the mixing disappears at higher jet densities.
3. In the mixing region which lies beyond the end of the core, the axial rate of decay in the composition of the jet is nearly independent of the density ratio.

(B) With regard to other test cases and to the influence of jet Mach number:

1. The measurements well define the important relationship of local species concentration to the spreading of the mixing region.
2. In the case of $M_j = 3$ jets discharging into the still ambient, the core length increases as the jet density is decreased and, correspondingly, the initial jet velocity is increased. Values of 15 and 25 jet radii were measured respectively at ambient-to-jet density ratios equal to 0.6 and 6.0.
3. Increasing jet Mach number from 3 to 4 results in an increased core length from 21 to 38 jet radii in the case of high density jets ($\rho_\infty/\rho_j = 0.6$) discharging into the still ambient and from 30 to 45 jet radii in the case of low density jets ($\rho_\infty/\rho_j \approx 10$) discharging into the $M_\infty = 2$ outer stream.

The short-duration technique used to simulate low altitude plume flowfields has been successfully applied in this investigation of nonreacting jets. The jet apparatus is capable of varying gasdynamic parameters over a broad range and validity of the fast response diagnostics has been proven. The short-duration technique represents an effective and reliable tool for investigating fundamental plume phenomena.

REFERENCES

1. Dash, S.M., Pergament, H.S., and Thorpe, R.D., "The JANNAF Standard Plume Flowfield Model-Modular Approach and Preliminary Results", JANNAF 11th Plume Technology Meeting, Huntsville, AL, May 1979.
2. Schetz, J.A., "Injection and Mixing in Turbulent Flow", *Progress in Astronautics and Aeronautics*, Vol. 68, 1980.
3. "Free Turbulent Shear Flows", Vol. 1 - Conference Proceedings, Vol. 2 - Summary of Data, NASA SP-321, NASA Langley Research Center, 1972.
4. Padova, C., "Non-Reacting Turbulent Mixing Experiments - Phase II - Test Engineering Report. Supplement No. 1 - Data Plots", Calspan Report No. 6632-A-2, September 1982.
5. Wittliff, C.E., Wurster, W.H. and Marrone, P.V., "Non-Reacting Supersonic Mixing Experiments", Calspan Technical Memorandum submitted to AFRPL, May 1978.
6. Wurster, W.H., "Supplementary Discussions on Non-Reacting Supersonic Mixing Measurements Program", Calspan Technical Memorandum submitted to AFRPL, September 1978.
7. Sheeran, W.J., Hendershot, K.C., and Wilson, H.E., "Applications of a Tube Wind Tunnel in Supersonic Testing", AIAA Paper No. 69-335, Presented at AIAA 4th Aerodynamic Testing Conference, Cincinnati, Ohio, April 1969.
8. Sheeran, W.J. and Hendershot, K.C., "A Tube Wind Tunnel Technique for Rocket Propulsion Testing", Journal of Spacecraft and Rockets, Vol. 7, No. 8, pp. 1008-1010, August 1970.
9. Ludwig, H., "The Tube Wind Tunnel - A Special Type of Blowdown Tunnel", AGARD Report 143, July 1957.
10. Johnson, C.B., Boney, L.R., Ellison, J.C. and Erickson, W.D., "Real-Gas Effects on Hypersonic Nozzle Contours with a Method of Calculation", NASA TN D-1622, April 1963.
11. Bontrager, P.J., "Development of Thermocouple-Type Total Temperature Probes in the Hypersonic Flow Regime", AEDC-TR-69-25, 1969.
12. Padova, C. and Wurster, W.H., "Non-Reacting Turbulent Mixing Experiments Phase O, Test Report", August 1981.
13. Padova, C., "Non-Reacting Turbulent Mixing Experiments - Phase I/81 Data Package and Supplement", November and December 1981.
14. Cable, A.J., and Cox, R.N., "The Ludwig Pressure Tube Supersonic Wind Tunnel", *Aero. Quart.*, May 1963.

TABLE I
NOZZLE COORDINATES

M = 2 Nozzle		M = 3 Nozzle		M = 4 Nozzle	
X	Y	X	Y	X	Y
0	1.1545	0	0.7290	0	0.4585
.050	1.1550-	0.050	0.7295	0.050	0.4590
.100	1.1550+	0.100	0.7305	0.100	0.4600
.150	1.1555	0.150	0.7325	0.150	0.4625
.200	1.1565	0.200	0.7350	0.200	0.4655
.250	1.1570	0.250	0.7380	0.250	0.4690
.300	1.158	0.300	0.742	0.300	0.4735
.400	1.160	0.400	0.751	0.400	0.4840
.500	1.163	0.500	0.762	0.500	0.4955
.600	1.167	0.600	0.775	0.600	0.5085
.700	1.171	0.700	0.789	0.700	0.522
.800	1.175	0.800	0.803	0.80	0.536
.900	1.179	0.900	0.819	0.90	0.551
1.000	1.184	1.00	0.835	1.00	0.566
1.250	1.197	1.25	0.875	1.25	0.604
1.500	1.210	1.50	0.914	1.50	0.642
1.750	1.223	1.75	0.954	1.75	0.680
2.000	1.236	2.00	0.994	2.00	0.718
2.500	1.263	2.25	1.033	2.25	0.756
3.000	1.289	2.50	1.072	2.50	0.794
3.500	1.315	3.00	1.142	2.75	0.831
4.000	1.341	3.50	1.204	3.00	0.869
4.500	1.367	4.00	1.259	3.25	0.905
5.000	1.393	4.50	1.309	3.50	0.941
5.500	1.420	5.00	1.351	3.75	0.976
6.000	1.443	5.50	1.388	4.00	1.009
6.500	1.463	6.00	1.419	4.50	1.073
7.000	1.478	6.50	1.443	5.00	1.132
7.500	1.489	7.00	1.463	5.50	1.185
8.000	1.496	7.50	1.478	6.00	1.233
8.250	1.4990	8.00	1.488	6.50	1.276
8.500	1.4995	8.50	1.495	7.00	1.314
8.708	1.5000	9.00	1.499	7.50	1.347
		9.50	1.500	8.00	1.376
				8.50	1.401
				9.00	1.422
				9.50	1.440
				10.00	1.455
				10.50	1.467
				11.00	1.476
				11.50	1.484
				12.00	1.490
				12.50	1.494
				13.00	1.496
				13.50	1.498
				14.00	1.499
				14.50	1.500

Table II
SPECIFICATIONS FOR HYDROGEN/NITROGEN GAS MIXTURES

RANGE OF MINOR COMPONENT	PREPARATION TOLERANCE	CERTIFICATION ACCURACY
10% TO 50%	± 5% OF COMPONENT	2% OF COMPONENT
.005% TO 10%	± 10% OF COMPONENT	2% OF COMPONENT

- **CONCENTRATIONS ARE SPECIFIED IN VOLUME PERCENT**
- **COMPONENT CERTIFICATION BASED ON NBS TRACEABLE STANDARDS**

Table III
MATRIX^a OF TEST CASES

M	M _j	ρ_{∞}/ρ_j	MW _j	T _{oj} (°R)	GAS COMPOSITION (% H ₂ , BALANCE N ₂)
0	3	0.6	15.12	528	49.6
↓	↓	1.0	10.29	↓	68.2
↓	↓	2.0	5.397	↓	87.0
↓	↓	6.0	2.016	650	100.0
↓	2	0.6	25.89	528	8.19
↓	↓	1.0	12.21	↓	60.8
↓	↓	2.0	6.047	↓	84.5
2	↓	0.6	22.01	↓	23.1
↓	↓	1.0	13.64	↓	55.3
↓	↓	3.0	4.642	↓	89.9
↓	↓	9.0	2.016	750	100.0
↓	2	10.0	3.212	528	95.4
↓	3		2.016	↓	100.0

^aCONDITIONS INTO WHICH THE JETS EXHAUST WERE:

T_{o∞} = 470°R, MW = 28, FOR WIND-ON CASES (M_∞ = 2)

T_{o∞} = 523°R, MW = 28, FOR NO-WIND CASES (M_∞ = 0)

Table IV
COMPLETED DATA POINTS

		$\frac{x}{R_j} = 100$	80	60	40	20	10
$M_j = 4$							
NO-WIND ρ_∞/ρ_j	$= 0.6$		2.47	2.54			
	$= 1.0$	2.1		2.36	1.6		1.7
WIND-ON	$= 0.6$	2.14			2.18		
	$= 1.0$	1.10		2.37	1.5		1.8
	$= 3.0$		2.48	2.38	2.16	2.24	
	$= 9.0$	1.11		2.39	2.17	2.25	
$M_j = 3$							
NO-WIND ρ_∞/ρ_j	$= 0.6$		2.50	2.53			
	$= 1.0$	2.6		2.34	2.19	2.33	
	$= 2.0$			2.51			
	$= 6.0$			2.52			
WIND-ON	$= 10.0$	2.7		2.35	2.20	2.32	
$M_j = 2$							
NO-WIND ρ_∞/ρ_j	$= 0.6$	2.9		2.41	2.21	2.28	
WIND-ON	$= 10.0$	2.11		2.40		2.31	

TABLE V
DATA POINTS SURVEYING THE NOZZLE BOUNDARY LAYERS

Nozzle	P_{∞}/P_j	Boundary Layer Surveyed <u>Internal</u>	<u>External</u>
$M_j = 4$	1.0	01.9	
	↓	2.46	2.46
	3.0	1.12	
	10.0	1.13	
$M_j = 3$	1.0	2.44	
	10.0	2.45	2.45
$M_j = 2$	0.6	2.42	
	10.0	2.43	2.43

Table VI
MEASURED NOZZLE PARAMETERS

NOMINAL		MEASUREMENTS			
MACH NO.	P_j/P_oj	P_j/P_oj		MACH NO.	
		AVERAGE	STAND. DEV. (%)		
2	0.1278	0.0753	8.4	2.34	$\pm .06$
3	0.0272	0.0210	7.1	3.17	$\pm .04$
4	0.00659	0.00622	9.1	4.04	$\pm .06$

TABLE VII

INITIAL AND REFERENCE PARAMETERS FOR THE MIXING MEASUREMENTS

Run	P _{ref} (psia)	xH ₂	MW _j	T _{oj} (°R)	P _{oj} (psi)	P _j (psi)	T _{o60} (°R)	P _{o20} (psi)	P _∞ (psi)
1.5	1.55	.608	12.210	532	268.5	.1780	472	11.7481	.4308
1.6	1.61	.845	6.047	535	260.7	.0242	528	9.0	.0081
1.7	1.59	.845	6.047	536	265.4	.0686	↓	0.0	.0105
1.8	1.68	.608	12.210	532	263.2	.2058	472	13.110	.2826
1.10	1.64	.608	12.210	529	275.4	.2372	472	11.5340	.3187
1.11	1.62	1.0	2.016	751	249.1	-.0935	↓	11.4252	.2806
2.1	1.55	.945	6.047	537	264.3	.0381	528	0.0	0.0
2.6	1.99	.682	10.285	525	87.67	.0213	↓	↓	-.0132
2.7	1.76	1.0	2.016	521	81.13	-.1270	472	11.4982	.0301
2.9	1.72	.082	25.888	528	9.363	-.0193	528	0.0	-.0049
2.11	1.64	.954	3.212	528	19.034	.0590	472	11.7269	.3324
2.14	1.66	.231	22.013	523	245.5	.2823	↓	11.5190	.2616
2.16	1.76	.899	4.642	533	236.0	-.2138		12.1382	.1832
2.17	1.86	1.0	2.016	737	234.0	-.1882		11.8693	.0502
2.18	1.80	.231	22.013	525	245.8	.1631	↓	11.6699	.1721
2.19	1.91	.682	10.285	526	81.22	.1110	528	0.0	-.0228
2.20	1.78	1.0	2.016	528	84.68	.0514	472	11.8232	.0251
2.21	1.66	.082	25.888	515	9.526	-.7835	528	0.0	-.0013
2.24	1.60	.899	4.642	534	236.1	-.0756	472	11.8687	.3108
2.25	1.52	1.0	2.016	712	219.5	.0620	↓	11.1244	.2109
2.28	1.60	.082	25.888	505	20.234	-.0636	528	0.0	0.0
2.31	.09	.954	3.212	531	21.514	1.2888	472	11.4827	1.6112

T_{ref} = 528°R in all cases.

TABLE VII (Cont'd)
INITIAL AND REFERENCE PARAMETERS FOR THE MIXING MEASUREMENTS

Run	P _{ref} (psia)	xH ₂	MW _j	T _{oj} (°R)	P _{oj} (psi)	P _j (psi)	T _{o∞} (°R)	P _{o∞} (psi)	P _∞ (psi)
2.32	1.80	1.0	2.016	528	89.67	.0550	472	11.2425	-.0764
2.33	1.79	.682	10.285	522	80.43	.0014	528	0.0	-.0165
2.34	1.82	.682	10.285	522	81.87	-.0161	528	0.0	-.0275
2.35	1.80	1.0	2.016	523	85.56	-.0306	472	11.2159	-.1557
2.36	1.62	.810	6.957	533	270.0	.0206	528	0.0	.0025
2.37	1.60	.553	13.640	532	242.67	.1426	472	9.9815	.0107
2.38	1.60	.899	4.642	534	238.5	-.0997	↓	9.9529	-.0845
2.39	1.61	1.0	2.016	709	238.2	.0138	↓	9.9460	-.0703
2.40	.027	.954	3.207	534	22.274	1.6367	↓	11.4262	1.7315
2.41	1.62	.082	25.890	508	18.014	-.0338	528	0.0	-.0050
2.47	1.84	.608	12.210	533	267.21	-.0782	528	0.0	-.0318
2.48	1.65	.899	4.642	534	274.3	-.1424	472	9.8191	-.0312
2.50	1.75	.496	15.122	523	85.44	.1038	528	0.0	-.0143
2.51	1.81	.870	5.397	524	89.75	-.0931	↓	↓	-.0012
2.52	1.82	1.0	2.016	652	87.77	-.0713	↓	↓	.0221
2.53	1.81	.496	15.122	520	89.81	.0469	↓	↓	-.0068
2.54	1.85	.608	12.210	532	275.9	-.0900	↓	↓	.0087

T_{ref} = 528°R in all cases.

TABLE VIII
INITIAL VELOCITIES AND ACTUAL DENSITY RATIOS
FOR THE MIXING MEASUREMENTS

Run	u_j (fps)	u_∞ (fps)	ρ_∞/ρ_j
1.5	3400.	1614.	0.99
1.6	4845.	0.	1.12
1.7	4849.	↓	1.12
1.8	3400.	1614.	0.99
1.10	3390.	↓	0.99
1.11	9940.	↓	8.47
2.1	4854.	0.	1.12
2.6	3380.	↓	0.97
2.7	7605.	1614.	9.86
2.9	1776.	0.	0.60
2.11	5043.	1614.	9.76
2.14	2510.	↓	0.60
2.16	5519.	↓	2.92
2.17	9847.	↓	9.30
2.18	2515.	↓	0.61
2.19	3383.	0.	0.97
2.20	7656.	1614.	10.00
2.21	1754.	0.	0.59
2.24	5524.	1614.	2.93
2.25	9679.	↓	8.99
2.28	1737.	0.	0.58
2.31	5057.	1614.	9.81
2.32	7656.	↓	10.00
2.33	3370.	0.	0.96
2.34	3370.	↓	0.96
2.35	7620.	1614.	9.90
2.36	4508.	0.	0.97
2.37	3216.	1614.	0.99
2.38	5524.	↓	2.93
2.39	9658.	↓	8.95
2.40	5075.	↓	9.88
2.41	1742.	0.0	0.58
2.47	3403.	↓	0.55
2.48	5524.	1614.	2.93
2.50	2782.	0.0	0.66
2.51	4662.	↓	1.84
2.52	8508.	↓	6.13
2.53	2774.	↓	0.65
2.54	3400.	↓	0.55

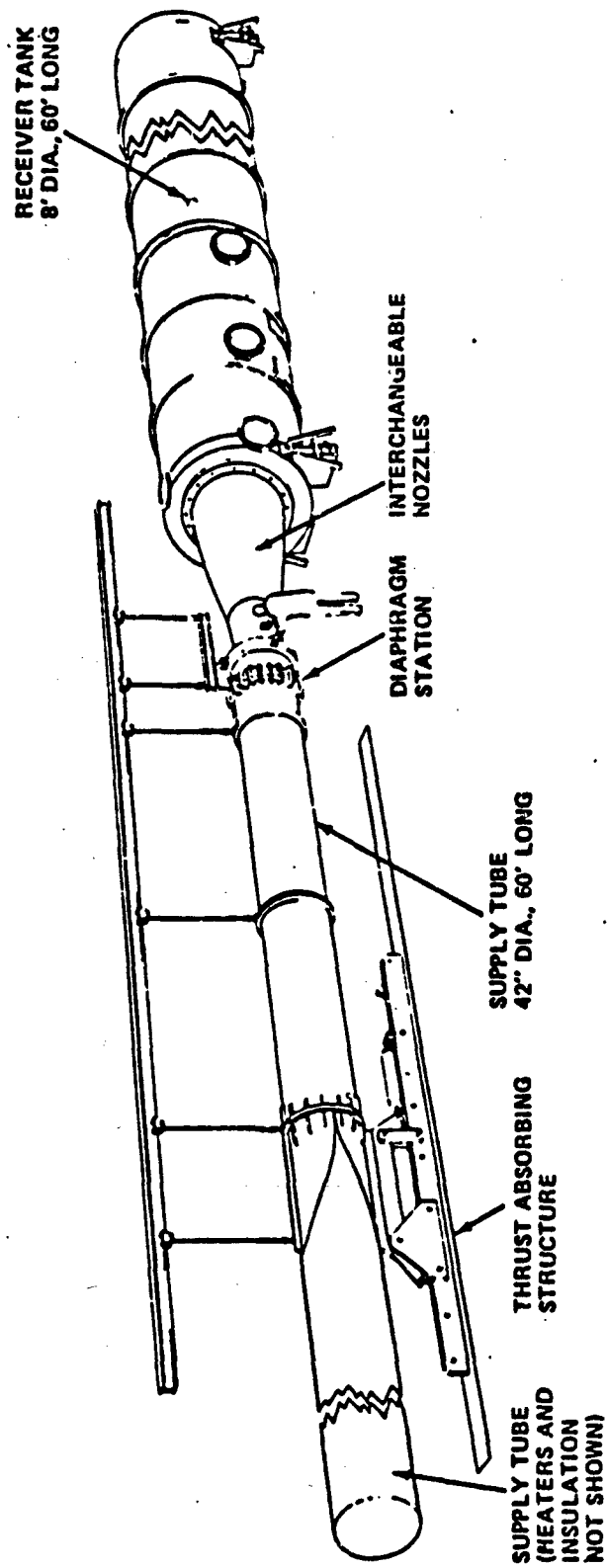


Figure 1 CALSPAN LUDWIG TUBE WIND TUNNEL

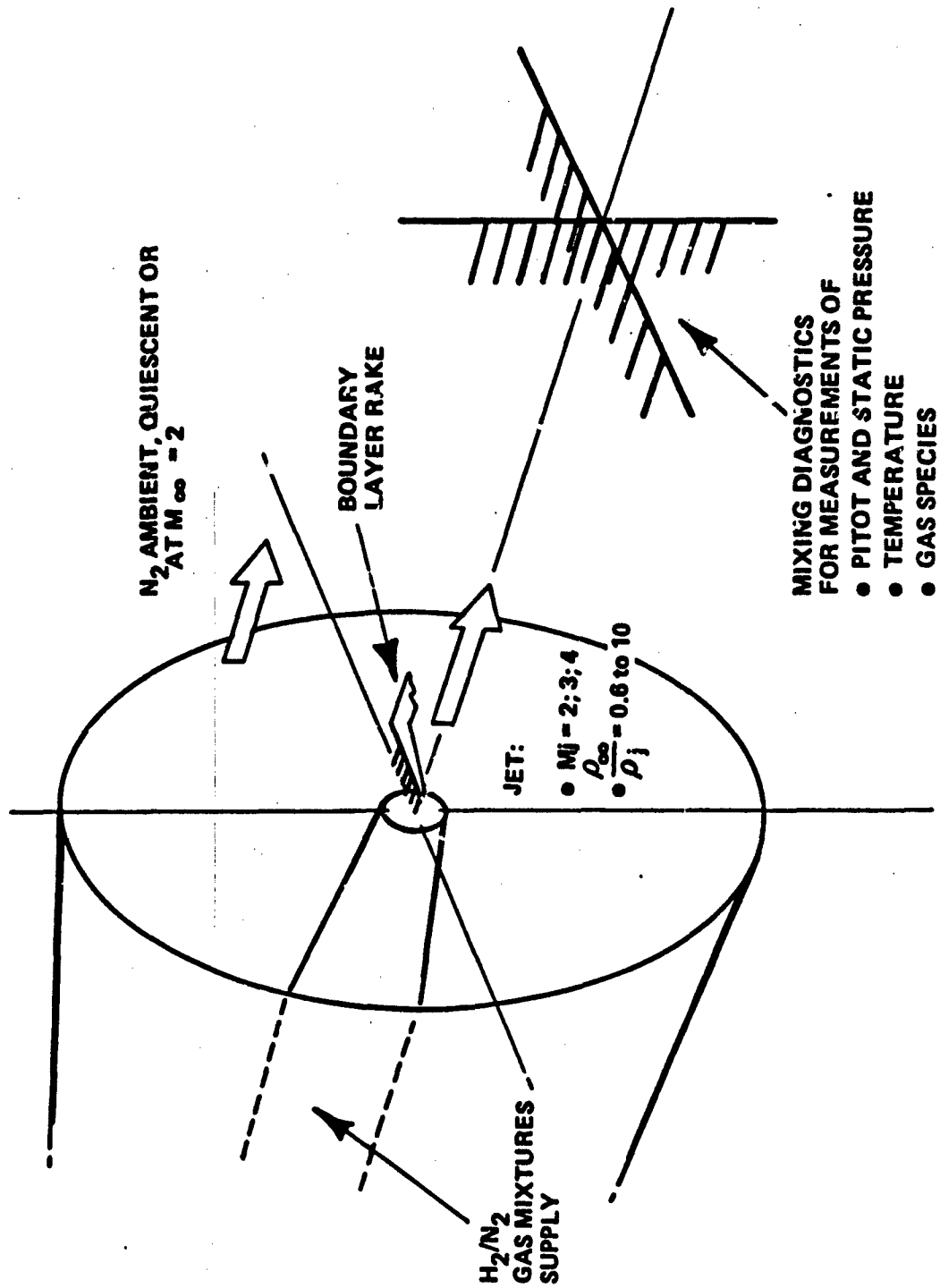


Figure 2 SCHEMATIC OF JET MIXING EXPERIMENT

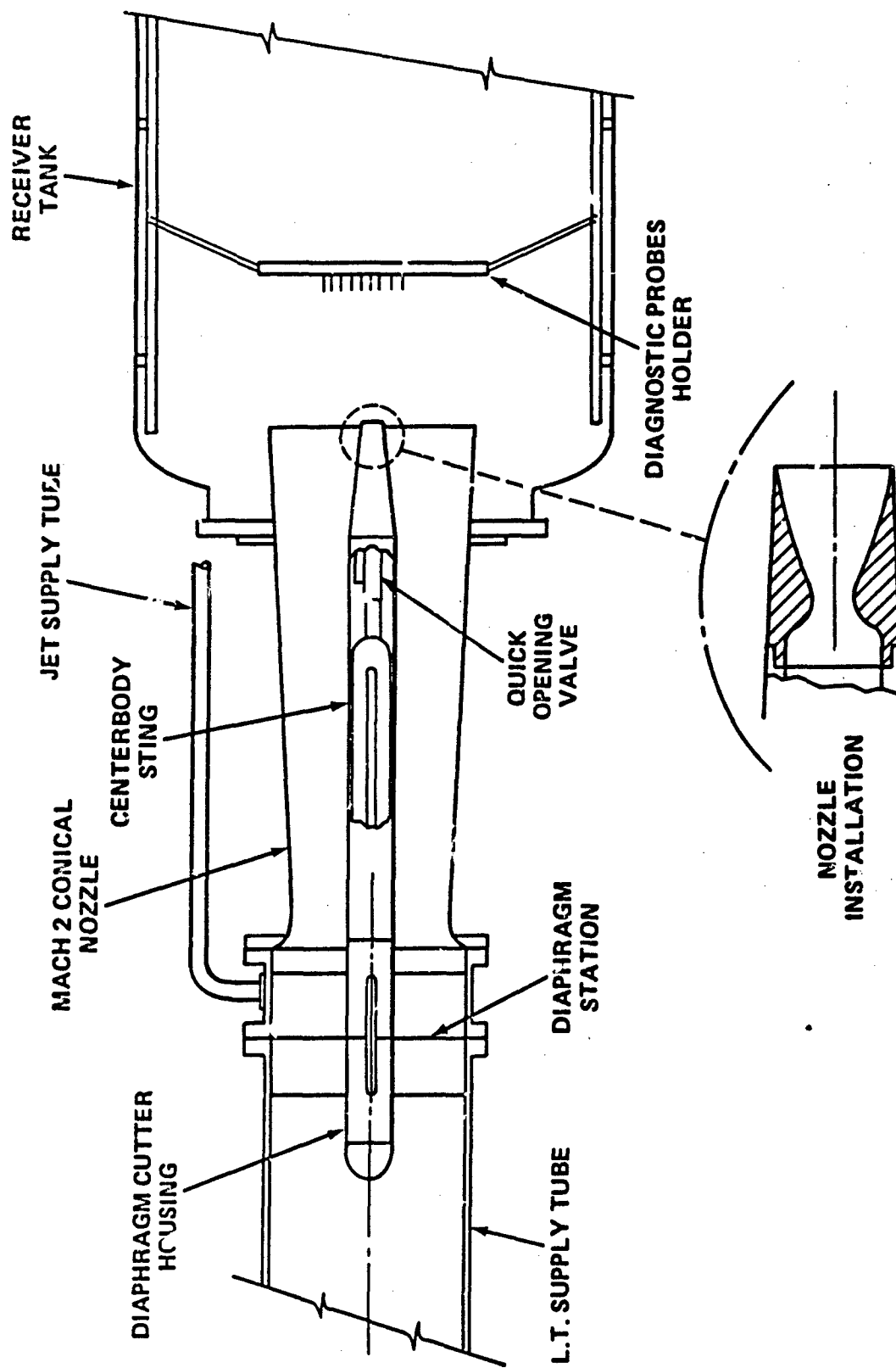
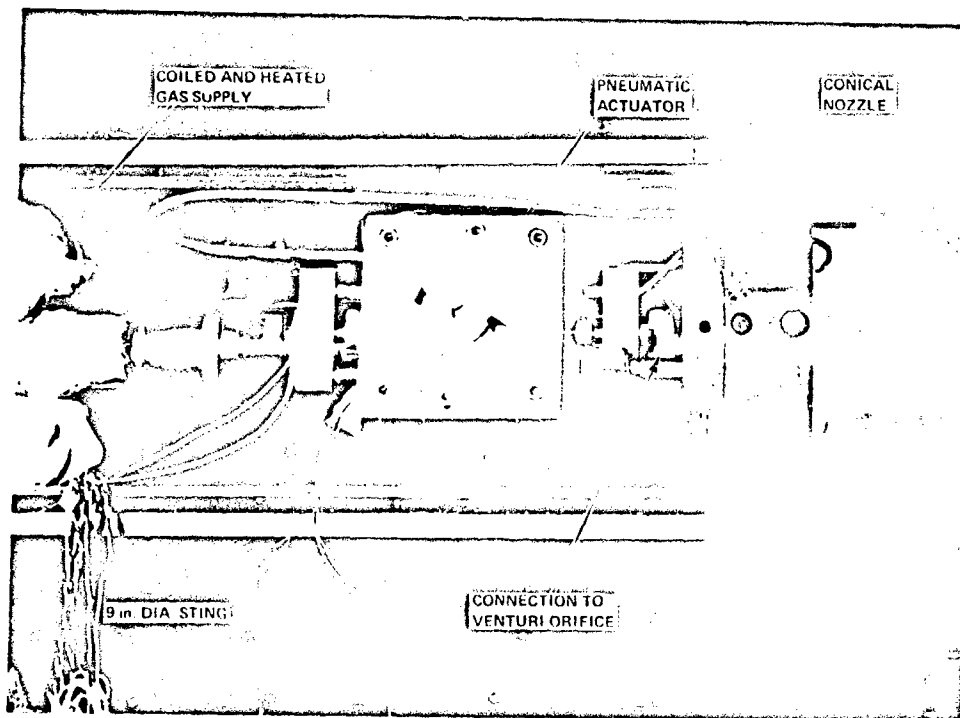
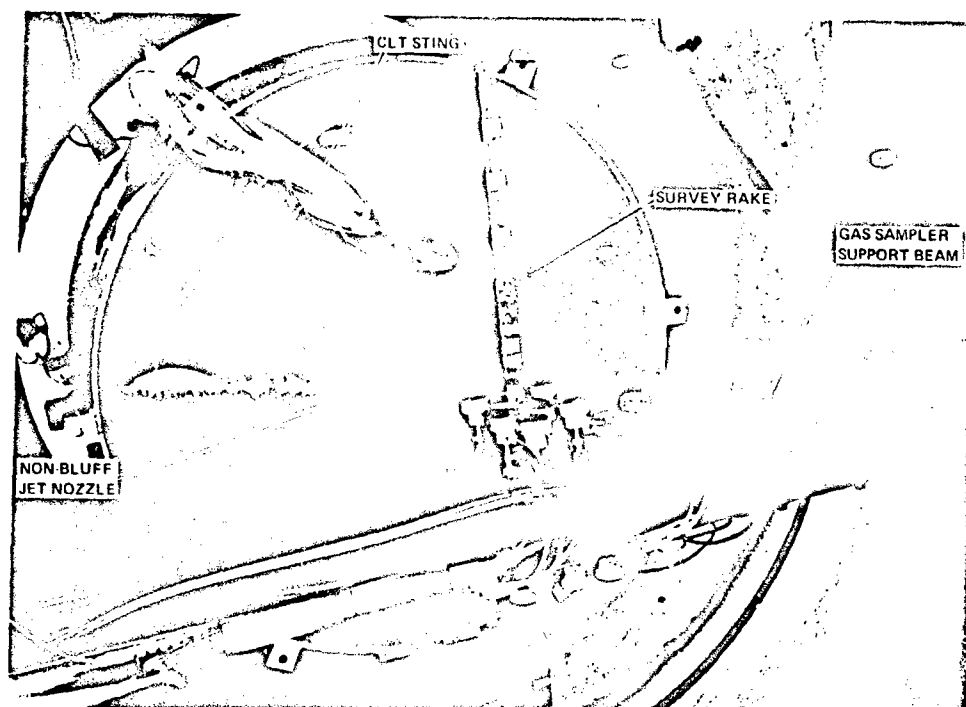


Figure 3 LUDWIG TUBE FACILITY CONFIGURATION FOR TURBULENT MIXING EXPERIMENTS



(a) GAS SUPPLY AND PNEUMATIC ACTUATOR



(b) JET MODEL

Figure 5 VIEWS OF THE APPARATUS

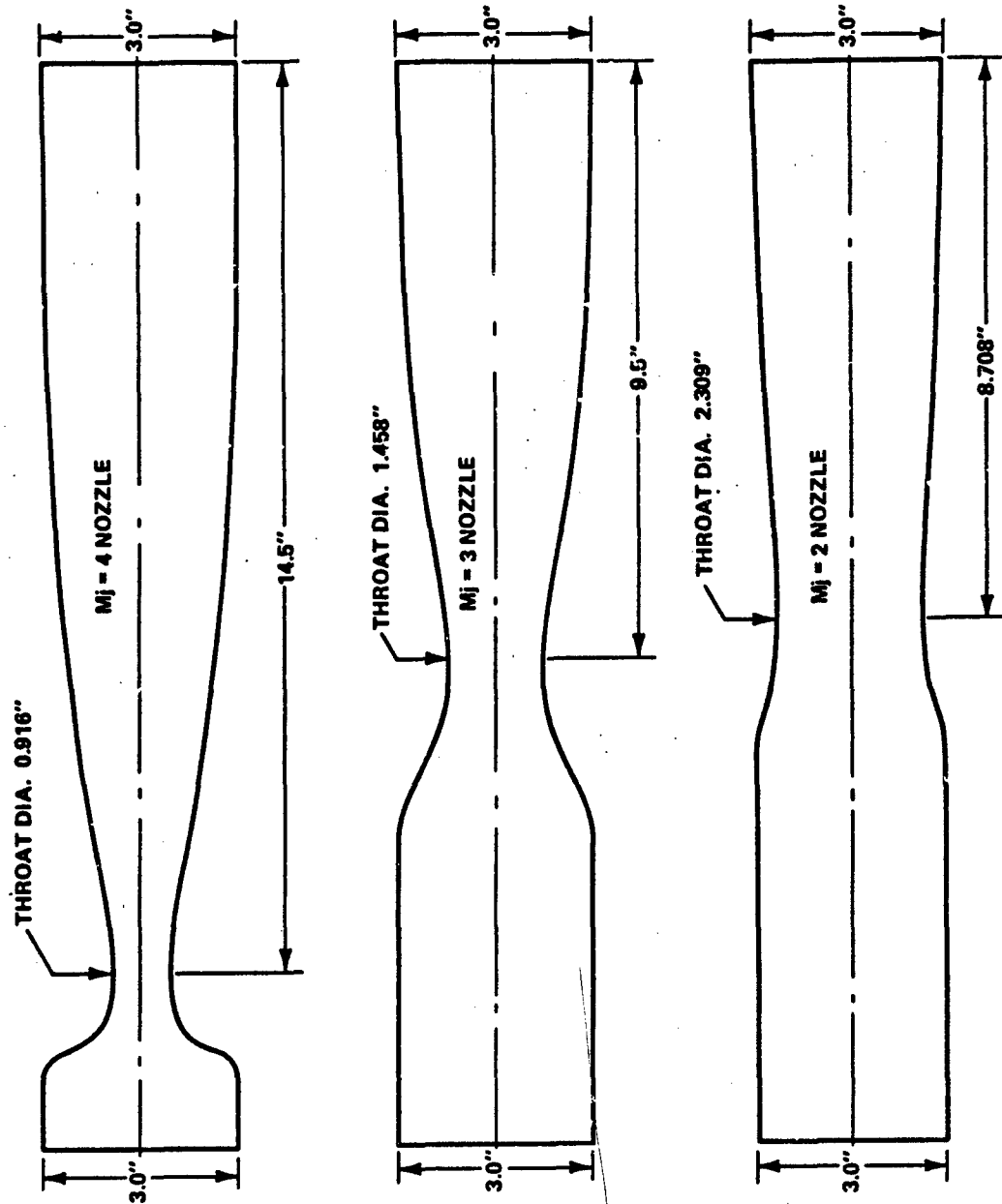


Figure 6 NOZZLE CONTOURS

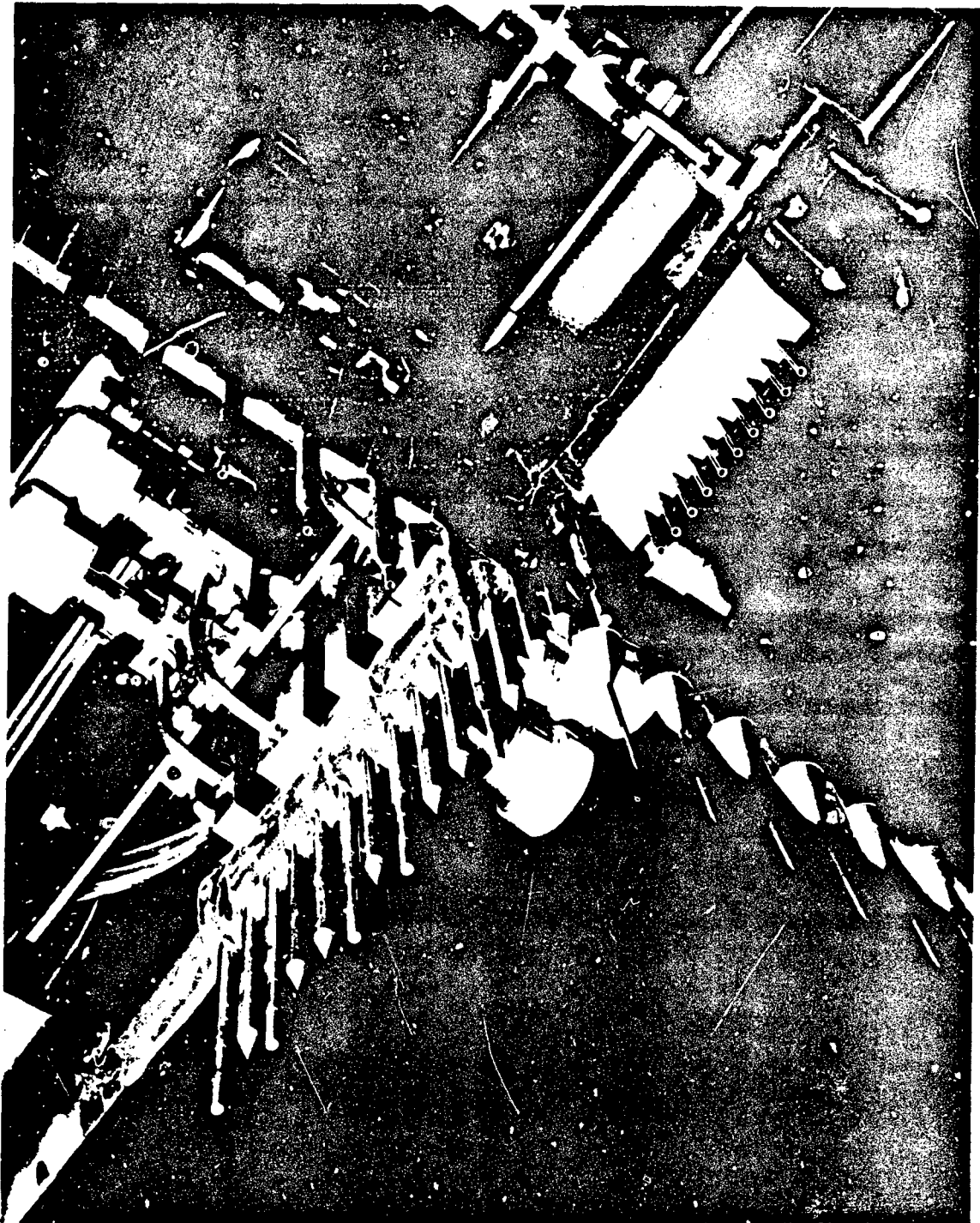


Figure 7 VIEW OF THE INSTRUMENTED RAKE FOR MIXING SURVEYS

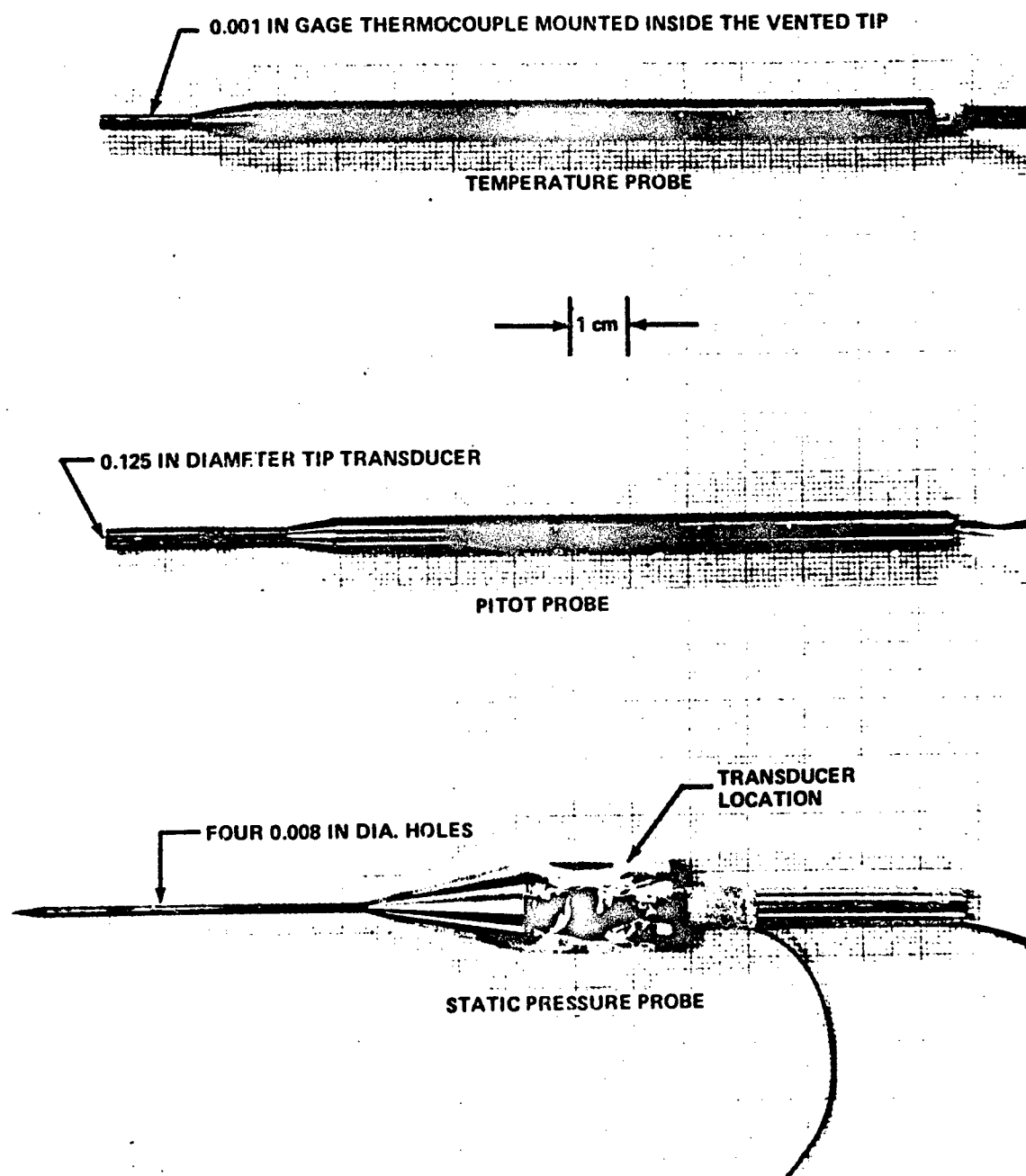


Figure 8 VIEW OF THE PROBES FOR GASDYNAMIC MEASUREMENTS: (a) SINGLE PROBES

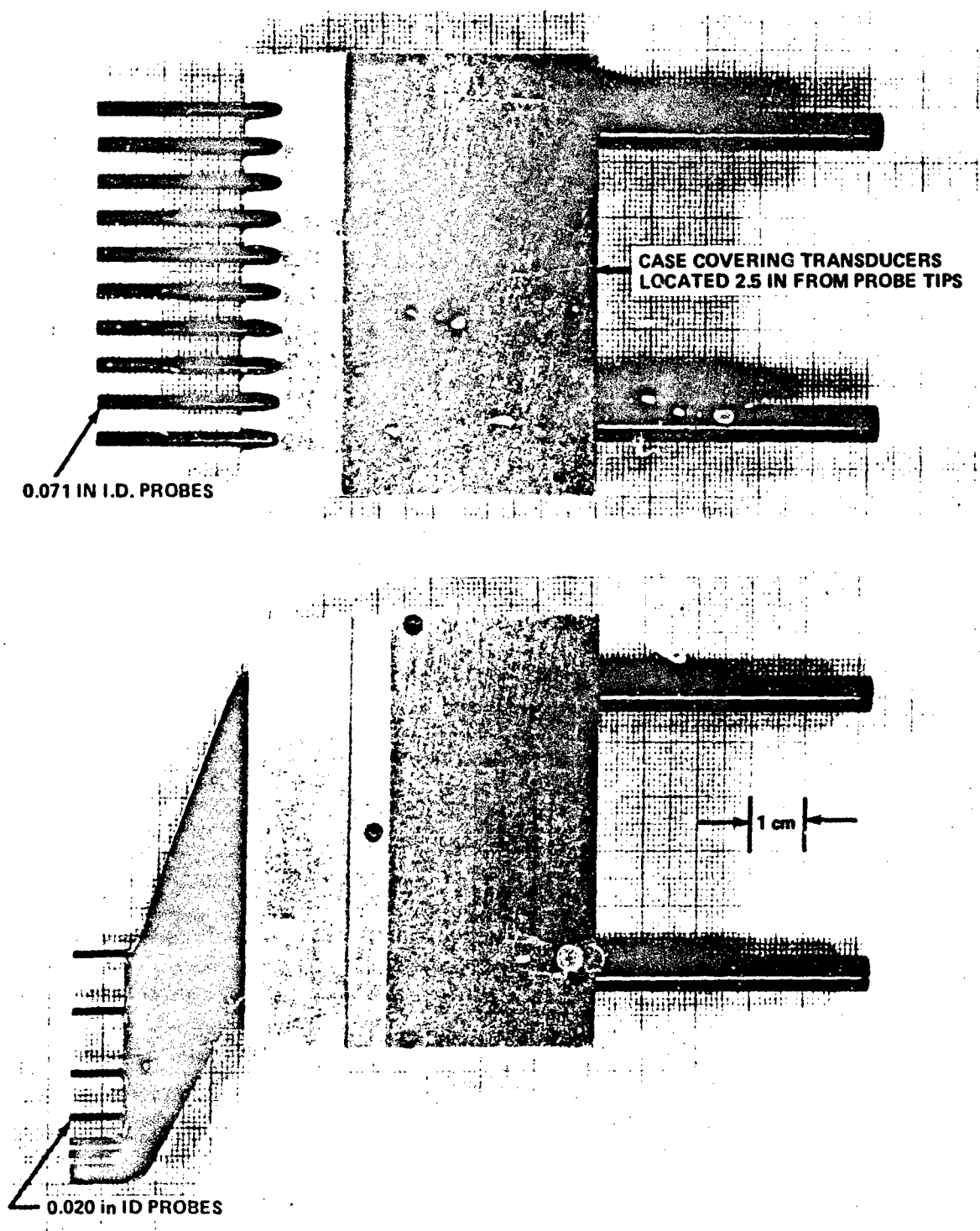


Figure 8 (Cont.) VIEW OF THE PROBES FOR GASDYNAMIC MEASUREMENTS:
(b) PITOT PRESSURE RAKES

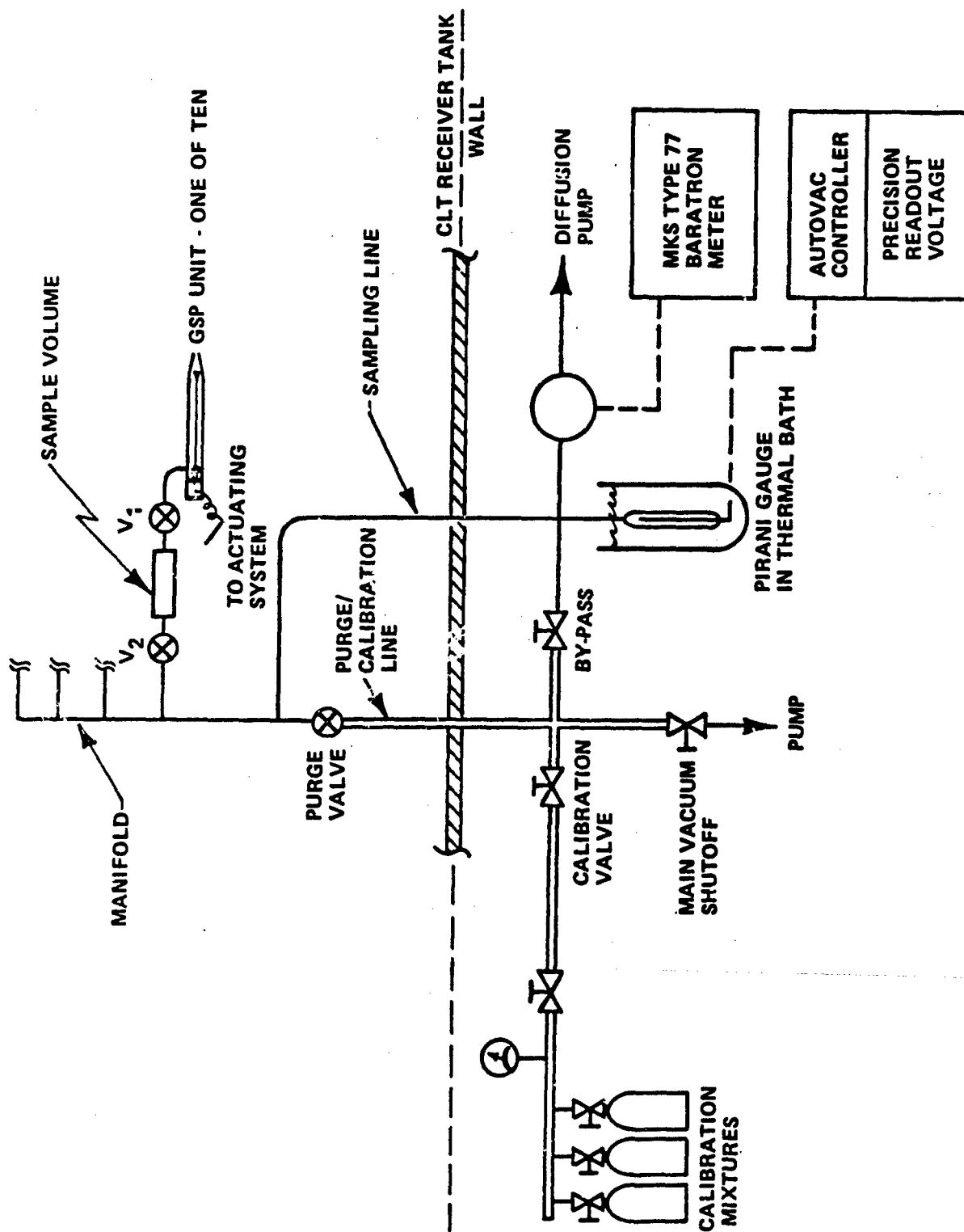
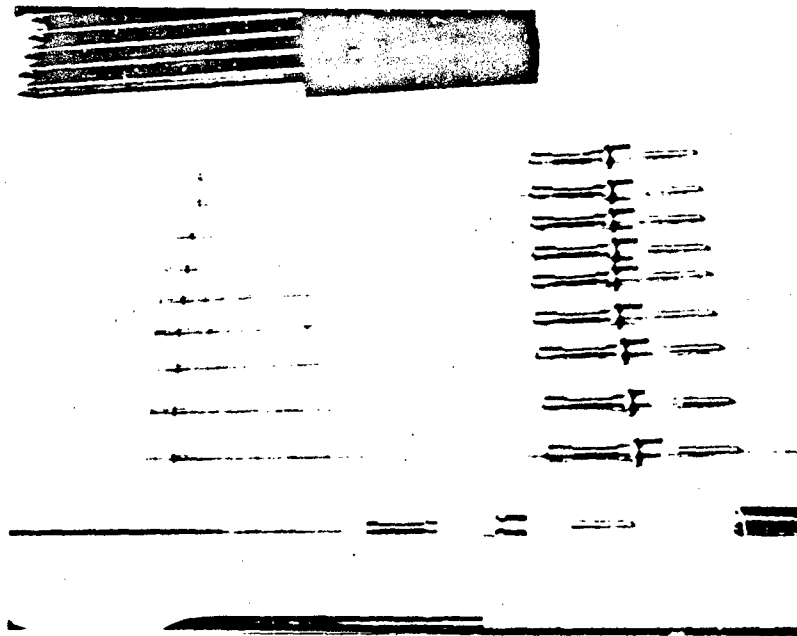
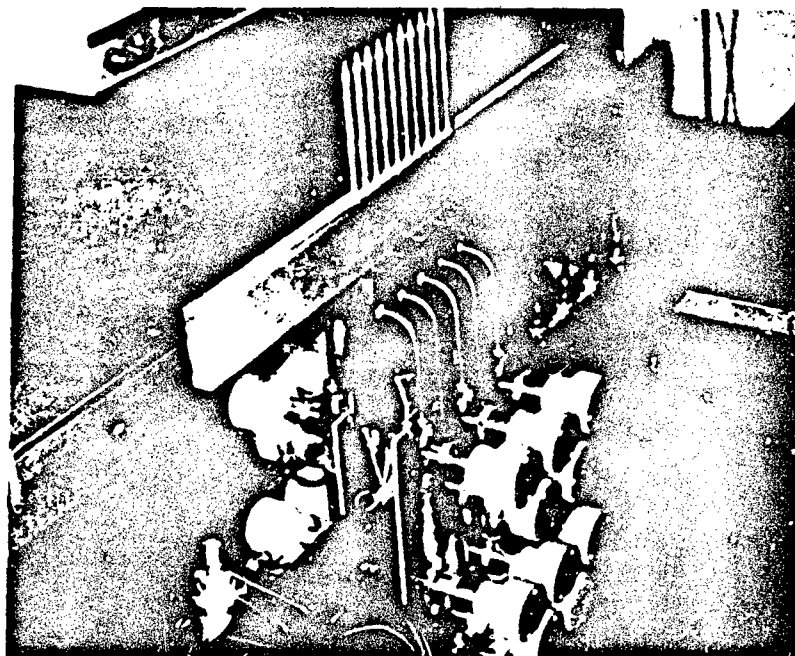


Figure 9 SCHEMATIC OF HEAT CONDUCTIVITY GAS SAMPLER SYSTEM (HCGS)



(a) KEY ELEMENTS OF THE STEM-SEAL ACTUATOR SYSTEM (SEE TEXT FOR DETAILS)



(b) ASSEMBLED GAS SAMPLER PROBE SYSTEMS

Figure 10 VIEW OF THE PROBES FOR GAS SAMPLING

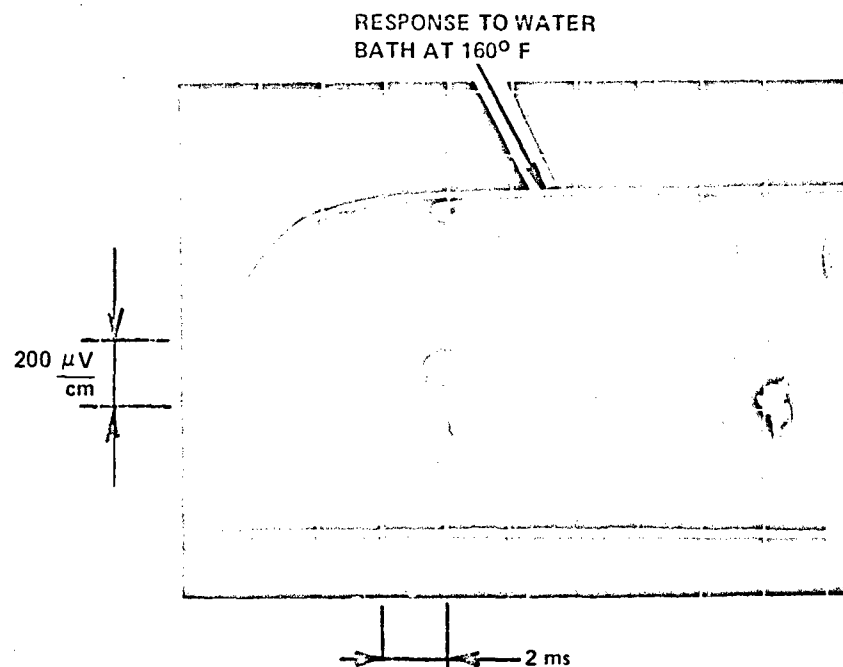


Figure 11 RESPONSE TO WATER IMMERSION OF TEMPERATURE PROBE. THERMOCOUPLE JUNCTION BUTT-WELDED FROM CHROMEL-CONSTANTAN WIRE .003 INCHES DIAMETER

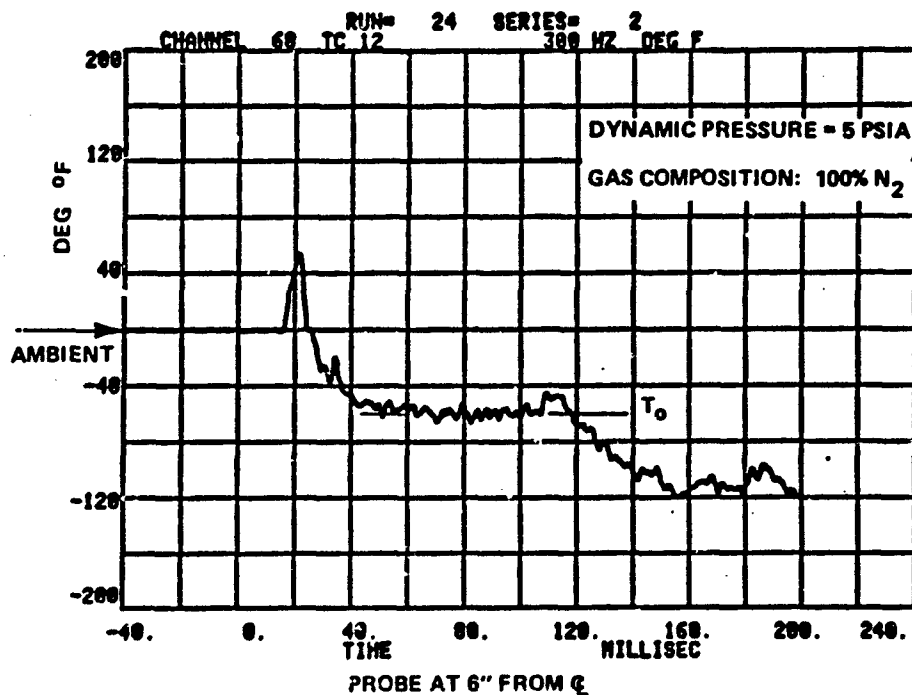
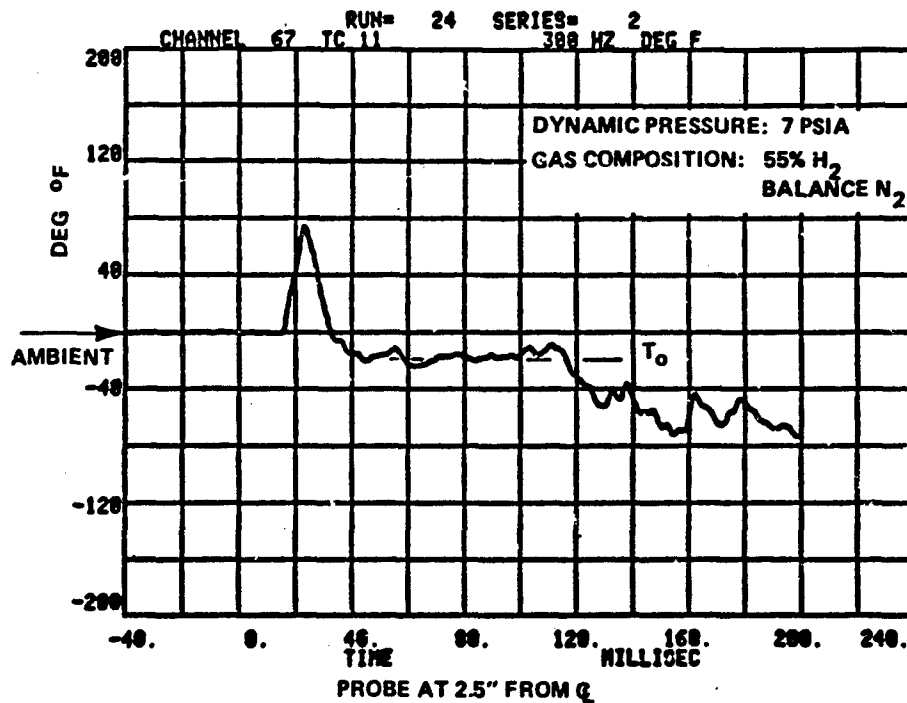


Figure 12 RESPONSE OF THE TEMPERATURE PROBES IN THE JETS AT VARIOUS COMPOSITIONS AND LEVELS OF DYNAMIC PRESSURE

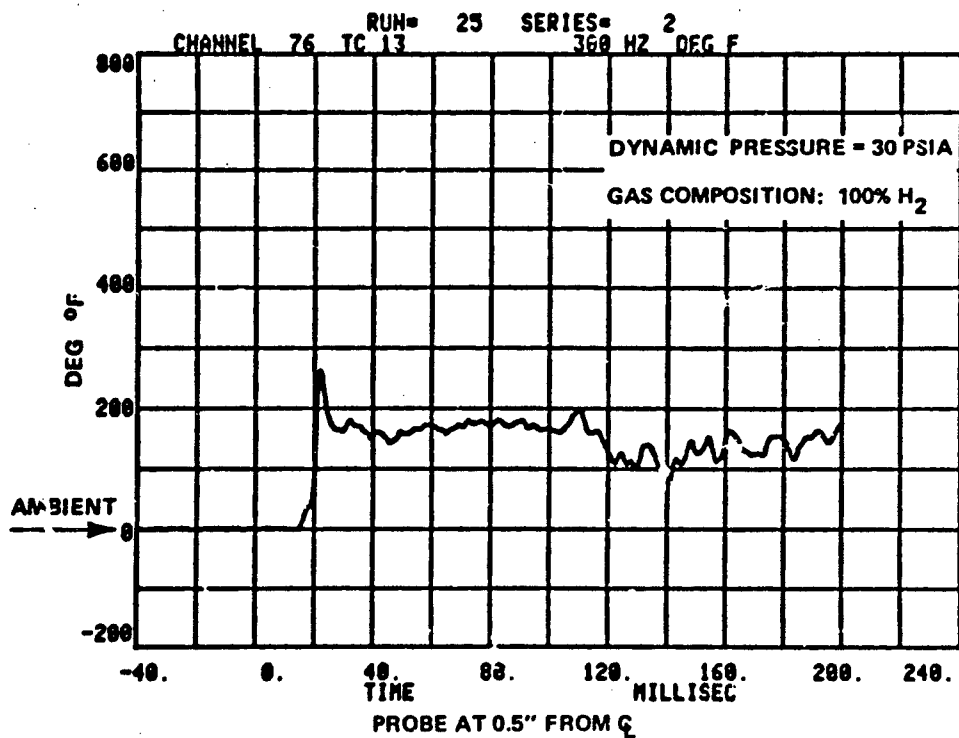
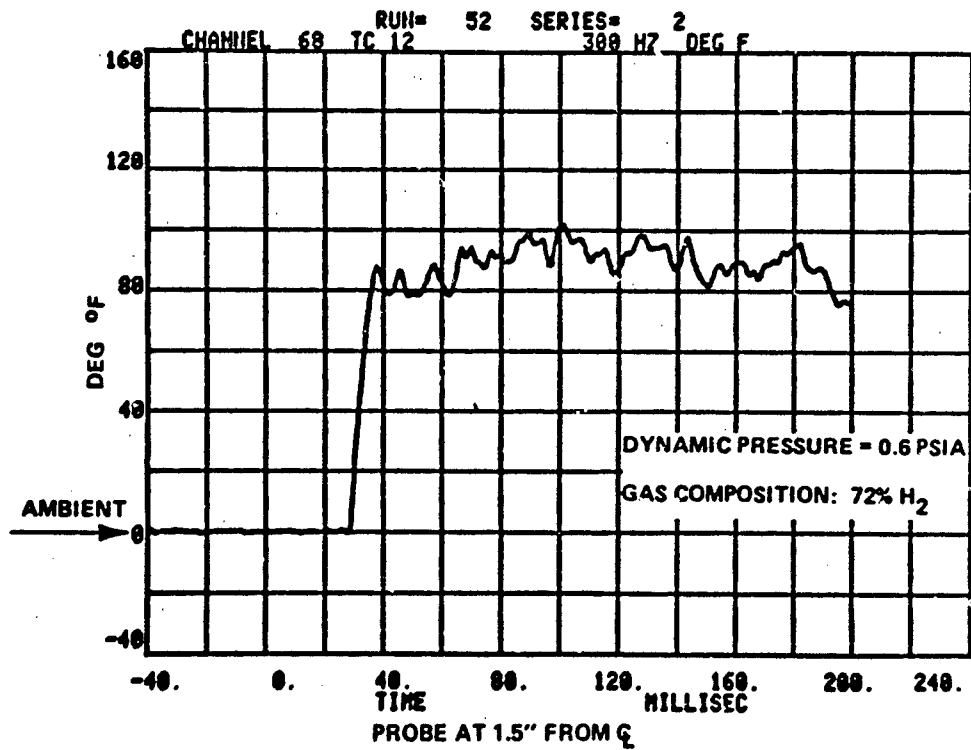


Figure 12 RESPONSE OF THE TEMPERATURE PROBES IN THE JETS AT VARIOUS COMPOSITIONS AND LEVELS OF DYNAMIC PRESSURE (CONTINUED)

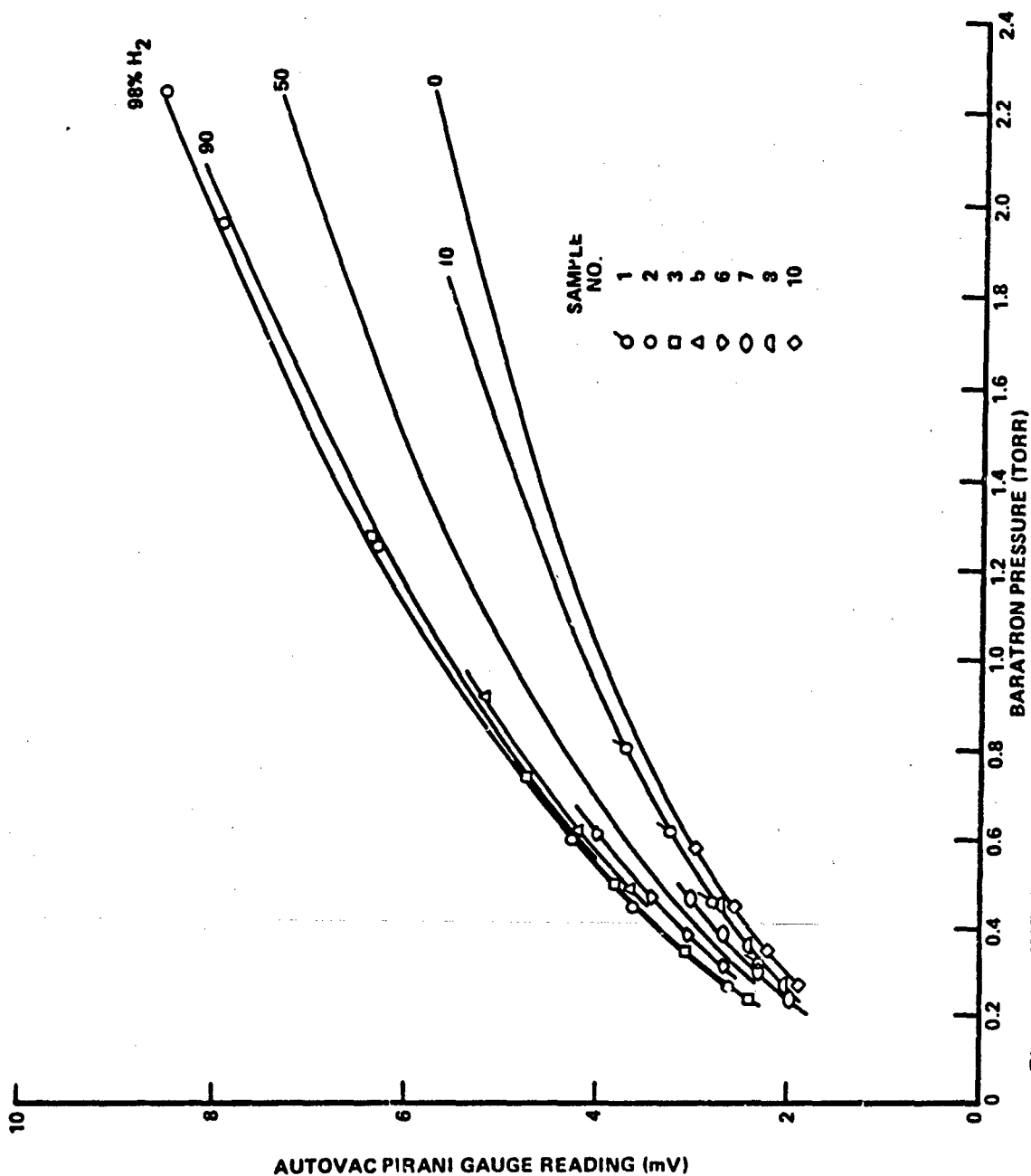


Figure 13 INFLUENCE OF GAS COMPOSITION ON THE MEASUREMENT OF PRESSURE USING PIRANI AND BARATRON GAUGES

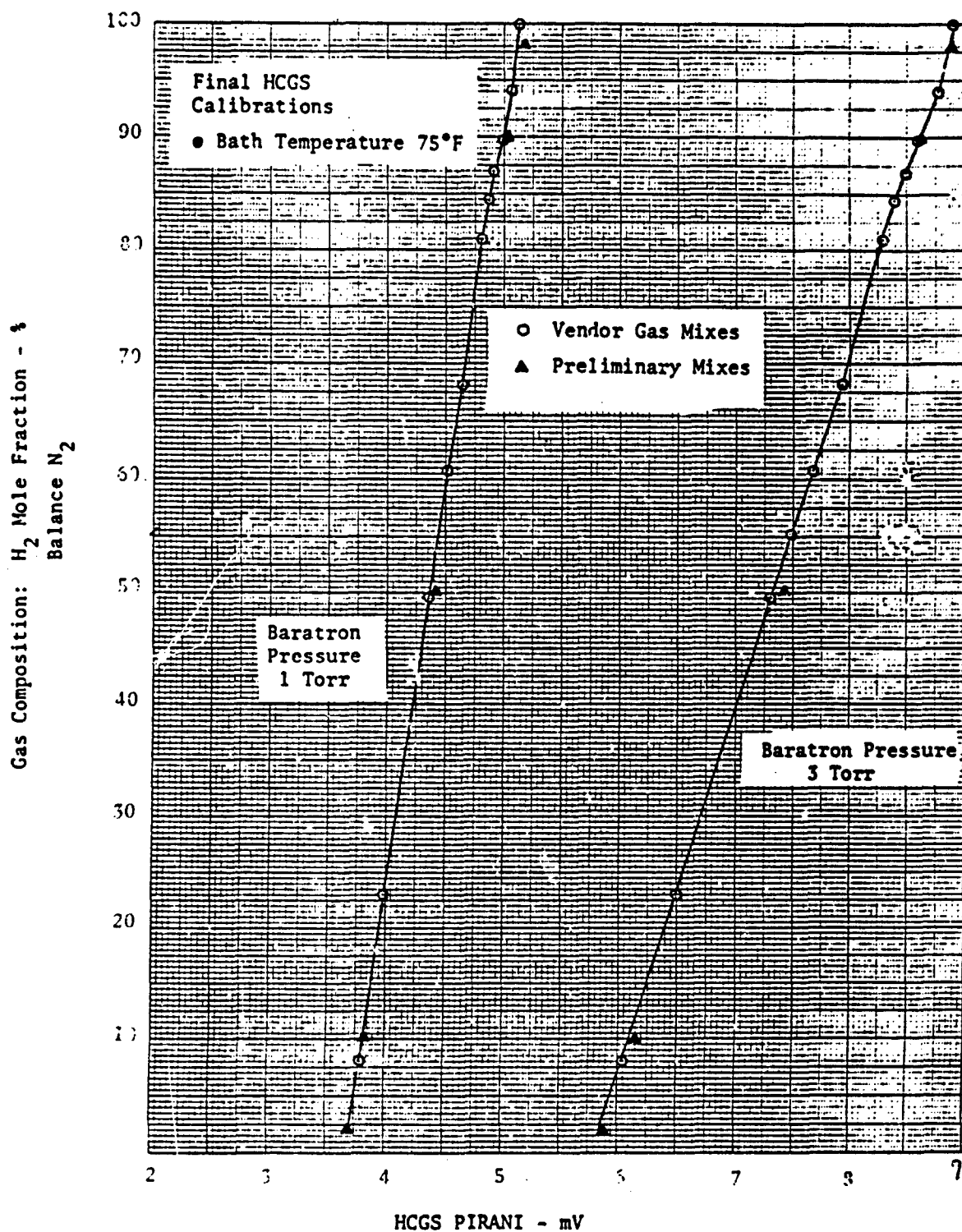


Figure 14 GAS SAMPLER CALIBRATION

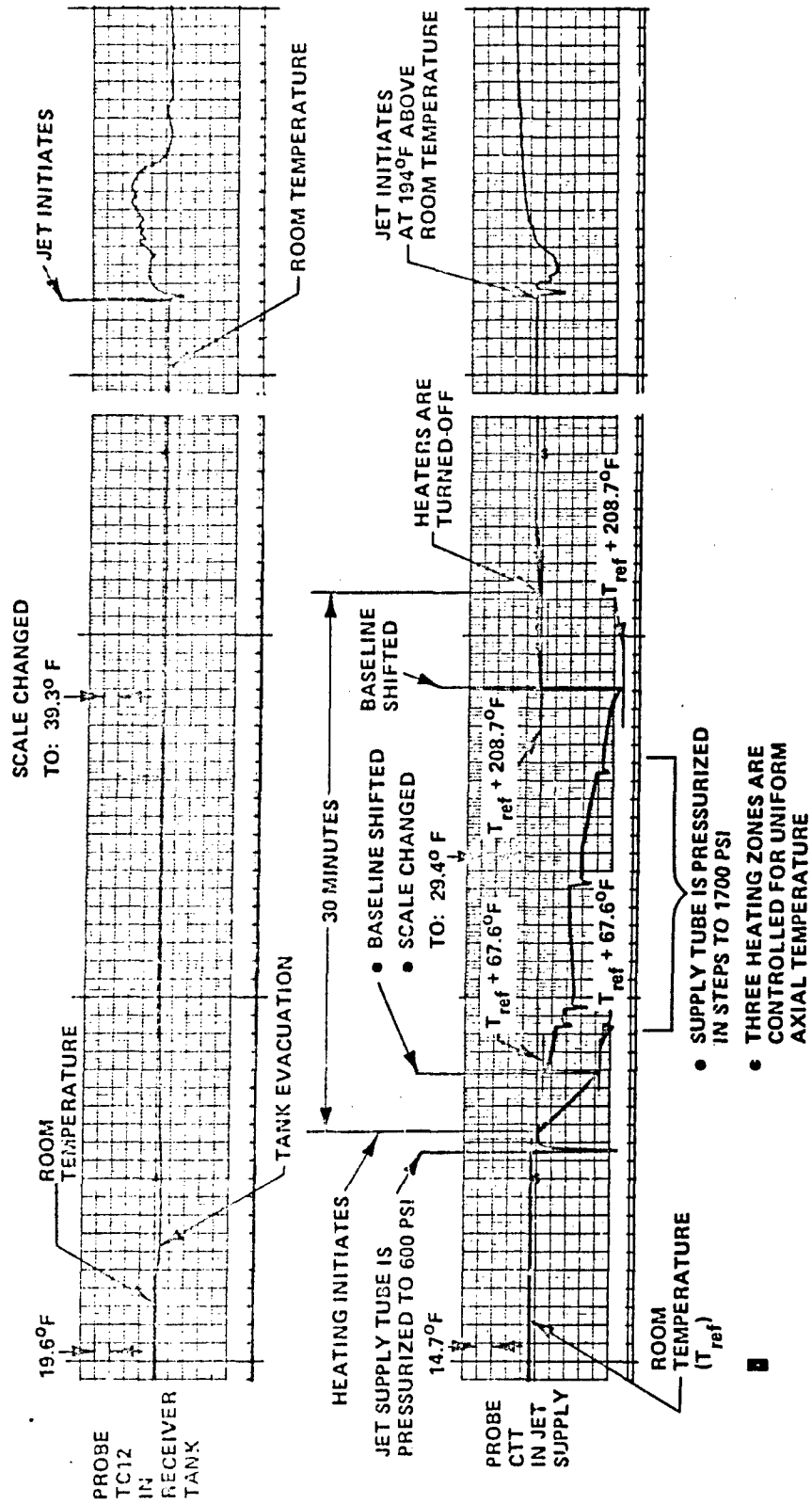


Figure 15 PRE-TEST MONITORING OF REFERENCE TEMPERATURES

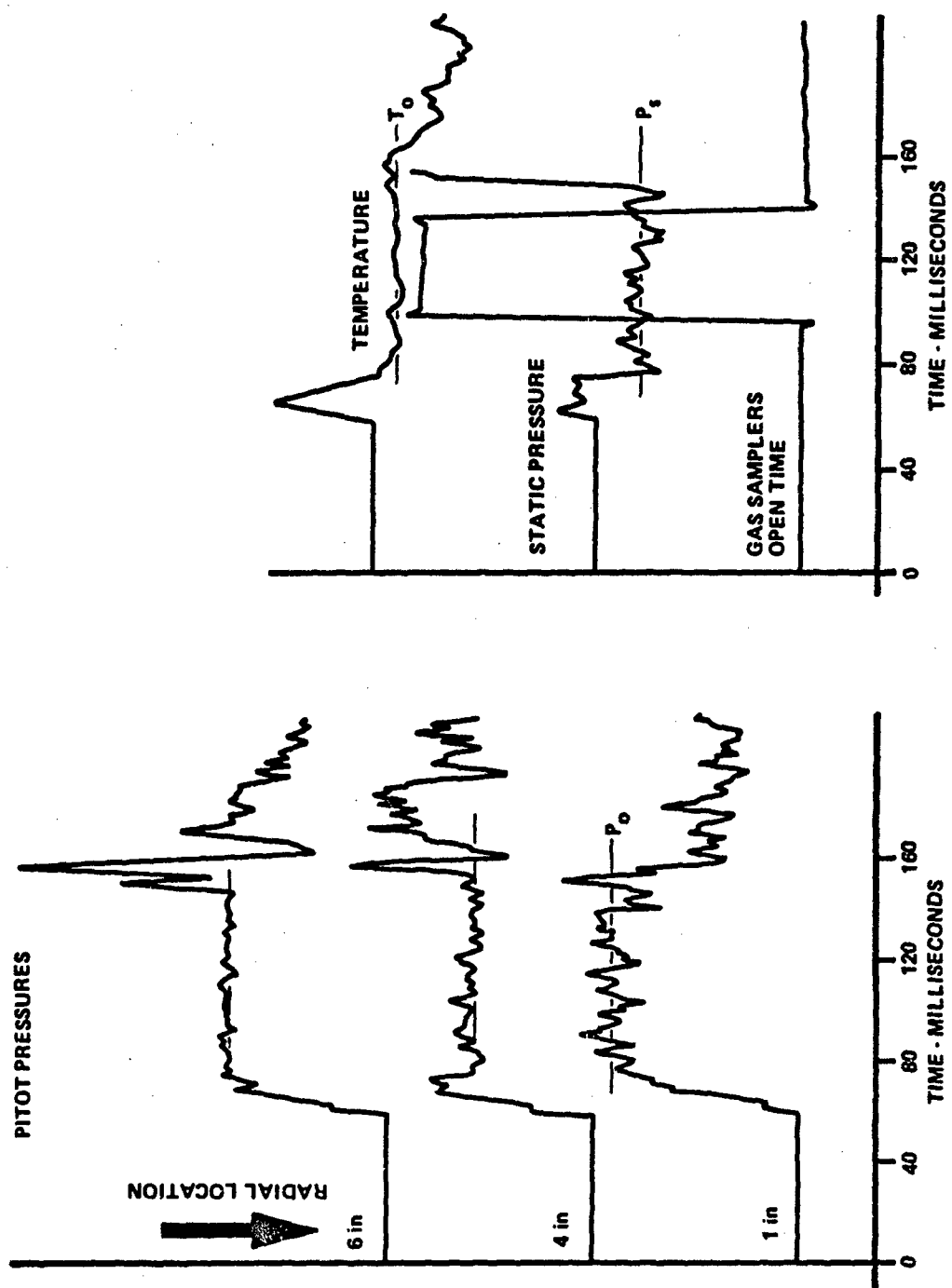


Figure 16 HISTORIES OF FLOW VARIABLES MEASURED IN THE MIXING REGION

RUN 238	CH POSITION	OUTPUT (AU)	UNITS	TIMES (MS)	TIMEE (MS)
65	NT0	6.55564	DEG	60.00	100.00
67	TC 11	-65.8140	DEG	60.00	100.00
68	TC 12	-22.3515	DEG	60.00	100.00
70	TC 15	-51.2018	DEG	60.00	100.00
74	TC 14	5.2789	DEG	60.00	100.00
76	TC 13	19.6858	DEG	60.00	100.00
77	CTT	-9.0755	DEG	60.00	100.00
78	LTP0	9.9529	PSI	60.00	100.00
79	LTP0P1	6.6686	PSI	60.00	100.00
80	CTP	-205.1623	PSI	60.00	100.00
81	NPO	238.5247	PSI	60.00	100.00
82	QU	7.0872	PSI	60.00	100.00
84	T 10	5.8463	PSI	60.00	100.00
86	T 8	6.4345	PSI	60.00	100.00
88	T 5	5.6349	PSI	60.00	100.00
90	T 4	4.7444	PSI	60.00	100.00
91	GP	-2112.7285	PSI	60.00	100.00
92	LTPS	--.0845	PSI	60.00	100.00
93	NPS	--.0997	PSI	60.00	100.00
94	LTPS	--.0793	PSI	60.00	100.00
95	NPS	--.1660	PSI	60.00	100.00
96	S 10	--.4203	PSI	60.00	100.00
97	S 2	--.6320	PSI	60.00	100.00

Figure 17 SAMPLE OF AVERAGED DATA FROM THE DDAS

RUN 2.38	CH POSITION	OUTPUT (AU)	UNITS	TIMES (MS)	TIME (MS)
98	S 4	5356	PSI	60.00	100.00
99	S 10	4476	PSI	60.00	100.00
100	S 5	3556	PSI	60.00	100.00
101	S 4	5465	PSI	60.00	100.00
102	S 3	3558	PSI	60.00	100.00
103	S 2	5949	PSI	60.00	100.00
104	S 3	3921	PSI	60.00	100.00
105	TR 10	5920	PSI	60.00	100.00
106	TR 9	9814	PSI	60.00	100.00
107	TR 8	7384	PSI	60.00	100.00
108	TR 7	9666	PSI	60.00	100.00
109	TR 6	2791	PSI	60.00	100.00
110	TR 5	4218	PSI	60.00	100.00
111	TR 4	6673	PSI	60.00	100.00
112	TR 3	5388	PSI	60.00	100.00
113	TR 2	9475	PSI	60.00	100.00
114	TR 10	7718	PSI	60.00	100.00
115	BL 9	2578	PSI	60.00	100.00
116	BL 8	0168	PSI	60.00	100.00
117	BL 7	2298	PSI	60.00	100.00
118	BL 6	7405	PSI	60.00	100.00
119	BL 3	1866	PSI	60.00	100.00
120	BL 1	2940	PSI	60.00	100.00
121	GP 1	.250	H2 FRAC	60.00	100.00
122	GP 2	.528	H2 FRAC	60.00	100.00
123	GP 3	.680	H2 FRAC	60.00	100.00
124	GP 4	.750	H2 FRAC	60.00	100.00
125	GP 5	.780	H2 FRAC	60.00	100.00
126	GP 6	.740	H2 FRAC	60.00	100.00
127	GP 7	.620	H2 FRAC	60.00	100.00
128	GP 8	.465	H2 FRAC	60.00	100.00
129	GP 9	.155	H2 FRAC	60.00	100.00
130	GP 10	.085	H2FRAC	60.00	100.00

Figure 17 Continued

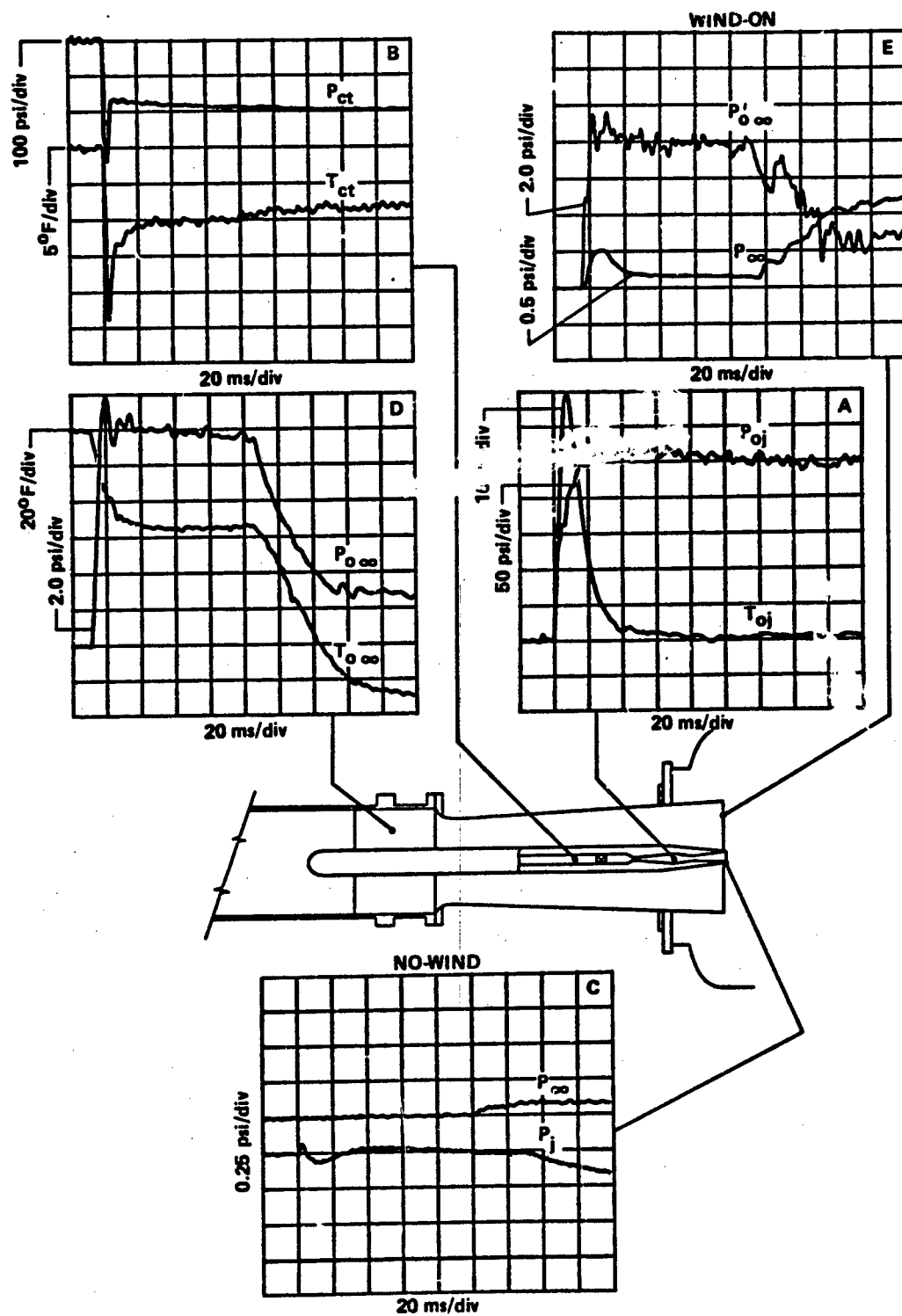
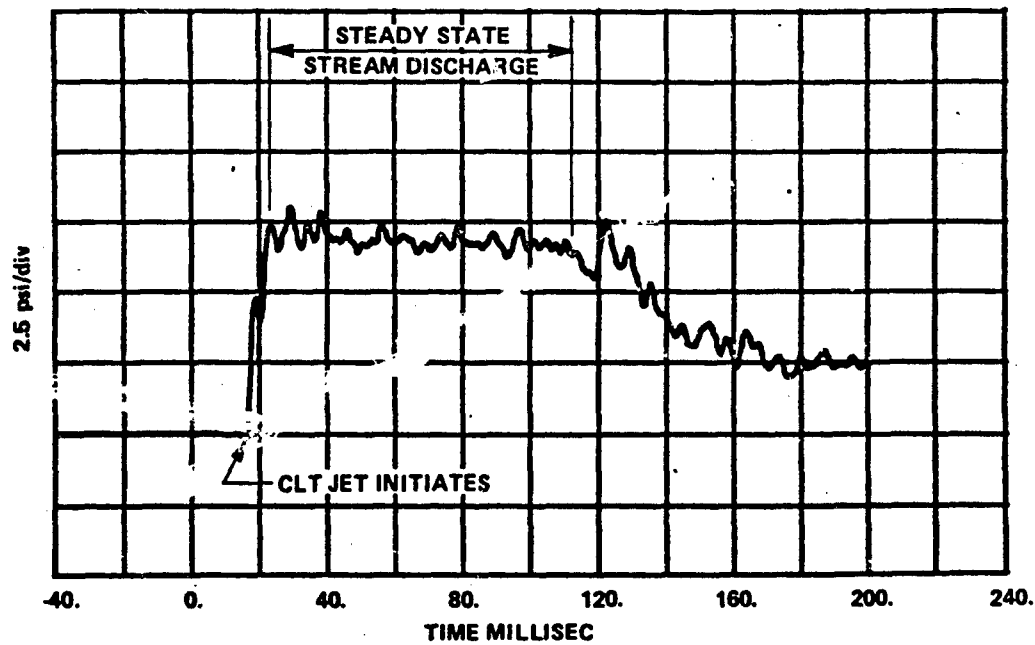
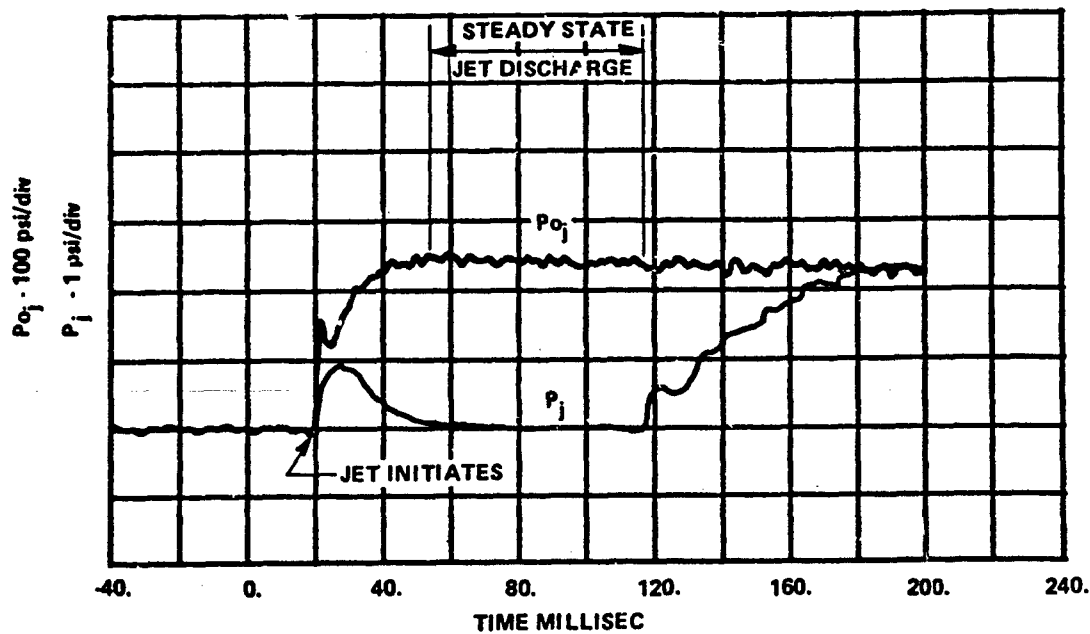


Figure 18 HISTORIES OF FLOW VARIABLES ILLUSTRATING THE JET/STREAM CHARACTERISTICS



(a) PITOT PRESSURE AT THE EXIT PLANE OF THE CLT NOZZLE



(b) PRESSURES IN THE JET

Figure 19 SYNCHRONIZATION OF THE CLT AND JET DISCHARGES

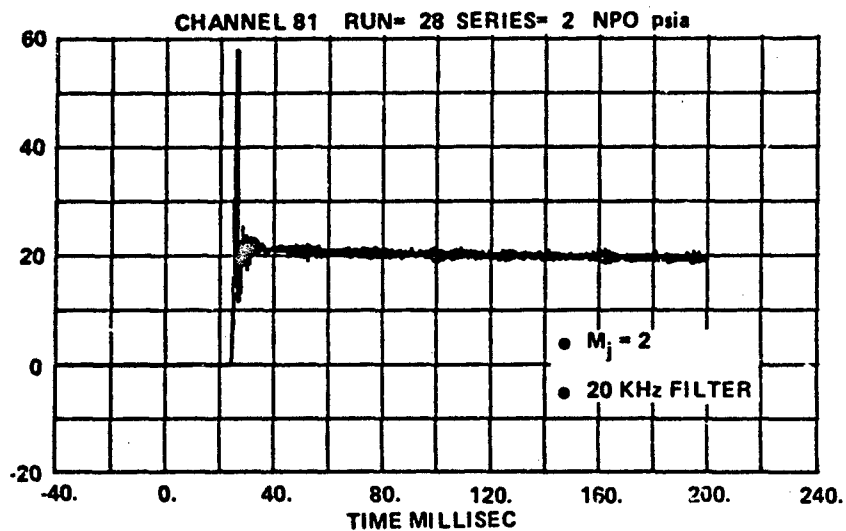
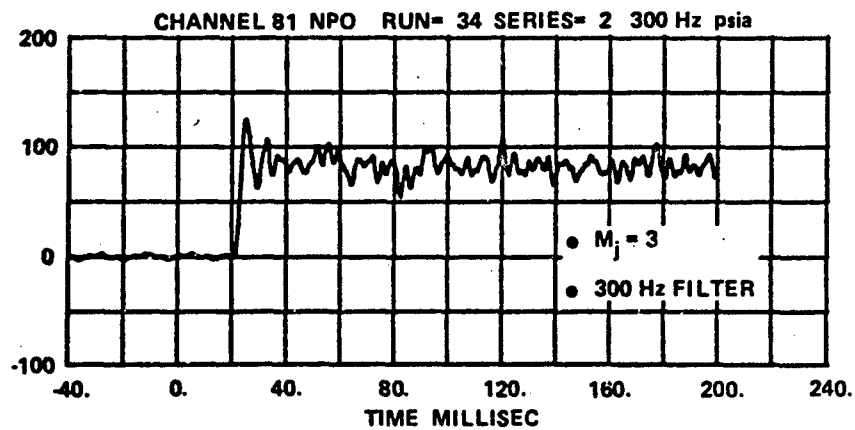
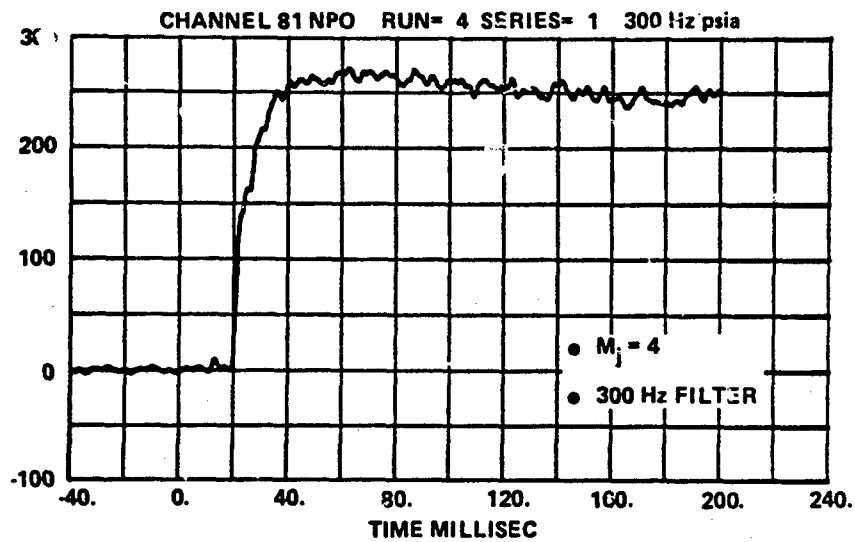
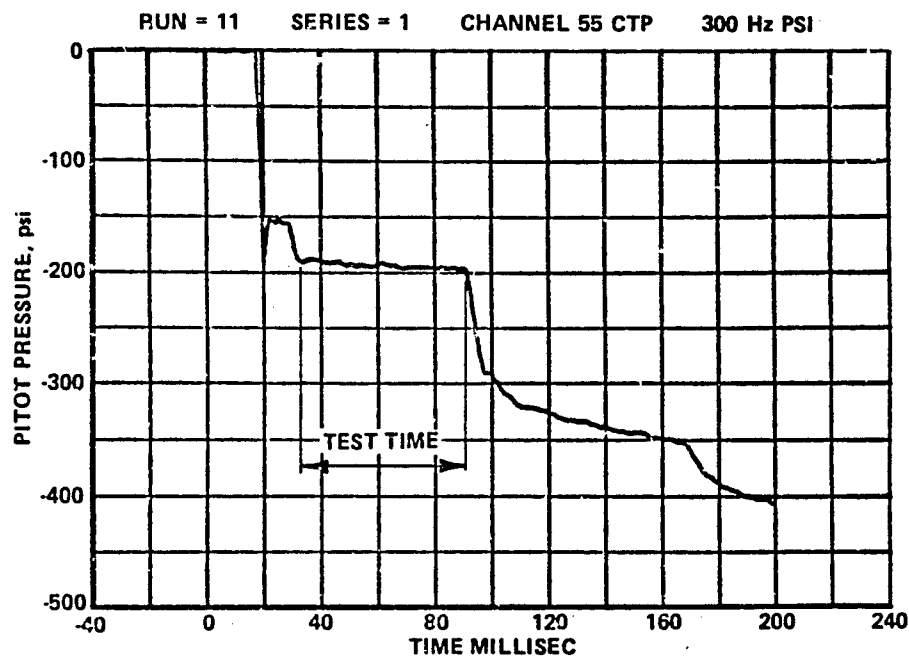
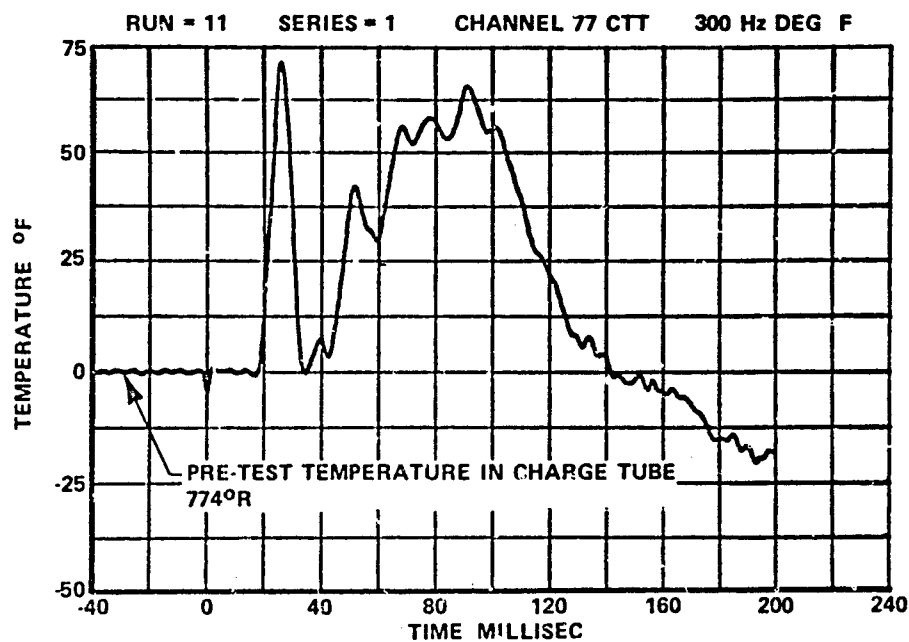


Figure 20 HISTORIES OF PLENUM PRESSURE FOR $M = 4, 3, 2$ JETS



(a) CHARGE TUBE PRESSURE



(b) CHARGE TUBE TEMPERATURE

Figure 21 HISTORIES OF JET VARIABLES IN A HEATED-JET TEST CASE

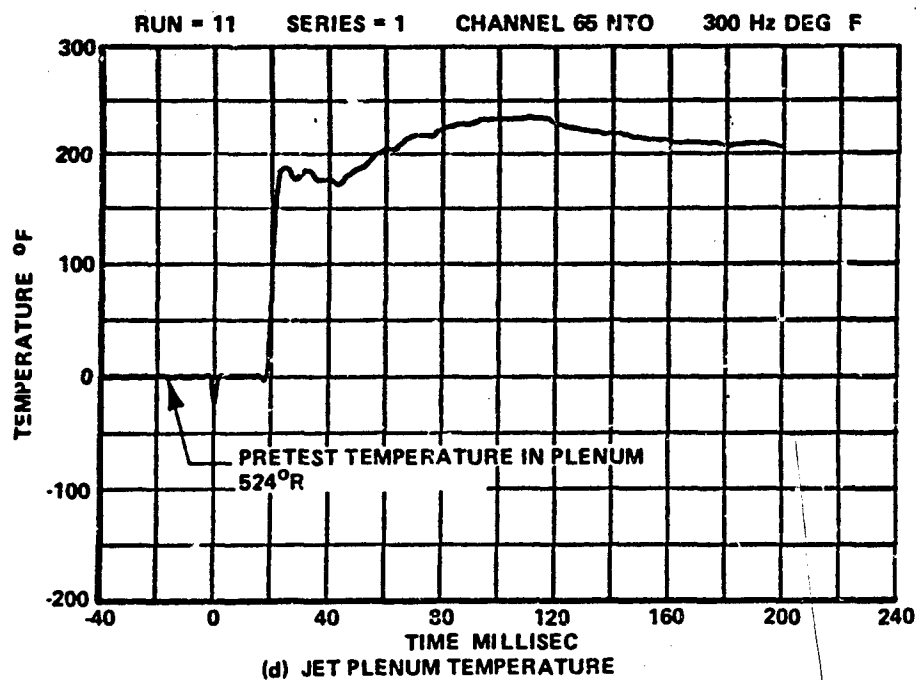
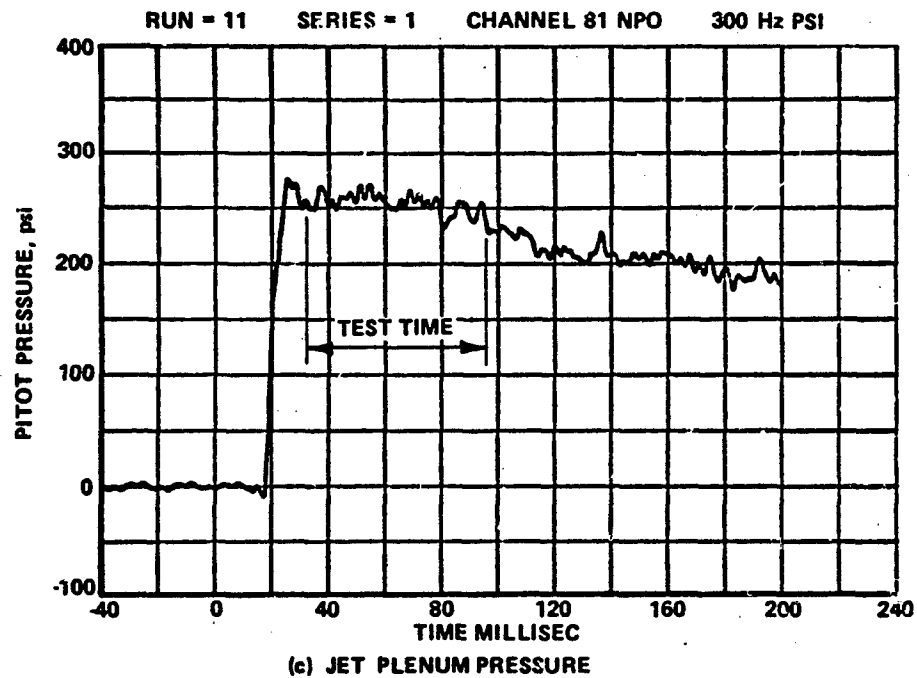


Figure 21 HISTORIES OF JET VARIABLES IN A HEATED-JET TEST CASE (Cont.)

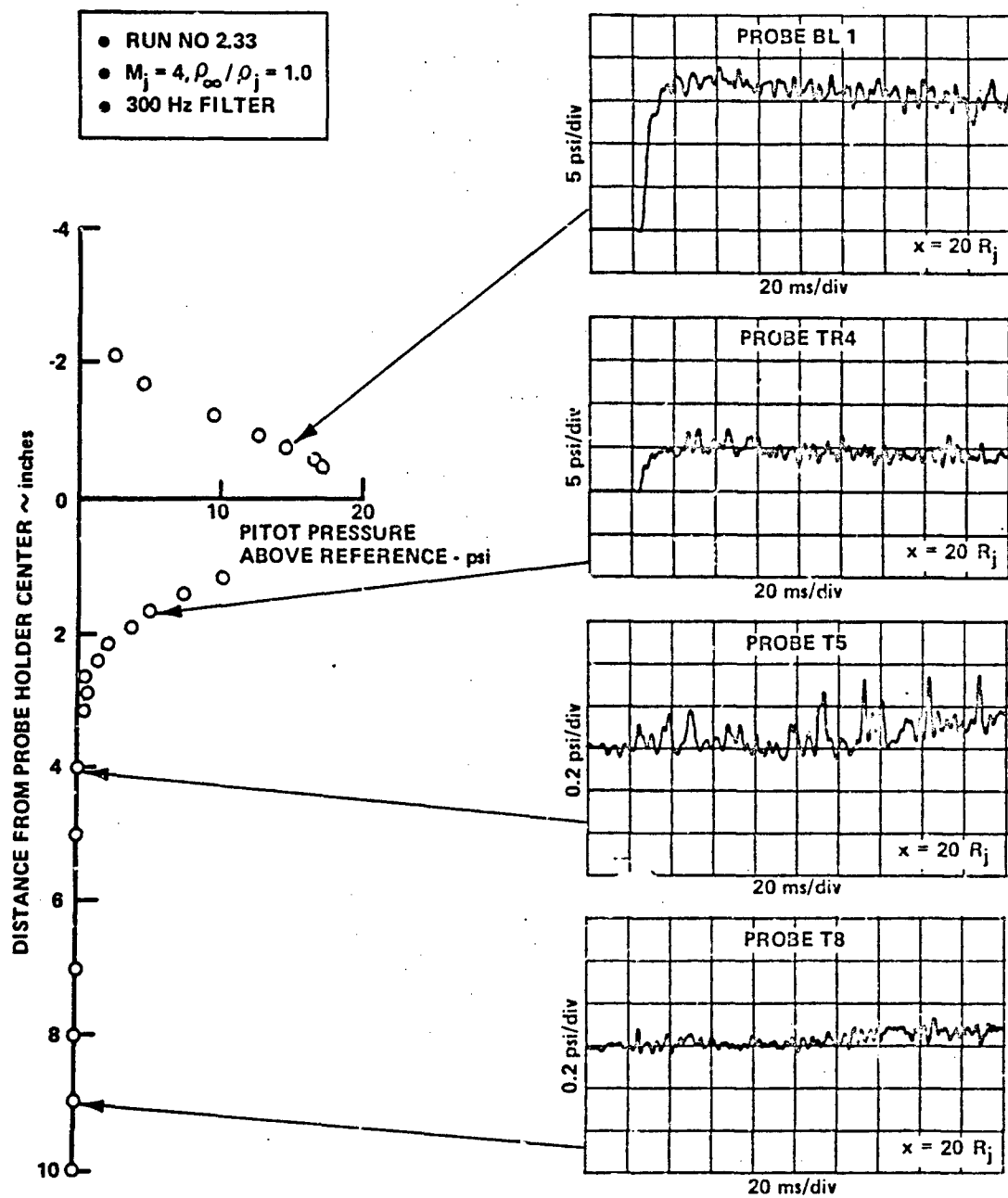
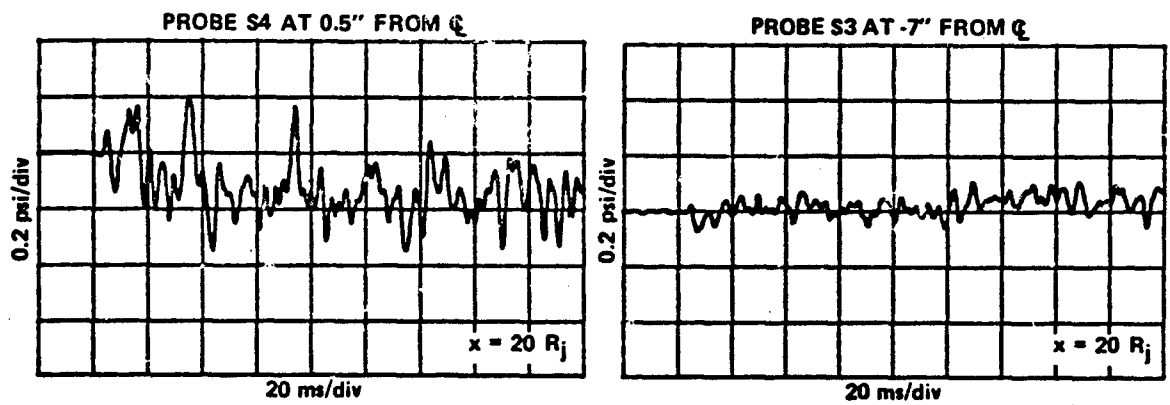
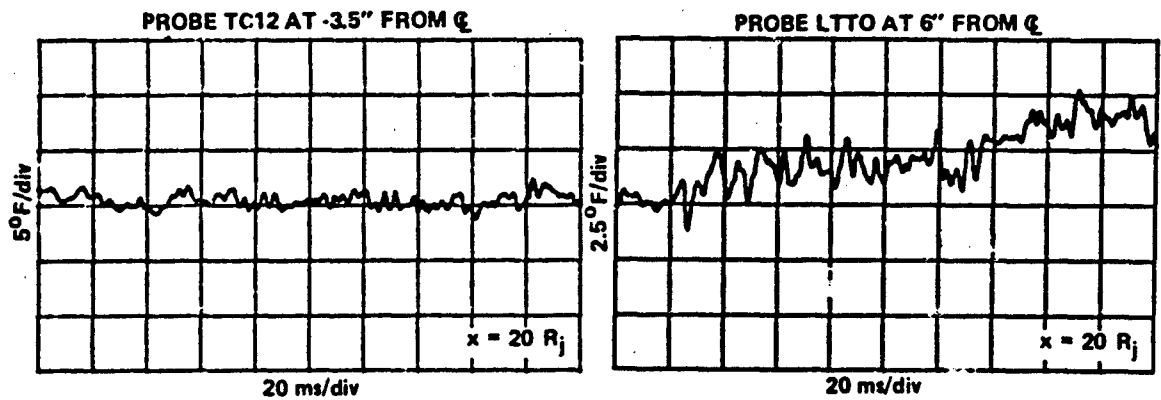


Figure 22 RADIAL VARIATION OF THE MEASUREMENTS IN A TYPICAL NO-WIND TEST CASE . (a) PITOT PRESSURES



(b) STATIC PRESSURES



(c) RECOVERY TEMPERATURES

Figure 22 RADIAL VARIATION OF THE MEASUREMENTS IN A TYPICAL NO-WIND TEST CASE (Cont.)

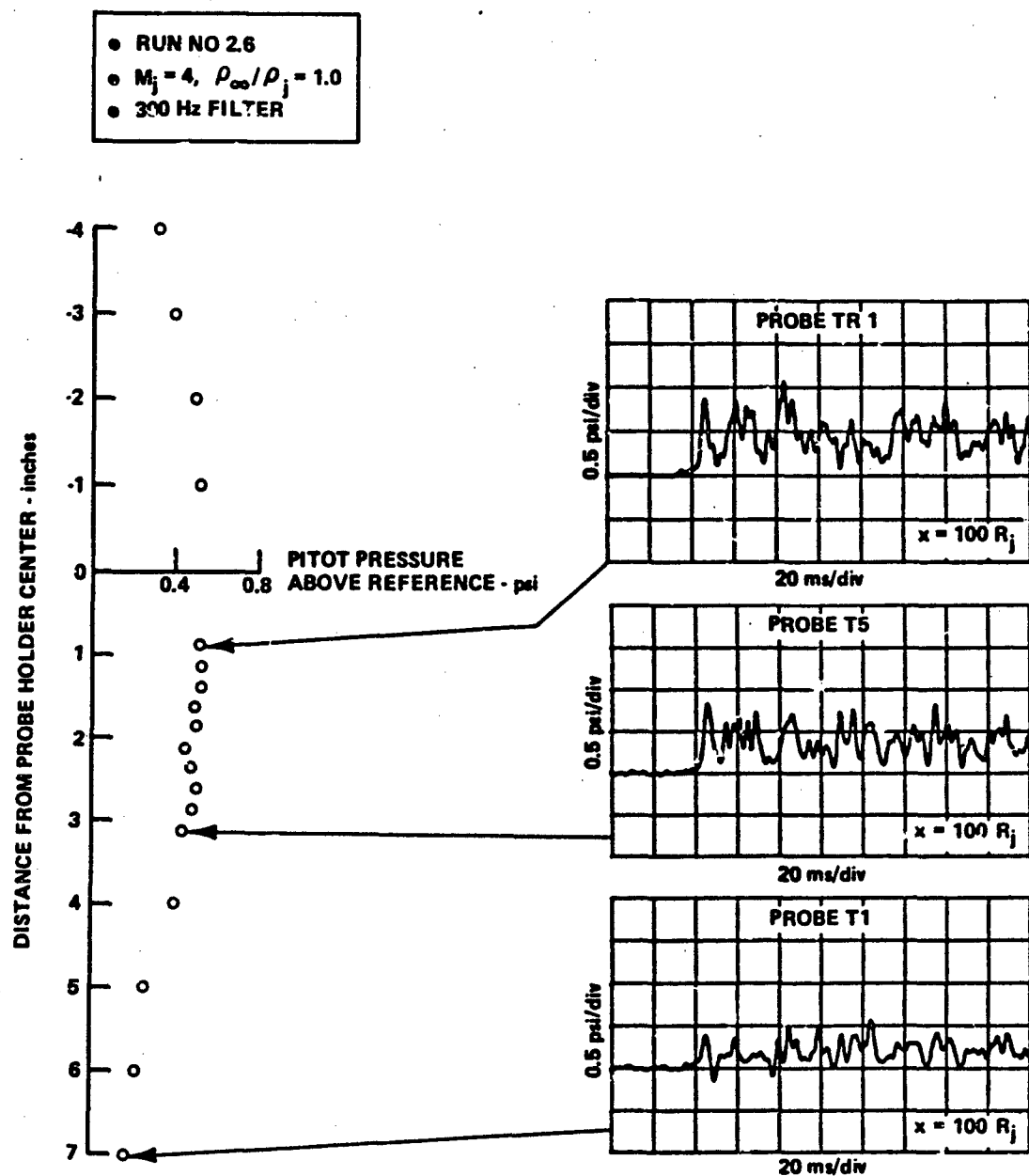


Figure 22 RADIAL VARIATION OF THE MEASUREMENTS IN A TYPICAL NO-WIND TEST CASE (d) PITOT PRESSURES (Cont.)

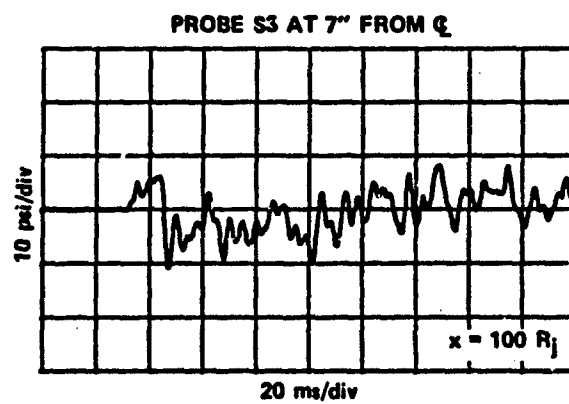
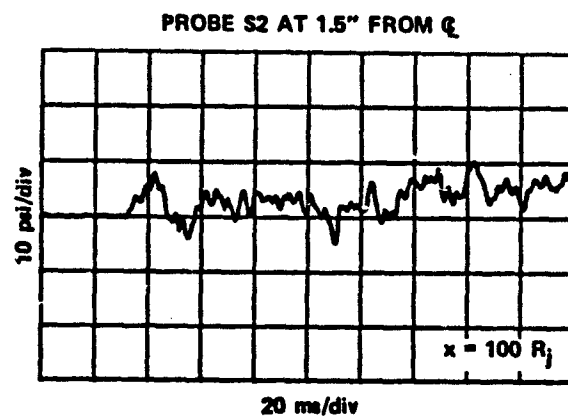


Figure 22 RADIAL VARIATION OF THE MEASUREMENTS IN A TYPICAL NO-WIND TEST CASE (e) STATIC PRESSURE (Cont.)

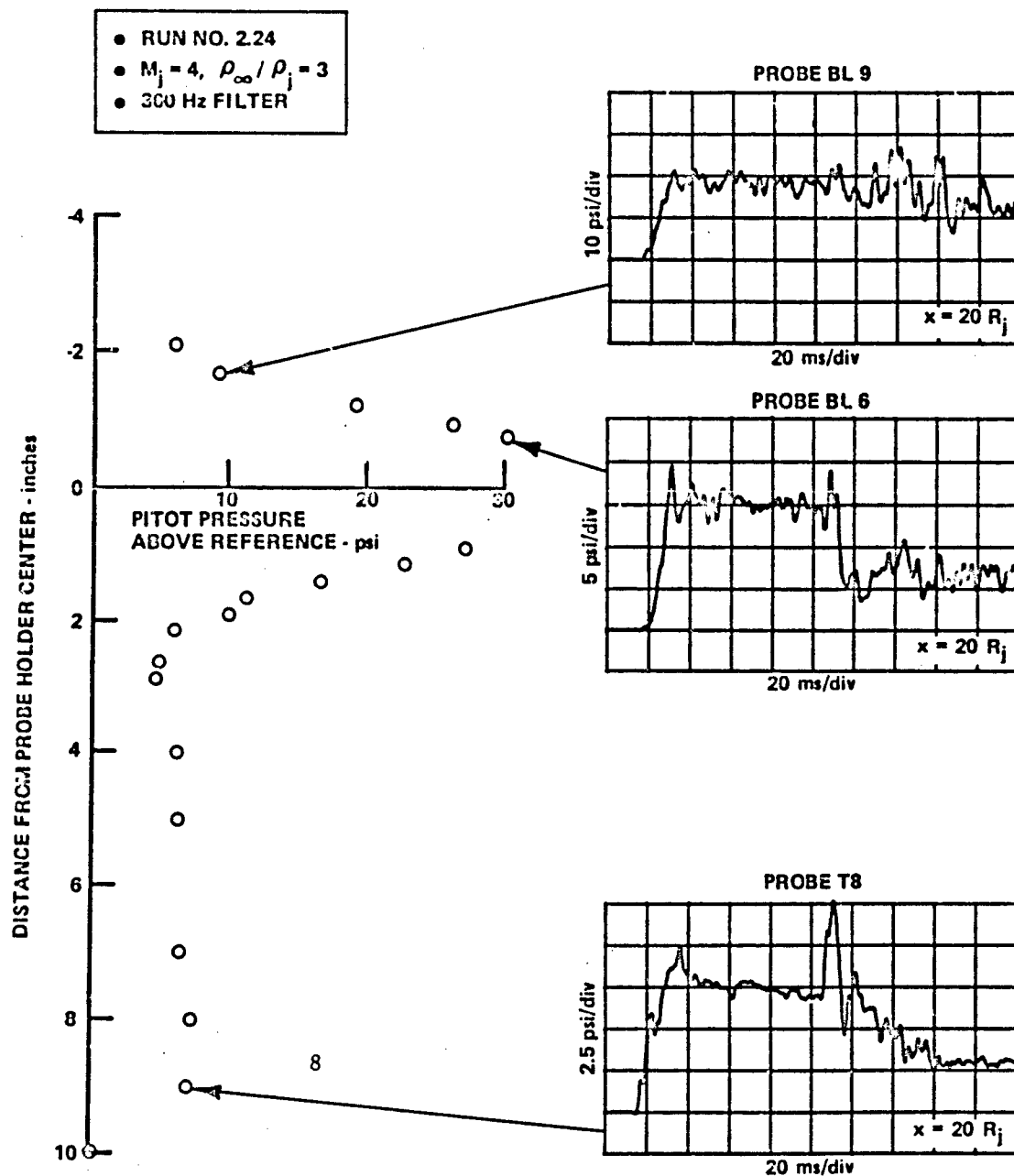


Figure 23 RADIAL VARIATION OF THE MEASUREMENTS IN A TYPICAL WIND-ON TEST CASE (a) PITOT PRESSURES

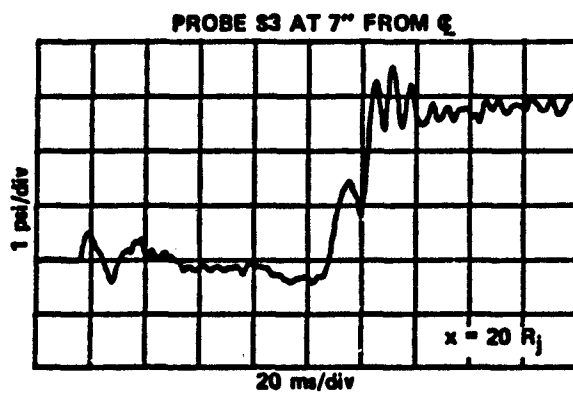
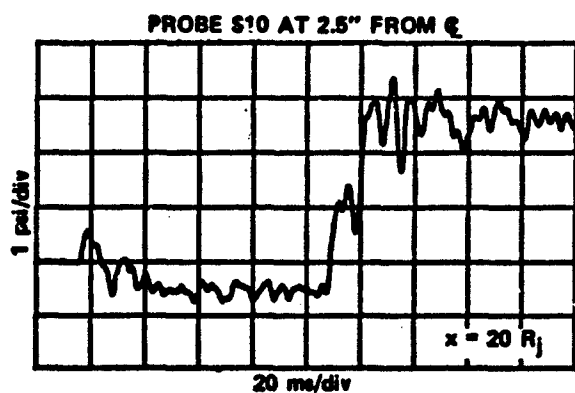
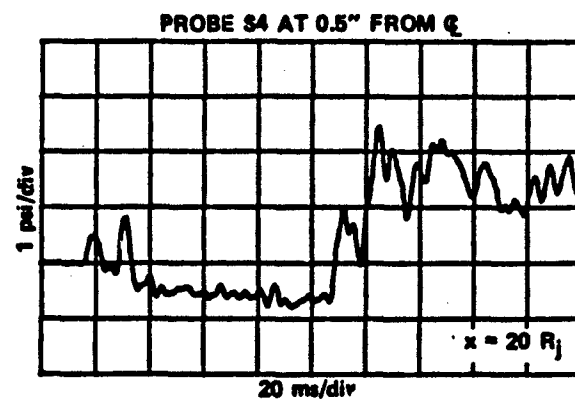


Figure 23 RADIAL VARIATION OF THE MEASUREMENTS IN A TYPICAL WIND-ON TEST CASE (b) STATIC PRESSURES. (Cont.)

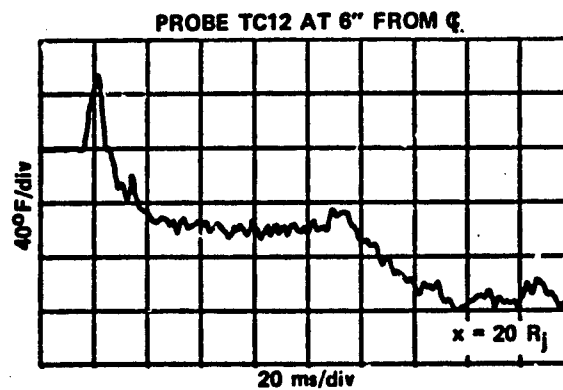
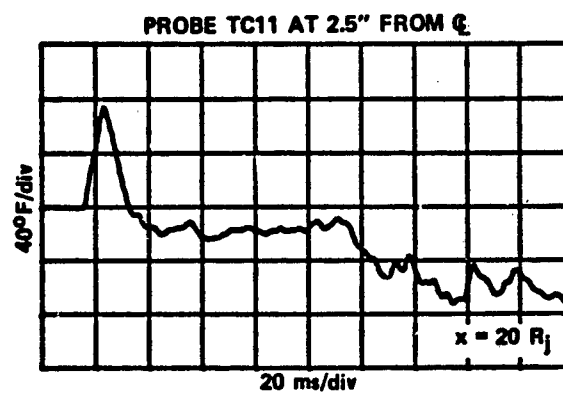
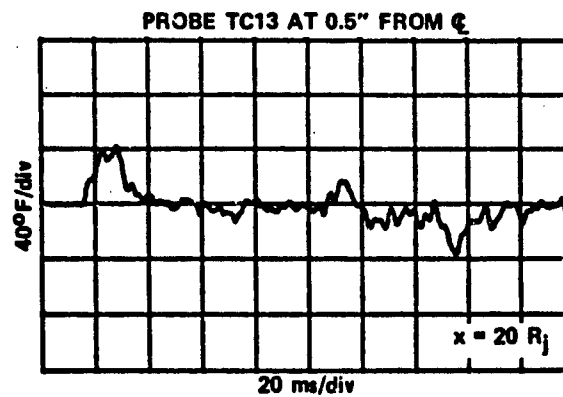


Figure 23 RADIAL VARIATION OF THE MEASUREMENTS IN A TYPICAL WIND-ON TEST CASE (c) RECOVERY TEMPERATURES. (Cont.)

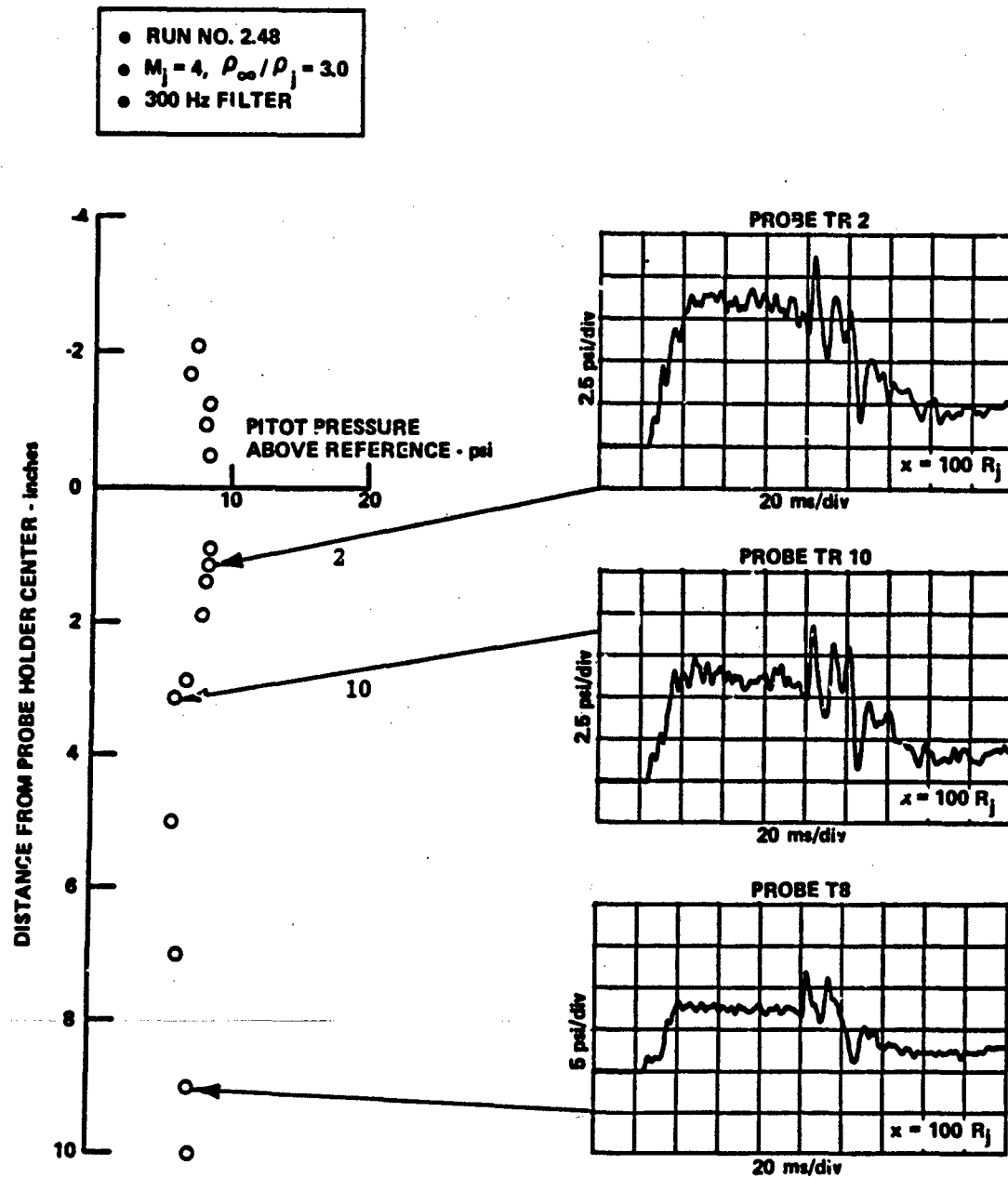


Figure 23 RADIAL VARIATION OF THE MEASUREMENTS IN A TYPICAL WIND-ON TEST CASE (d) PITOT PRESSURES (Cont.)

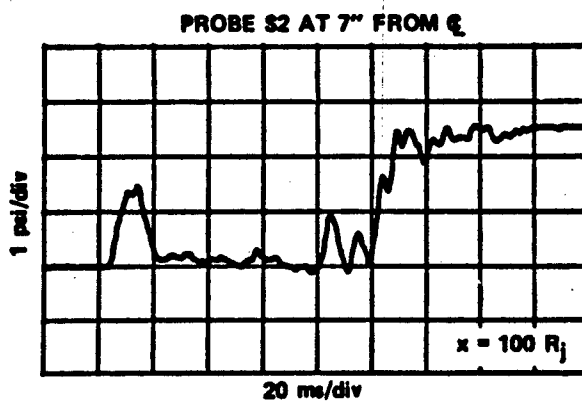
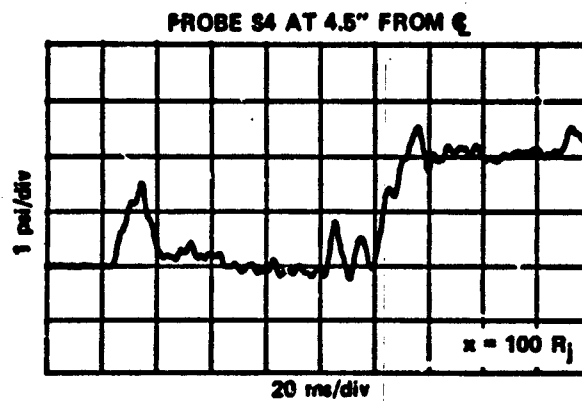
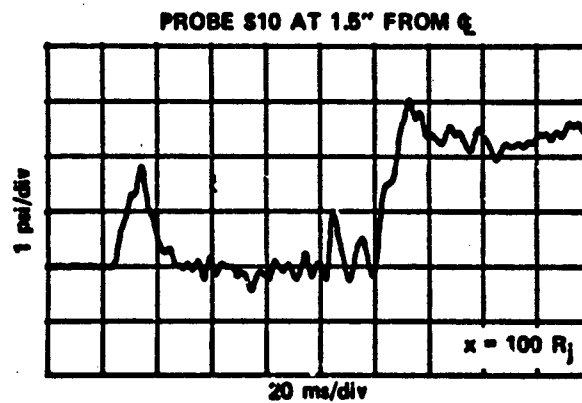


Figure 23 RADIAL VARIATION OF THE MEASUREMENTS IN A TYPICAL WIND-ON TEST CASE (e) STATIC PRESSURE (Cont.)

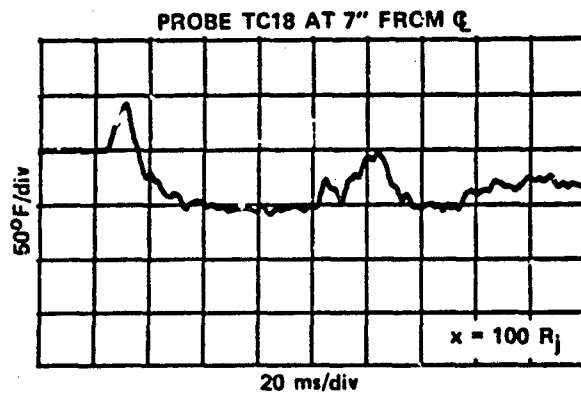
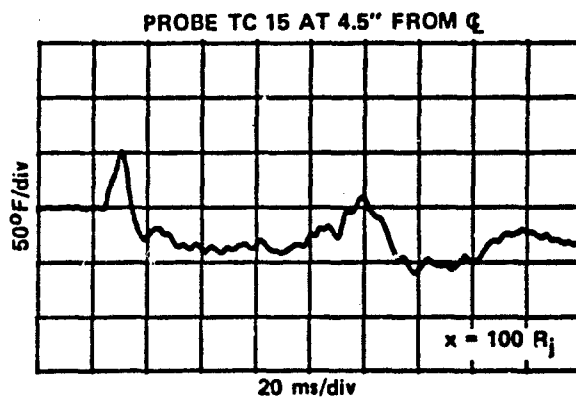
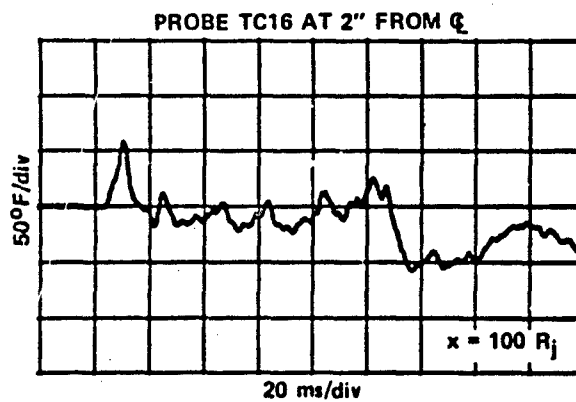


Figure 23 RADIAL VARIATION OF THE MEASUREMENTS IN A TYPICAL WIND-ON TEST CASE (f) RECOVERY TEMPERATURE (Cont.)

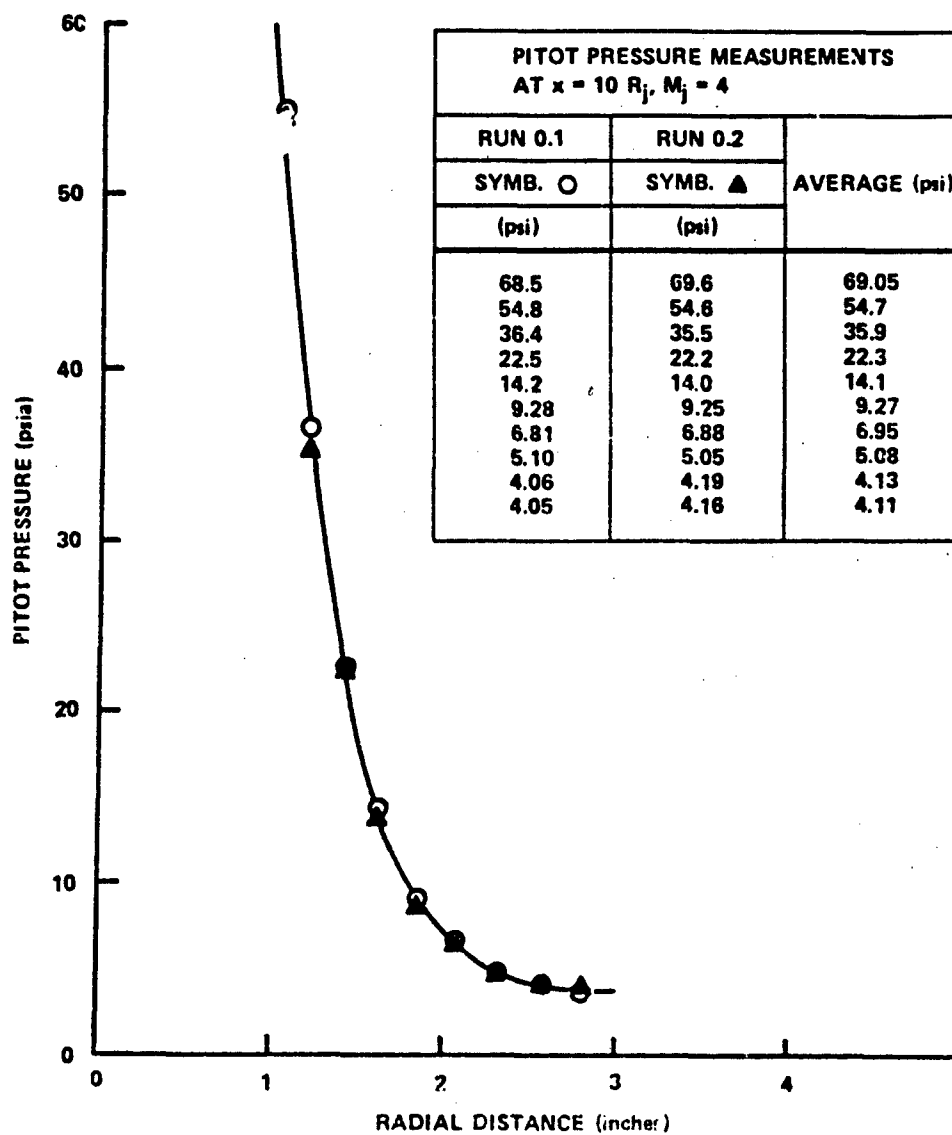


Figure 24 REPRODUCIBILITY OF THE DATA

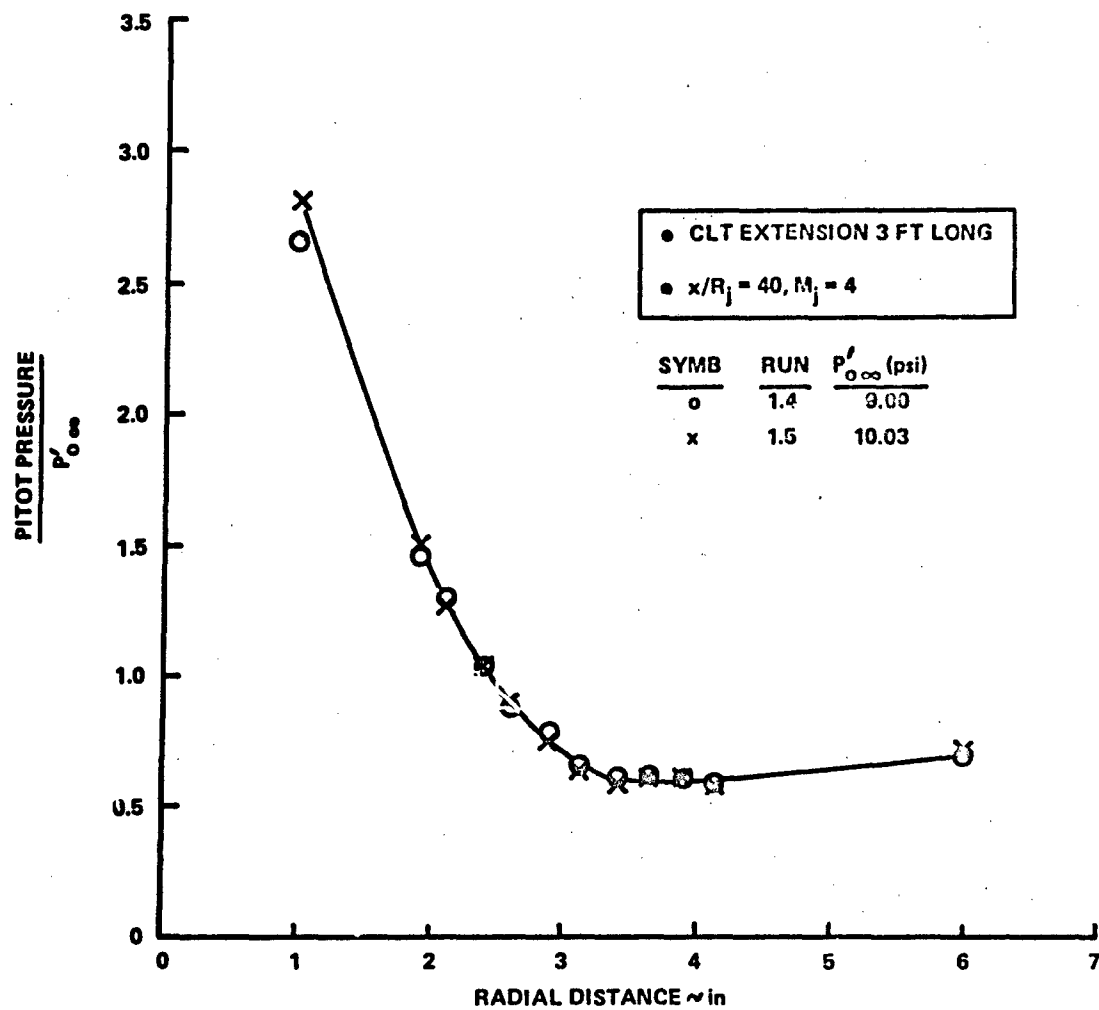


Figure 25 COMPARISON OF RADIAL PITOT PRESSURES WITH AND WITHOUT CLT NOZZLE EXTENSION

TEST NO. 2.10

CONDITIONS

MJ = 4.0

MA = 2.0

MMA/RMJ = 2.92

A/RJ = 40.0

JET PARAMETERS

XM2 = 0.90

MWJ = 4.042

TOJ = 533. R

POJ = 237.76 PSIA

PJ = 1.546 PSIA

UJ = 5519. FPS

AMBIENT PARAMETERS

TOA = 472. R

POA = 13.898 PSIA

PA = 1.943 PSIA

UA = 1614. FPS

MIXING SURVEY

STUT PRESSURE, PSIA

Z	R	PO
-3.000	2.923	7.7261
-2.000	1.945	10.0809
-1.000	1.012	19.4541
0.075	1.114	16.0485
1.125	1.342	14.7745
1.375	1.576	12.9306
1.625	1.815	11.1961
1.875	2.057	10.4979
2.125	2.300	9.1863
2.625	2.790	7.7571
3.125	3.283	7.0900
4.000	4.150	7.2900
5.000	5.144	8.1227

M2 MOLE FRACTION

Y	R	XM2
-5.0	4.502	0.060
-3.0	2.503	0.570
-2.0	1.505	0.815
-1.0	0.514	0.906
0.0	0.514	0.906
1.0	1.505	0.810
2.0	2.503	0.570
3.0	3.502	0.240
4.0	4.502	0.050
5.0	5.501	0.060

STATIC PRESSURE, PSIA

Y	Z	R	P
1.5	0.0	2.004	1.1654
2.5	0.0	3.002	1.2828
3.5	0.0	4.002	1.3577
-5.5	0.0	5.001	1.4210
0.0	-7.0	6.898	1.3910

RECOVERY TEMPERATURE, R

Y	Z	R	T
-0.5	0.0	0.120	527.
0.0	3.0	3.160	502.

Figure 26 ILLUSTRATIVE TEST RUN SUMMARY

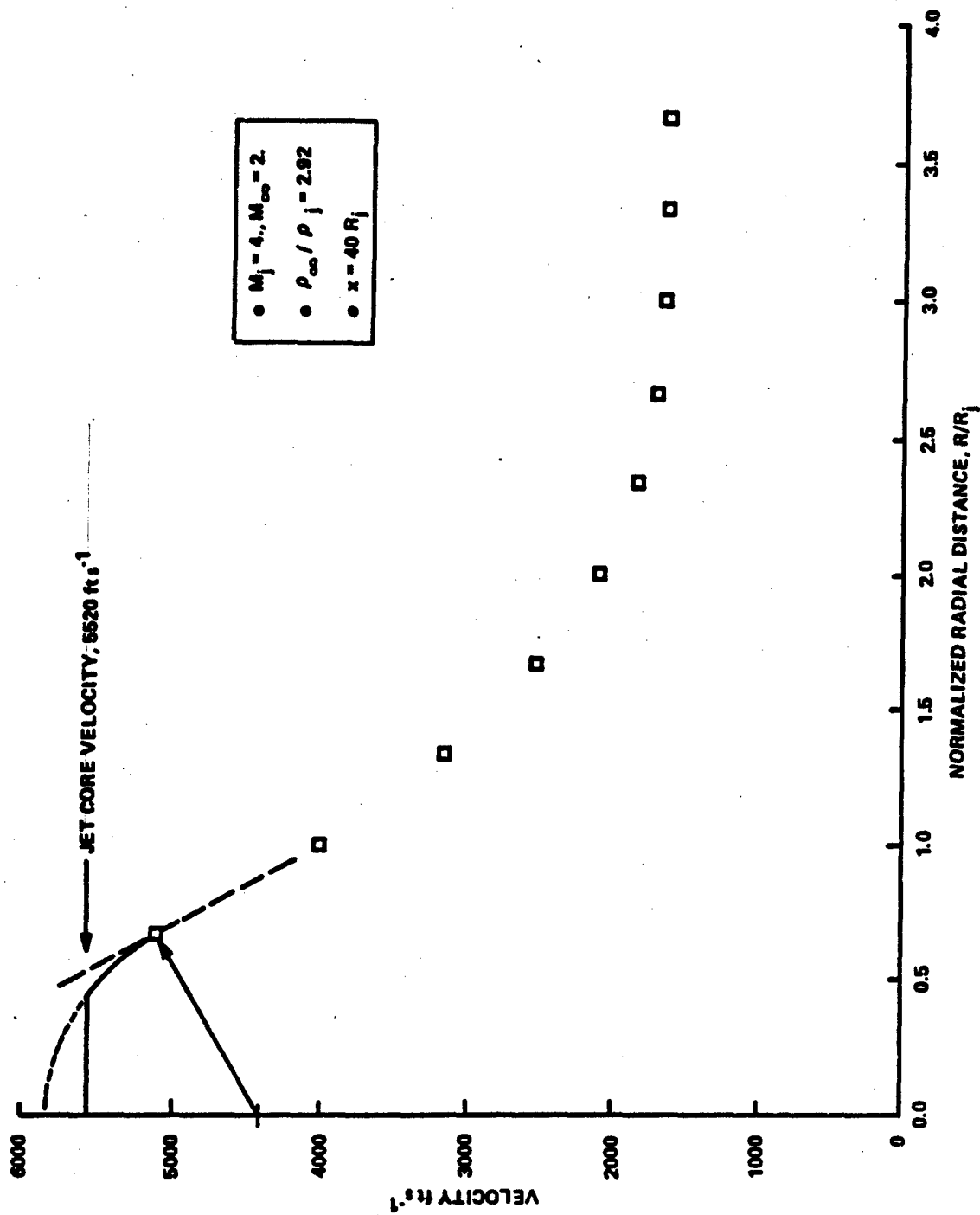


Figure 27 ILLUSTRATIVE CALCULATION OF RADIAL VELOCITY PROFILE

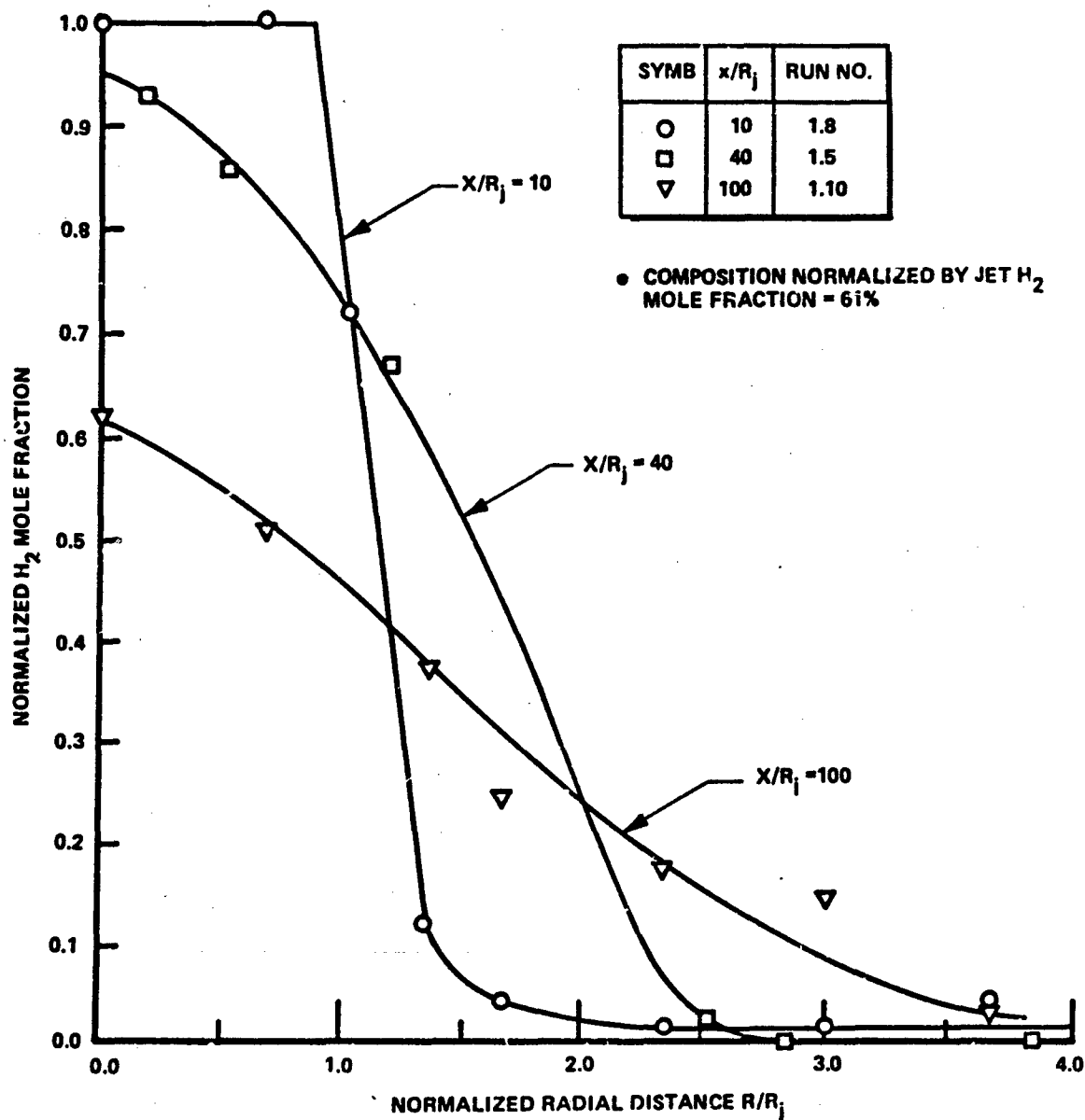


Figure 28 VARIATION OF HYDROGEN FRACTION PROFILE FROM NEAR TO FAR
 FIELD $M_j = 4$ JET DISCHARGING INTO SUPERSONIC STREAM WITH DENSITY
 MATCHED

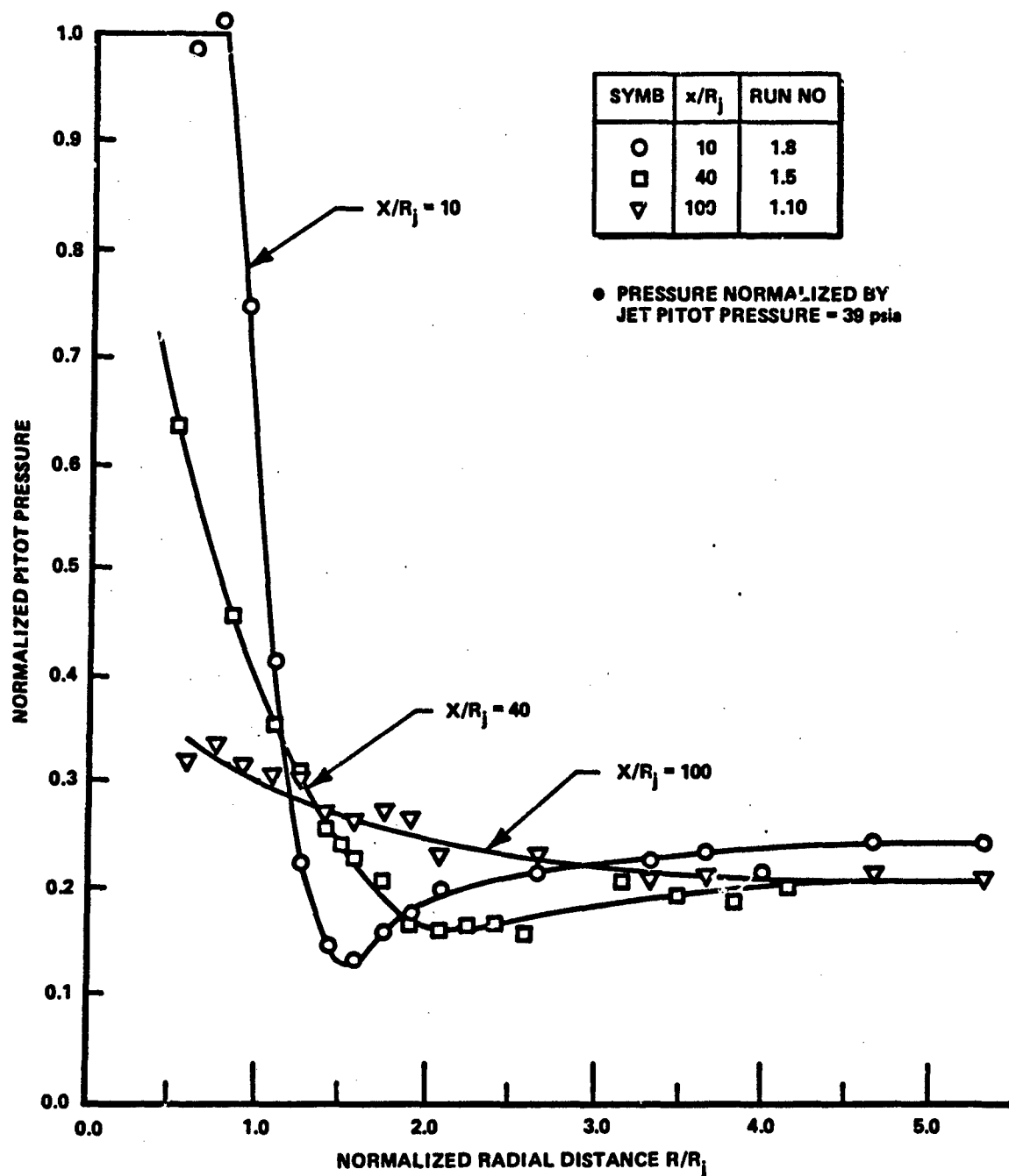


Figure 29 VARIATION OF PITOT PRESSURE FROM NEAR TO FAR FIELD $M_j = 4$ JET DISCHARGING INTO THE SUPERSONIC STREAM WITH DENSITY MATCHED

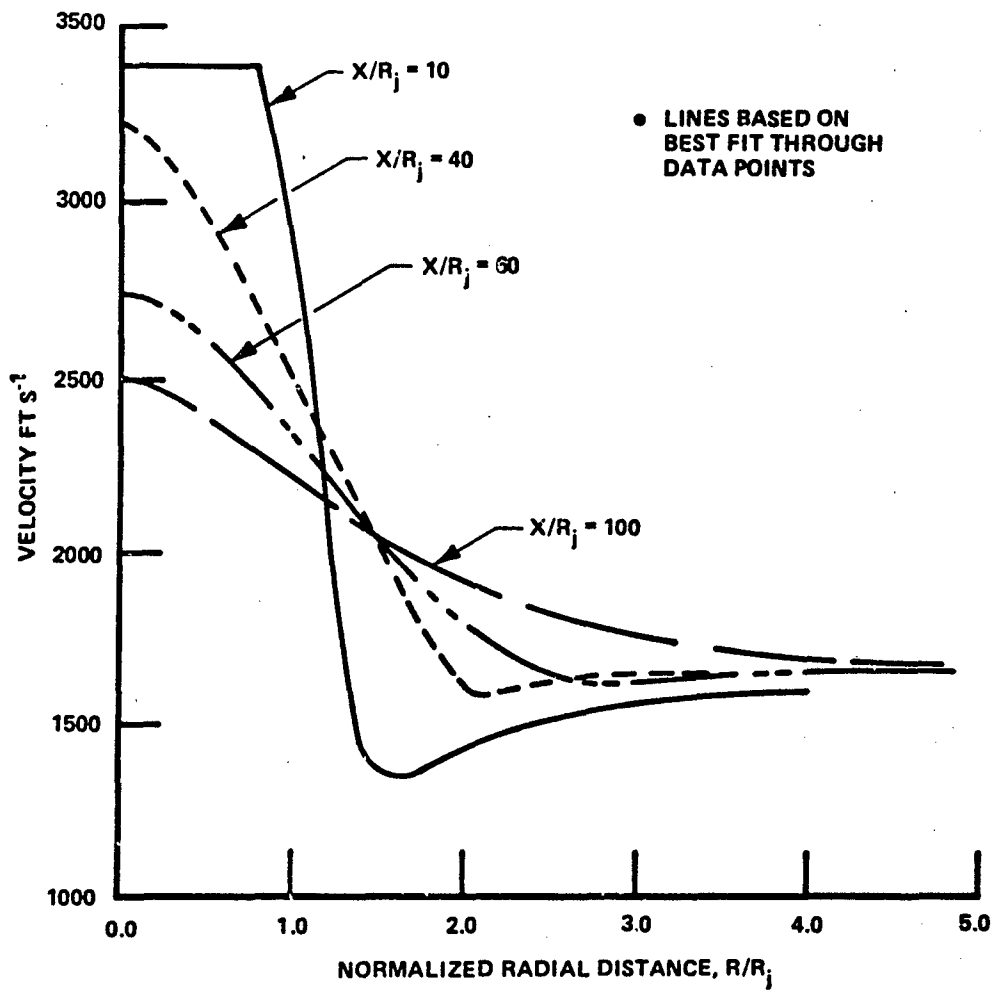


Figure 30 VELOCITY VARIATIONS FROM NEAR TO FAR FIELD. $M_i = 4.$,
 $M_\infty = 2$, DENSITY MATCHED

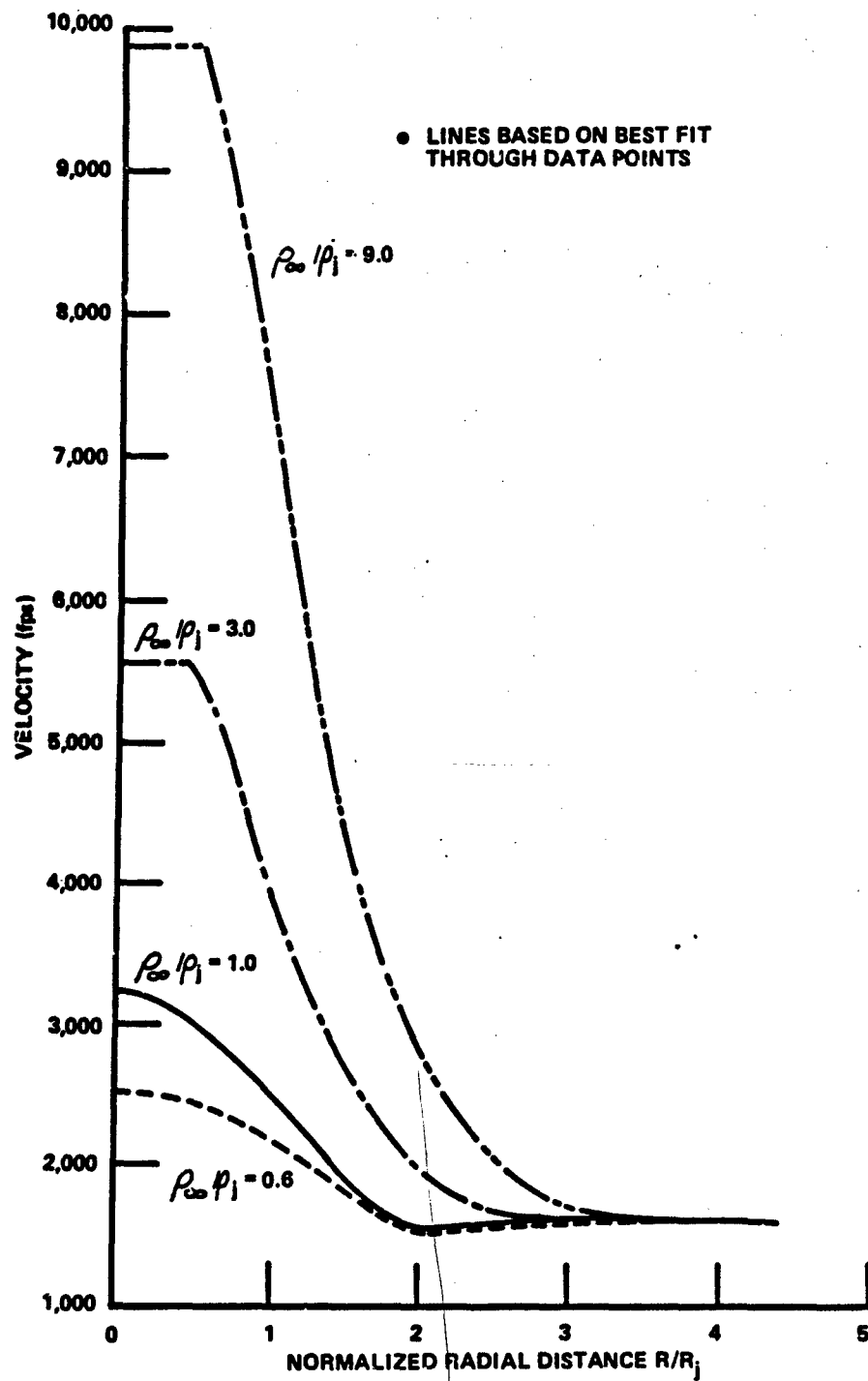


Figure 31 INFLUENCE OF DENSITY VARIATIONS ON VELOCITY SURVEYS AT $40 R_j$, $M_j = 4$, $M_{\infty} = 2$

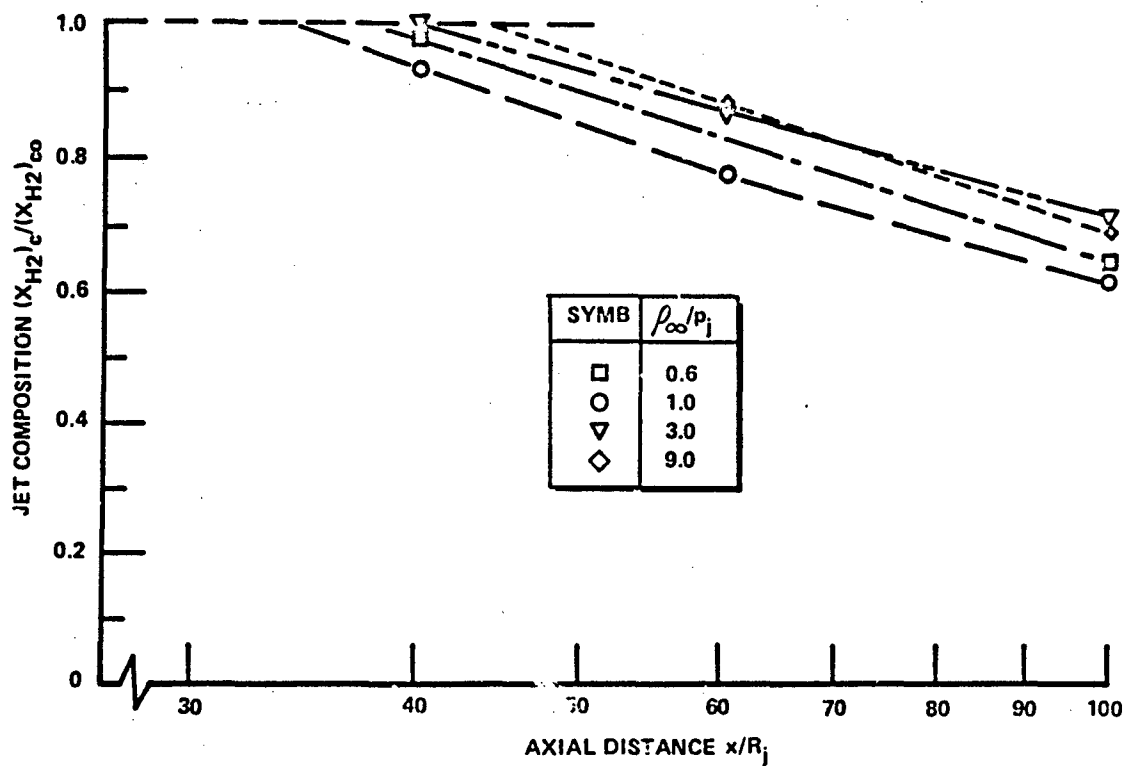


Figure 32 AXIAL DECAY OF JET CORE COMPOSITION

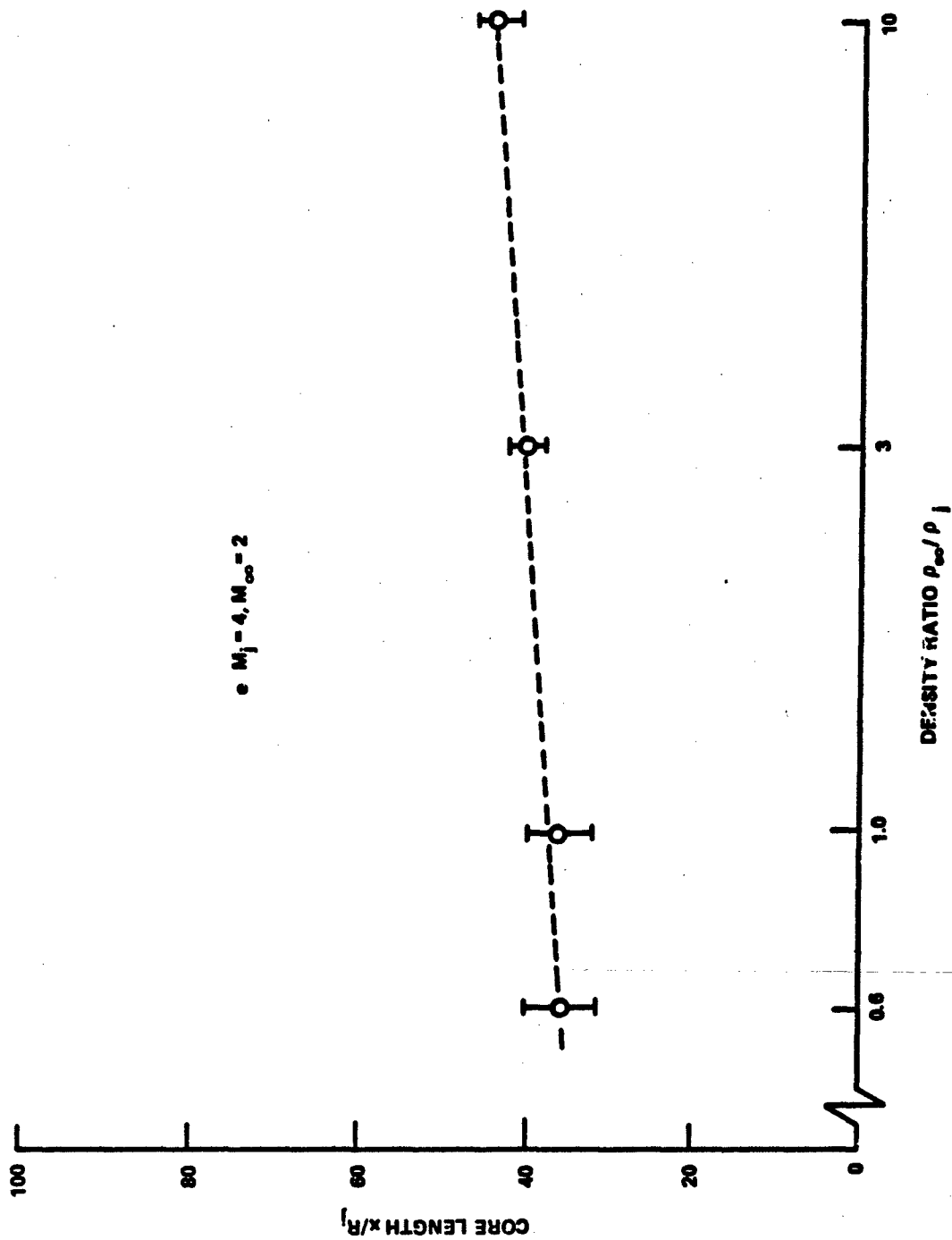


Figure 33 INFLUENCE OF DENSITY VARIATIONS ON CORE LENGTH

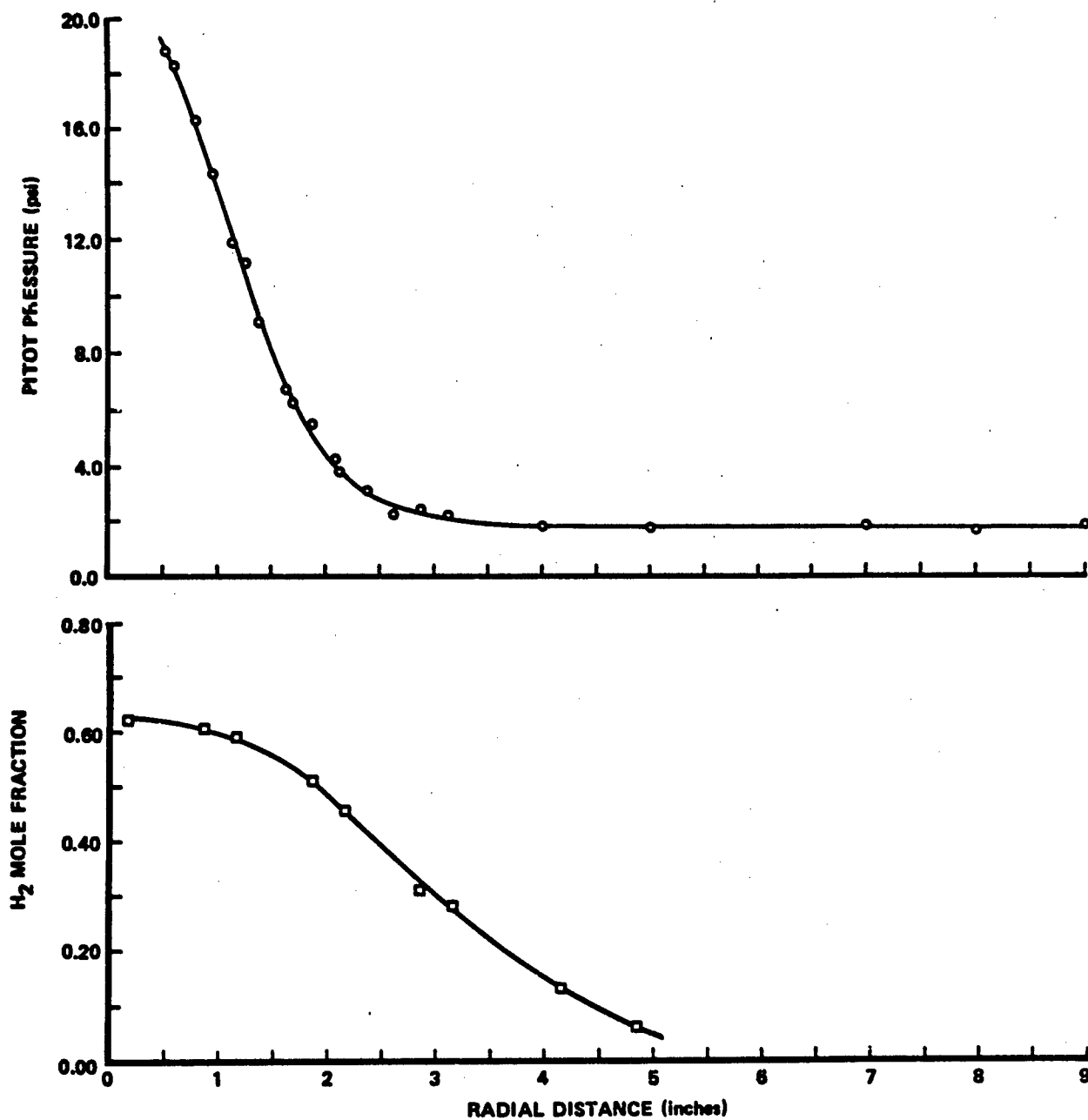


Figure 34 PITOT PRESSURE AND COMPOSITION IN THE MIXING JET AT $x = 20 R_j$. $M_j = 3$
JET DISCHARGING INTO STILL AMBIENT WITH DENSITY MATCHED

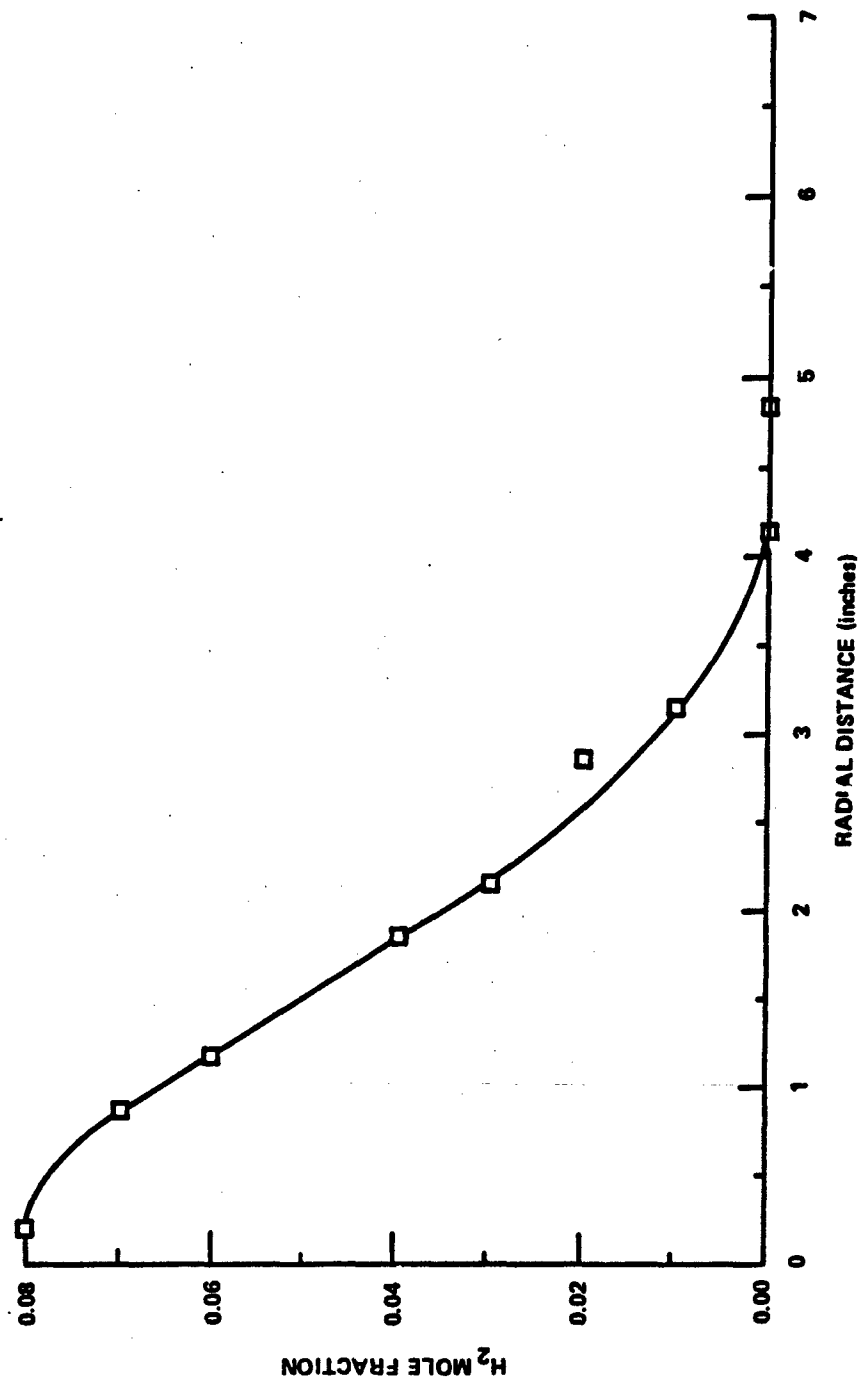


Figure 35 COMPOSITION PROFILE IN THE MIXING JET AT $x = 20$ RJ. $M_j = 2$ JET
DISCHARGING INTO STILL AMBIENT WITH $\rho_{\infty}/\rho_j = 0.6$

APPENDIX I
MIXING MEASUREMENTS

<u>Test Case No.</u>	<u>M_j</u>	<u>M_∞</u>	<u>p_∞/ρ_j</u>	<u>Page</u>
1	4	0	0.6	105
2	↓	0	1.0	107
3	↓	2	0.6	111
4	↓	↓	1.0	113
5	↓	↓	3.0	117
6	↓	↓	9.0	121
7	3	0	0.6	125
8	↓	↓	1.0	127
9	↓	↓	2.0	131
10	↓	↓	6.0	132
11	↓	2	10.0	133
12	2	0	0.6	137
13	↓	2	10.0	141

NOTE: For each Test Case, the measurements are presented by increasing value of x/R_j .

TEST CASE NO. 1

TEST NO. 2.54

CONDITIONS

MJ = 4.0 MA = 0.0 NMA/NMJ = 0.55 X/MJ = 0.0

JET PARAMETERS

XM2 = 0.61
MWJ = 12.210
TOJ = 532. R
POJ = 277.75 PSIA
PJ = 1.760 PSIA
UJ = 3400. FPS

AMBIENT PARAMETERS

TOA = 520. R
POA = 1.850 PSIA
PA = 1.859 PSIA
UA = 0. FPS

MIXING SURVEY

PITOT PRESSURE, PSIA

Z	R	PO
-2.100	2.309	4.8180
-1.250	1.490	6.4288
-0.950	1.212	6.5051
-0.800	1.077	6.9150
0.875	0.877	6.9144
1.125	1.092	6.6874
1.375	1.319	6.3610
1.625	1.554	6.0432
1.875	1.792	5.6500
2.125	2.033	5.2000
2.375	2.277	5.2537
2.625	2.521	5.0923
2.875	2.767	4.7782
3.125	3.013	4.4124
4.000	3.878	3.2406
5.000	4.872	2.8714
6.000	5.867	2.3572
7.000	6.864	2.1201
8.000	7.862	1.8794
9.000	8.860	1.9315

M2 MOLE FRACTION

Y	R	XM2
-7.0	6.502	0.190
-3.0	2.503	0.412
-1.0	0.523	0.475
0.0	0.523	0.473
1.0	1.508	0.460
3.0	3.503	0.355
9.0	9.501	0.046
12.0	12.501	0.0

STATIC PRESSURE, PSIA

Y	Z	R	P
-0.5	0.0	0.154	1.7892
1.5	0.0	2.006	1.8372
4.5	0.0	5.002	1.7717
7.0	0.0	7.502	1.7979

RECOVERY TEMPERATURE, R

Y	Z	R	T
0.5	0.0	1.012	545.
-1.5	0.0	1.012	546.
-2.0	0.0	1.508	530.
-2.5	0.0	2.006	530.
3.5	0.0	4.003	523.
4.5	0.0	5.002	520.
7.0	0.0	7.502	528.
11.0	0.0	11.501	528.

TEST CASE NO. 1

TEST NO. 2.47

CONDITIONS

MJ = 4.0 MA = 0.0 MHA/MJ = 0.55 A / MJ = 80.0

JET PARAMETERS

AMBIENT PARAMETERS

XM2 = 0.01
M2J = 12.210
TOJ = 533.0 R
POJ = 269.05 PSIA
PJ = 1.762 PSIA
UJ = 34030. FPS

TOA = 520.0 R
POA = 1.840 PSIA
PA = 1.808 PSIA
UA = 0. FPS

MIXING SURVEY

PITOT PRESSURE, PSIA

H2 MOLE FRACTION

Z	N	P0	Y	N	XM2
-2.100	2.202	3.7216	-5.0	4.301	0.320
-1.700	1.882	3.6357	-3.0	2.361	0.375
-1.250	1.467	3.4932	-1.0	0.367	0.395
-0.950	1.204	4.0045	0.0	0.044	0.394
-0.500	0.657	4.1172	1.0	1.041	0.385
0.875	1.028	3.9230	2.0	2.041	0.355
1.125	1.234	3.9076	3.0	3.041	0.330
1.375	1.453	3.8826	4.0	4.041	0.305
1.625	1.682	3.7604	6.0	6.040	0.270
1.875	1.915	3.7442			
2.375	2.392	3.4035			
2.625	2.634	3.4852			
2.875	2.877	3.3907			
3.125	3.121	3.2322			
5.000	4.971	2.5899			
6.000	5.964	2.3498			
7.000	6.959	2.1883			
8.000	7.956	2.0670			
9.000	8.953	2.0137			

STATIC PRESSURE, PSIA

RECOVERY TEMPERATURE, R

Y	Z	N	P	Y	Z	N	T
4.5	0.0	5.140	1.8017	0.5	0.0	1.142	545.
0.0	-7.0	7.099	1.7917	-1.5	0.0	0.003	542.
1.5	0.0	2.141	1.9227	3.5	0.0	4.191	532.
2.5	0.0	3.141	1.9485	4.5	0.0	5.140	530.
-0.5	0.0	0.157	1.9942	12.0	0.0	12.040	520.

TEST CASE NO. 2

TEST NO. 1.7

CONDITIONS

MJ = 4.0 MA = 0.0 RMA/MHJ = 1.12 X/ RJ = 10.0

JET PARAMETERS

XH2 = 0.85
MHJ = 0.047
TOJ = 536. R
POJ = 266.99 PSIA
PJ = 1.659 PSIA
UJ = 4649. FPS

AMBIENT PARAMETERS

TOA = 528. R
POA = 1.590 PSIA
PA = 1.601 PSIA
UA = 0. FPS

MIXING SURVEY

PITOT PRESSURE, PSIA

Y =-R	PO
0.500	38.7900
- 1.625	15.5034
- 1.875	7.0775
- 2.125	3.4882
- 2.375	2.3913
- 2.625	1.9437
- 2.875	1.7342
- 3.125	1.6997
- 6.000	1.6103
- 5.500	1.6050
- 5.000	1.6199
- 4.500	1.6359
- 7.000	1.6136
- 8.000	1.6335

H2 MOLE FRACTION

Y	R	XH2
0.0	0.0	0.850
1.0	1.000	0.850
1.5	1.500	0.760
2.0	2.000	0.500
2.5	2.500	0.270
3.5	3.500	0.055
4.5	4.500	0.025
5.5	5.500	0.035

STATIC PRESSURE, PSIA

Y	Z	R	P
0.0	-1.0	1.000	1.4684
0.0	-2.0	2.000	1.5039
0.0	-3.0	3.000	1.5656
0.0	-4.0	4.000	1.6082
0.0	-5.0	5.000	1.6121
0.0	-6.0	6.000	1.6154
0.0	-7.0	7.000	1.5866

TEST CASE NO. 2

TEST NO. 1.0

CONDITIONS

MJ = 4.0 MA = 0.0 RMA/MJ = 1.12 X/RJ = 40.0

JET PARAMETERS

AM2 = 0.85
MWJ = 6.047
TOJ = 535. R
POJ = 262.31 PSIA
PJ = 1.634 PSIA
UJ = 4845. FPS

AMBIENT PARAMETERS

TOA = 525. H
POA = 1.610 PSIA
PA = 1.610 PSIA
UA = 0. FPS

MIXING SURVEY

PITOT PRESSURE, PSIA

Y	R	PO
-6.0	5.750	1.8636
-4.125	3.875	2.6278
-3.875	3.625	2.8298
-3.625	3.375	3.1837
-3.375	3.125	3.5659
-3.125	2.875	3.8532
-2.875	2.625	4.7904
-2.625	2.375	5.2129
-2.375	2.125	6.0901
-2.125	1.875	7.4452
-1.875	1.625	8.3617
-1.0	0.750	14.5887
1.0	1.250	12.0900
2.0	3.250	3.0138
4.5	4.750	2.2314
5.0	5.250	1.8739
6.0	6.250	1.6691

M2 MOLE FRACTION

Y	R	AM2
-0.5	0.250	0.805
0.0	0.250	0.800
0.5	0.750	0.800
1.5	1.750	0.720
3.5	3.750	0.460
4.0	4.250	0.390
5.5	5.750	0.240

STATIC PRESSURE, PSIA

Y	Z	R	P
0.0	-1.0	1.031	1.4525
0.0	-2.0	2.016	1.4025
0.0	-3.0	3.010	1.3573
0.0	-4.0	4.008	1.3196
0.0	-5.0	5.006	1.2658
0.0	-6.0	6.005	1.2874
0.0	-7.0	7.004	1.6210

TEST CASE NO. 2

TEST NO. 2.36

CONDITIONS

MJ = 4.0 MA = 0.0 RMA/RMJ = 0.97 X/ RJ = 60.0

JET PARAMETERS

XM2 = 0.61
MWJ = 6.957
TOJ = 533. R
POJ = 271.62 PSIA
PJ = 1.641 PSIA
UJ = 4508. FPS

AMBIENT PARAMETERS

TOA = 528. R
POA = 1.620 PSIA
PA = 1.622 PSIA
UA = 0. FPS

MIXING SURVEY

PITOT PRESSURE, PSIA

Z	R	PO
-2.100	2.115	5.1067
-1.700	1.718	5.5848
-1.250	1.275	6.7045
-0.950	0.982	6.6648
-0.800	0.838	6.9844
-0.580	0.632	7.0118
-0.500	0.559	6.9529
1.125	1.152	6.3440
1.375	1.398	6.0286
1.625	1.644	5.5775
1.875	1.892	5.6406
2.125	2.140	4.6367
2.375	2.388	4.8078
2.625	2.637	4.1856
2.875	2.886	4.2349
3.125	3.135	4.0014
4.000	4.008	3.0684
5.000	5.006	2.3698
7.000	7.004	1.9181
8.000	8.004	2.0358
9.000	9.003	1.7197

M2 MOLE FRACTION

Y	R	XM2
-3.0	2.750	0.569
-2.0	1.750	0.610
-1.0	0.750	0.620
0.0	0.250	0.630
1.0	1.250	0.605
2.0	2.250	0.540
3.0	3.250	0.515
4.0	4.250	0.400

STATIC PRESSURE, PSIA

Y	Z	R	P
0.5	0.0	0.750	1.5318
1.5	0.0	1.750	1.5379
2.5	0.0	2.750	1.5355
3.5	0.0	3.750	1.5602
0.0	-7.0	7.004	1.5818

RECOVERY TEMPERATURE, R

Y	Z	R	T
-0.5	0.0	0.250	553.
-1.5	0.0	1.250	543.
-2.5	0.0	2.250	535.
-3.5	0.0	3.250	528.
4.5	0.0	4.750	520.
6.0	0.0	6.250	508.

TEST CASE NO. 2

TEST NO. 2.1

CONDITIONS

MJ = 4.0 MA = 0. MHA/MJ = 1.12 X/RJ = 100.

JET PARAMETERS

AMZ = 0.65
 MJ = 0.047
 T0J = 537. K
 P0J = 205.65 PSIA
 PJ = 1.500 PSIA
 UJ = 4034. FPS

AMBIENT PARAMETERS

TOA = 520. K
 POA = 1.550 PSIA
 PA = 1.550 PSIA
 UA = 0. FPS

MIXING SURVEY

PITOT PRESSURE, PSIA

Z	H	P0
-4.000	4.250	2.3462
-3.000	3.250	2.5299
-2.000	2.250	2.6173
-1.000	1.250	2.6788
0.075	0.025	2.6934
1.125	0.075	2.6986
1.375	1.125	2.6972
1.675	1.025	2.6924
2.125	1.075	2.6809
2.375	2.125	2.6751
2.625	2.375	2.6644
2.875	2.025	2.6507
3.125	2.875	2.6343
4.000	3.750	2.6344
5.000	4.750	2.6112
6.000	5.750	2.6046
7.000	6.750	2.6020

H2 MOLE FRACTION

Y	H	AMZ
-5.0	5.000	0.420
-3.0	3.010	0.435
-2.0	2.010	0.445
-1.0	1.031	0.465
1.0	1.031	0.465
2.0	2.010	0.450
3.0	3.010	0.435

STATIC PRESSURE, PSIA

Y	Z	H	P
0.5	0.0	0.559	1.0310
1.5	0.0	1.521	1.5937
2.5	0.0	2.512	1.5503
3.5	0.0	3.509	1.5500
0.0	-5.0	5.250	1.5104
0.0	-7.0	7.250	1.5008

RECOVERY TEMPERATURE, K

Y	Z	H	T
-0.5	0.0	0.559	543.
-1.5	0.0	1.521	550.

TEST CASE NO. 3

TEST NO. 2.18

CONDITIONS

MJ = 4.0 MA = 2.0 RMA/RMJ = 0.61 X/RJ = 40.0

JET PARAMETERS

XH2 = 0.23
MWJ = 22.013
TOJ = 525. R
POJ = 247.60 PSIA
PJ = 1.963 PSIA
UJ = 2515. FPS

AMBIENT PARAMETERS

TOA = 472. R
POA = 13.470 PSIA
PA = 1.972 PSIA
UA = 1614. FPS

MIXING SURVEY

PITOT PRESSURE, PSIA

Z	R	P0
-2.100	2.037	13.5690
-1.700	1.652	16.6523
-1.250	1.231	23.4136
-0.950	0.965	24.2438
-0.800	0.840	26.6305
-0.580	0.676	28.3356
0.475	1.118	23.2099
1.125	1.346	20.0804
1.375	1.581	17.5817
1.625	1.820	14.5695
1.875	2.062	12.9987
2.125	2.305	9.7635
2.625	2.795	8.8115
2.875	3.041	8.4765
4.000	4.155	8.4802
5.000	5.149	9.5493
6.000	6.145	9.1265
7.000	7.143	8.9449
8.000	8.140	9.4720
9.000	9.139	9.4724

H2 MOLE FRACTION

Y	R	XH2
-5.0	4.502	0.010
-3.0	2.503	0.080
-2.0	1.505	0.155
-1.0	0.515	0.219
0.0	0.515	0.200
1.0	1.505	0.160
2.0	2.503	0.080
3.0	3.502	0.010
4.0	4.502	0.0
5.0	5.501	0.0

STATIC PRESSURE, PSIA

Y	Z	R	P
0.5	0.0	1.008	1.2126
1.5	0.0	2.004	1.3382
2.5	0.0	3.003	1.4351
3.5	0.0	4.002	1.4233
-5.5	0.0	5.002	1.4246
0.0	-7.0	6.893	1.3785

RECOVERY TEMPERATURE, R

Y	Z	R	T
-0.5	0.0	0.125	526.
-1.5	0.0	1.008	504.
-3.0	0.0	2.503	499.

TEST CASE NO. 3

TEST NO. 2.14

CONDITIONS

MJ = 4.0 MA = 2.0 RMA/RMJ = 0.60 X/MJ = 100.

JET PARAMETERS

XH2 = 0.23
MwJ = 22.013
T0J = 523. R
P0J = 247.16 PSIA
PJ = 1.942 PSIA
UJ = 2510. FPS

AMBIENT PARAMETERS

T0A = 472. R
P0A = 13.179 PSIA
PA = 1.922 PSIA
UA = 1614. FPS

MIXING SURVEY

PITOT PRESSURE, PSIA

Z	R	P0
-3.000	3.198	2.4666
-2.000	2.219	2.6859
-1.000	1.275	2.8331
0.875	0.910	2.9105
1.125	1.119	2.8740
1.375	1.343	2.8465
1.625	1.574	2.7813
1.875	1.811	2.7699
2.375	2.292	2.5687
2.625	2.535	2.5958
2.875	2.780	2.5697
4.000	3.889	2.3979
6.000	5.876	2.3439

H2 MOLE FRACTION

Y	R	XH2
-3.0	2.455	0.110
-2.0	1.458	0.130
-1.0	0.474	0.150
0.0	0.570	0.145
1.0	1.557	0.130
3.0	3.553	0.070
4.0	4.552	0.050
5.0	5.552	0.035

STATIC PRESSURE, PSIA

Y	Z	R	P
0.5	0.0	1.061	1.1363
1.5	0.0	2.055	1.2126
2.5	0.0	3.054	1.2606
3.5	0.0	4.053	1.1973
-5.5	0.0	4.952	1.2576
0.0	-7.0	7.171	1.2657

RECOVERY TEMPERATURE, R

Y	Z	R	T
-0.5	0.0	0.158	520.
-1.5	0.0	0.962	513.
0.0	12.0	11.863	468.

TEST CASE NO. 4

TEST NO. 1.8

CONDITIONS

MJ = 4.0 MA = 2.0 MMA/MMJ = 0.99 1/ MJ = 10.0

JET PARAMETERS

XH2 = 0.01
MHJ = 12.210 R
TOJ = 532. R
POJ = 204.00 PSIA
PJ = 1.880 PSIA
UJ = 3400. FPS

AMBIENT PARAMETERS

TOA = 472. R
POA = 13.110 PSIA
PA = 1.903 PSIA
UA = 1014. FPS

MIXING SURVEY

PITOT PRESSURE, PSIA

Y =-R	P0
- 0.875	38.2821
- 1.125	39.2087
- 1.375	28.9820
- 1.625	10.0799
- 1.875	8.8057
- 2.125	5.7504
- 2.375	5.3140
- 2.625	0.3803
- 2.875	0.9078
- 3.125	7.8460
- 4.000	8.4401
- 4.500	10.4529
- 5.000	8.9134
- 5.500	9.3788
- 6.000	0.5310
- 7.000	9.0495
- 8.000	9.0428

H2 MOLE FRACTION

Y	R	XH2
0.0	0.0	.61
1.0	1.000	.61
1.5	1.500	.44
2.0	2.000	.07
2.5	2.500	.027
3.5	3.500	.011
4.5	4.500	.011
5.5	5.500	.027

STATIC PRESSURE, PSIA

Y	Z	R	P
0.0	-1.0	1.000	1.7380
0.0	-3.0	5.000	1.7878
0.0	-2.0	2.000	1.7154
0.0	-6.0	0.000	1.7733

TEST CASE NO. 4

TEST NO. 1.5

CONDITIONS

MJ = 4.0 MA = 2.0 RHA/RHJ = 0.99 X/RJ = 40.0

JET PARAMETERS

XH2 = 0.61
MWJ = 12.210
TOJ = 532. R
POJ = 270.05 PSIA
PJ = 1.728 PSIA
UJ = 3400. FPS

AMBIENT PARAMETERS

TOA = 472. R
POA = 13.298 PSIA
PA = 1.981 PSIA
UA = 1614. FPS

MIXING SURVEY

PITOT PRESSURE, PSIA

Y	R	PO
-6.0	5.750	7.4058
-4.125	3.875	6.2464
-3.875	3.625	6.0076
-3.625	3.375	5.5542
-3.375	3.125	5.3805
-3.125	2.875	5.6112
-2.875	2.625	5.1803
-2.625	2.375	5.9342
-2.375	2.125	10.0390
-2.125	1.875	12.0854
-1.875	1.625	13.8262
-1.0	0.750	24.0624
1.0	1.250	17.7547
2.0	2.250	9.4308
4.5	4.750	5.0907
5.0	5.250	7.6206
6.0	6.250	7.9254

H2 MOLE FRACTION

Y	R	XH2
-0.5	0.250	0.570
0.5	0.750	0.525
1.5	1.750	0.410
3.5	3.750	0.015
4.0	4.250	0.0
5.5	5.750	0.0

STATIC PRESSURE, PSIA

Y	Z	R	P
0.0	-1.0	1.031	1.3815
0.0	-2.0	2.016	1.1022
0.0	-4.0	4.008	1.0515
0.0	-5.0	5.006	0.9959
0.0	-6.0	6.005	0.9897
0.0	-7.0	7.004	0.9848

TEST CASE NO. 4

TEST NO. 2.37

CONDITIONS

MJ = 4.0

MA = 2.0

RMA/RMJ = 0.99

X/RJ = 60.0

JET PARAMETERS

XH2 = 0.55
MWJ = 13.640
TOJ = 532. R
POJ = 244.27 PSIA
PJ = 1.743 PSIA
UJ = 3216. FPS

AMBIENT PARAMETERS

TOA = 472. R
POA = 11.562 PSIA
PA = 1.611 PSIA
UA = 1614. FPS

MIXING SURVEY

PITOT PRESSURE, PSIA

Z	R	PO
-2.100	2.209	10.9820
-1.700	1.811	12.3214
-1.250	1.365	16.0624
-0.950	1.069	16.8990
-0.800	0.922	17.7406
-0.580	0.709	18.6067
-0.550	0.680	18.8561
-0.500	0.632	18.9803
1.125	1.044	15.3439
1.375	1.291	13.8652
1.625	1.539	12.9270
1.875	1.786	10.2565
2.125	2.035	9.7903
2.375	2.284	8.4419
2.625	2.533	9.5323
2.875	2.782	8.6109
3.125	3.032	7.9047
4.000	3.905	6.7590
5.000	4.904	7.5275
7.000	6.903	8.4441
8.000	7.903	8.1800

H2 MOLE FRACTION

Y	R	XH2
-3.0	2.802	0.190
-2.0	1.803	0.300
-1.0	0.806	0.375
0.0	0.224	0.430
1.0	1.204	0.370
2.0	2.202	0.265
3.0	3.202	0.110
4.0	4.201	0.0
5.0	5.201	0.0

STATIC PRESSURE, PSIA

Y	Z	R	P
0.5	0.0	0.707	1.0560
1.5	0.0	1.703	1.1984
2.5	0.0	2.702	1.4010
3.5	0.0	3.701	1.3839

RECOVERY TEMPERATURE, R

Y	Z	R	T
-0.5	0.0	0.316	524.
-1.5	0.0	1.304	514.
-3.5	0.0	3.302	489.
4.5	0.0	4.701	466.

TEST CASE NO. 4

TEST NO. 1.10

CONDITIONS

MJ = 4.0 MA = 2.0 MHA/MHJ = 0.50 X/RJ = 100.

JET PARAMETERS

AMJ = 0.01
MHJ = 12.210
TOJ = 329. H
POJ = 277.04 PSIA
PJ = 1.077 PSIA
UJ = 3390. FPS

AMBIENT PARAMETERS

TOA = 472. H
POA = 13.174 PSIA
PA = 1.059 PSIA
UA = 1014. FPS

MAIN SURVEY

PITOT PRESSURE, PSIA

Y-R	PO
-0.875	12.4813
-1.125	13.0438
-1.375	12.2989
-1.625	11.9239
-1.875	11.9911
-2.125	10.3201
-2.375	10.3079
-2.625	10.7019
-2.875	10.4158
-3.125	9.1254
-3.500	8.4037
-3.000	8.2813
-4.000	9.1434
-7.000	8.4392
-8.000	8.3503

M2 MULE FRACTION

Y	R	AM2
0.0	0.0	0.380
1.0	1.000	0.310
2.0	2.000	0.230
2.5	2.500	0.150
3.5	3.500	0.110
4.5	4.500	0.090
5.5	5.500	0.020

STATIC PRESSURE, PSIA

Y	Z	H	P
0.0	-1.0	1.000	1.2105
0.0	-5.0	5.000	1.2000
0.0	-4.0	4.000	1.2040
0.0	-2.0	2.000	1.2173
0.0	-6.0	6.000	1.2933

TEST CASE NO. 5

TEST NO. 2.24

CONDITIONS

MJ = 4.0 MA = 2.0 RMA/RMJ = 2.93 X/RJ = 20.0

JET PARAMETERS

XH2 = 0.90
MWJ = 4.042
T0J = 534. R
P0J = 237.70 PSIA
PJ = 1.524 PSIA
UJ = 5524. FPS

AMBIENT PARAMETERS

T0A = 472. R
P0A = 13.469 PSIA
PA = 1.911 PSIA
UA = 1614. FPS

MIXING SURVEY

PITOT PRESSURE, PSIA

Z	R	P0
-2.100	2.115	7.6068
-1.700	1.718	10.7466
-1.250	1.275	20.7570
-0.950	0.982	27.8336
-0.800	0.838	31.8318
-0.500	0.559	34.6000
0.875	0.910	28.7872
1.125	1.152	24.3645
1.375	1.398	18.1957
1.625	1.644	12.9191
1.875	1.892	11.4979
2.125	2.140	7.6861
2.625	2.637	6.5944
2.875	2.886	6.2481
4.000	4.008	7.9072
5.000	5.006	7.9595
7.000	7.004	8.2538
8.000	8.004	9.2408
9.000	9.003	8.9898

H2 MOLE FRACTION

Y	R	XH2
-3.0	2.750	0.330
-2.0	1.750	0.770
-1.0	0.750	0.900
0.0	0.250	0.900
1.0	1.250	0.890
2.0	2.250	0.570
3.0	3.250	0.040
4.0	4.250	0.0

STATIC PRESSURE, PSIA

Y	Z	R	P
0.5	0.0	0.750	0.9486
1.5	0.0	1.750	1.0401
2.5	0.0	2.750	1.0871
3.5	0.0	3.750	1.1767
0.0	-7.0	7.004	1.3893

RECOVERY TEMPERATURE, R

Y	Z	R	T
-0.5	0.0	0.250	525.
-1.5	0.0	1.250	520.
-2.5	0.0	2.250	509.
4.5	0.0	4.750	472.
-6.0	0.0	5.750	468.

TEST CASE NO. 5

TEST NO. 2.16

CONDITIONS

MJ = 4.0 MA = 2.0 RMA/RMJ = 2.92 X/RJ = 40.0

JET PARAMETERS

XM2 = 0.90
MWJ = 4.642
T0J = 533. R
P0J = 237.76 PSIA
PJ = 1.546 PSIA
UJ = 5519. FPS

AMBIENT PARAMETERS

T0A = 472. R
P0A = 13.898 PSIA
PA = 1.943 PSIA
UA = 1614. FPS

MIXING SURVEY

PITOT PRESSURE, PSIA

Z	R	P0
-3.000	2.923	7.7261
-2.000	1.945	10.0809
-1.000	1.012	19.4541
0.875	1.114	16.6485
1.125	1.342	14.7745
1.375	1.576	12.9306
1.625	1.815	11.1961
1.875	2.057	10.4979
2.125	2.300	8.1863
2.625	2.790	7.7571
3.125	3.283	7.0900
4.000	4.150	7.2900
5.000	5.144	8.1227

M2 MOLE FRACTION

Y	R	XM2
-5.0	4.502	0.060
-3.0	2.303	0.570
-2.0	1.505	0.815
-1.0	0.514	0.906
0.0	0.514	0.906
1.0	1.505	0.810
2.0	2.303	0.570
3.0	3.502	0.240
4.0	4.502	0.050
5.0	5.501	0.060

STATIC PRESSURE, PSIA

Y	Z	R	P
1.5	0.0	2.004	1.1654
2.5	0.0	3.002	1.2828
3.5	0.0	4.002	1.3577
-3.5	0.0	5.001	1.4210
0.0	-7.0	6.898	1.3910

RECOVERY TEMPERATURE, R

Y	Z	R	T
-0.5	0.0	0.120	527.
0.0	3.0	3.160	502.

TEST CASE NO. 5

TEST NO. 2.38

CONDITIONS

MJ = 4.0 MA = 2.0 RMA/RMJ = 2.93 X/RJ = 60.0

JET PARAMETERS

X_{M2} = 0.90
M_{2J} = 4.642
T_{0J} = 534. R
P_{0J} = 240.10 PSIA
P_J = 1.500 PSIA
U_J = 5524. FPS

AMBIENT PARAMETERS

T_{0A} = 472. R
P_{0A} = 11.553 PSIA
P_A = 1.516 PSIA
U_A = 1614. FPS

MIXING SURVEY

PITOT PRESSURE, PSIA

Z	R	P0
-2.100	2.581	8.3716
-1.700	2.187	8.8578
-1.250	1.748	10.0100
-0.950	1.459	10.8298
-0.800	1.316	11.3405
-0.580	1.110	11.7806
-0.500	1.036	11.8940
1.125	0.800	12.5475
1.375	1.021	12.1388
1.625	1.252	11.2673
1.875	1.490	11.0218
2.125	1.731	8.8791
2.375	1.975	8.5000
2.625	2.219	7.3384
2.875	2.465	6.5814
3.125	2.712	7.1920
4.000	3.579	7.2349
5.000	4.573	6.3444
7.000	6.567	7.4403
9.000	8.564	8.0345

H2 MOLE FRACTION

Y	R	X _{M2}
-5.0	4.599	0.250
-3.0	2.615	0.580
-2.0	1.839	0.660
-1.0	0.729	0.750
0.0	0.015	0.780
1.0	1.491	0.740
2.0	2.464	0.620
3.0	3.452	0.465
4.0	4.445	0.155
5.0	5.441	0.085

STATIC PRESSURE, PSIA

Y	Z	R	P
0.5	0.0	1.025	1.0044
1.5	0.0	1.974	1.0051
2.5	0.0	2.957	1.1797
3.5	0.0	3.948	1.2444
0.0	-7.0	7.458	1.2442

RECOVERY TEMPERATURE, R

Y	Z	R	T
-0.5	0.0	0.153	548.
-1.5	0.0	1.100	553.
-3.5	0.0	3.109	566.
4.5	0.0	4.943	477.
-9.0	0.0	8.589	402.

TEST CASE NO. 5

TEST NO. 2.48

CONDITIONS

MJ = 4.0 MA = 2.0 RMA/RMJ = 2.93 A/ MJ = 80.0

JET PARAMETERS

XH2 = 0.90
MHJ = 4.642
T0J = 534. R
P0J = 275.95 PSIA
PJ = 1.508 PSIA
UJ = 5524. FPS

AMBIENT PARAMETERS

T0A = 472. R
P0A = 11.469 PSIA
PA = 1.019 PSIA
UA = 1014. FPS

MIXING SURVEY

PITOT PRESSURE, PSIA

Z	R	P0
-2.100	2.209	8.9807
-1.250	1.365	9.9054
-0.950	1.069	9.6330
-0.500	0.632	9.9972
0.875	0.800	10.0092
1.125	1.044	9.9601
1.375	1.291	9.8269
1.675	1.786	9.6087
2.875	2.702	8.5157
3.125	3.032	7.6490
5.000	4.904	7.5309
7.000	6.903	6.1698
8.000	7.903	9.0735
9.000	8.902	9.0461

H2 MOLE FRACTION

Y	R	XH2
-5.0	4.801	0.250
-3.0	2.802	0.505
-1.0	0.806	0.640
0.0	0.224	0.650
1.0	1.204	0.635
2.0	2.202	0.575
4.0	4.201	0.250
6.0	6.201	0.085
8.0	8.201	0.0

STATIC PRESSURE, PSIA

Y	Z	R	P
-0.5	0.0	0.316	1.4763
1.5	0.0	1.703	1.5382
2.5	0.0	2.702	1.4802
4.5	0.0	4.701	1.0195
0.0	-7.0	7.103	1.7175

RECOVERY TEMPERATURE, R

Y	Z	R	T
0.5	0.0	0.707	550.
-1.5	0.0	1.304	548.
-2.0	0.0	1.803	525.
-2.5	0.0	2.302	521.
3.5	0.0	3.701	509.
4.5	0.0	4.701	500.
7.0	0.0	7.201	483.
12.0	0.0	12.200	479.

TEST CASE NO. 6

TEST NO. 2-25

CONDITIONS

NJ = 4.0 MA = 2.0 RMA/RMJ = 8.99 X/RJ = 20.0

JET PARAMETERS

XH2 = 1.00
MWJ = 2.016
T0J = 712. R
P0J = 221.02 PSIA
PJ = 1.582 PSIA
UJ = 9679. FPS

AMBIENT PARAMETERS

TOA = 472. R
POA = 12.644 PSIA
PA = 1.731 PSIA
UA = 1614. FPS

MIXING SURVEY

PITOT PRESSURE, PSIA

Z	R	P0
-2.100	2.115	6.3849
-1.700	1.718	9.1254
-1.250	1.275	16.9163
-0.950	0.942	22.7798
-0.800	0.838	26.2521
-0.500	0.559	29.4254
0.875	0.910	23.8254
1.125	1.152	20.2786
1.375	1.398	15.3781
2.125	2.140	6.2484
2.375	2.388	4.7585
2.875	2.886	4.7523
3.125	3.135	4.5067
4.000	4.008	6.3042
5.000	5.006	6.9906
7.000	7.004	7.9590
8.000	8.004	9.0732
9.000	9.003	9.6643

H2 MOLE FRACTION

Y	R	XH2
-5.0	4.750	0.040
-3.0	2.750	0.390
-2.0	1.750	0.945
-1.0	0.750	1.000
0.0	0.250	1.000
1.0	1.250	1.000
2.0	2.250	0.845
3.0	3.250	0.250
4.0	4.250	0.0

STATIC PRESSURE, PSIA

Y	Z	R	P
0.5	0.0	0.750	0.8353
1.5	0.0	1.750	0.9486
2.5	0.0	2.750	1.1117
0.0	-7.0	7.004	1.4007

RECOVERY TEMPERATURE, R

Y	Z	R	T
-0.5	0.0	0.250	703.
-1.5	0.0	1.250	696.
-2.5	0.0	2.250	655.
-4.5	0.0	4.750	478.
-6.0	0.0	5.750	474.

TEST CASE NO. 6

TEST NO. 2.17

CONDITIONS

MJ = 4.0 MA = 2.0 RMA/RMJ = 9.30 X/RJ = 40.0

JET PARAMETERS

XM2 = 1.00
MWJ = 2.016
TOJ = 737. R
POJ = 235.86 PSIA
PJ = 1.672 PSIA
UJ = 7847. FPS

AMBIENT PARAMETERS

TOA = 472. R
POA = 13.729 PSIA
PA = 1.910 PSIA
UA = 1614. FPS

MIXING SURVEY

PITOT PRESSURE, PSIA

Z	R	PO
-3.000	2.957	6.2608
-1.000	1.106	14.0224
0.875	1.200	12.1569
1.125	1.414	11.2030
1.375	1.638	10.1984
1.625	1.869	9.1198
1.875	2.105	8.7999
2.625	2.526	6.6746
3.125	3.313	6.3600
4.000	4.174	6.0579
5.000	5.154	6.3722

M2 MOLE FRACTION

Y	R	XM2
-5.0	4.332	0.260
-3.0	2.333	0.820
-2.0	1.335	0.980
-1.0	0.751	1.000
0.0	0.611	0.800
1.0	1.674	3.970
2.0	2.673	0.775
3.0	3.672	0.460
4.0	4.672	0.090
5.0	5.671	0.020

STATIC PRESSURE, PSIA

Y	Z	R	P
2.5	0.0	3.172	1.4285
0.5	0.0	1.176	1.1511
1.5	0.0	2.173	1.2733
3.5	0.0	4.172	1.5152
-5.5	0.0	4.831	1.4180
0.0	-7.0	6.913	1.4195

RECOVERY TEMPERATURE, R

Y	Z	R	T
-0.5	0.0	0.208	754.
-1.5	0.0	0.839	740.
0.0	3.0	3.191	662.
4.5	0.0	5.171	526.

TEST CASE NO. 6

TEST NO. 2.39

CONDITIONS

MJ = 4.0 MA = 2.0 NMA/NMJ = 0.95 A/ MJ = 0.0

JET PARAMETERS

AM2 = 1.00
M4J = 2.010
T0J = 709. R
P0J = 239.81 PSIA
PJ = 1.024 PSIA
UJ = 9058. FPS

AMBIENT PARAMETERS

T0A = 472. R
P0A = 11.550 PSIA
PA = 1.540 PSIA
UA = 1014. FPS

MIXING SURVEY

PITOT PRESSURE, PSIA

M2 MOLE FRACTION

Z	N	P0	Y	R	AM2
-2.100	2.435	5.0050	-3.0	4.000	0.440
-1.700	2.040	0.0057	-3.0	2.000	0.745
-1.250	1.599	7.1332	-2.0	1.079	0.815
-0.950	1.308	7.0518	-1.0	0.720	0.875
-0.600	1.104	0.0274	0.0	0.400	0.007
-0.000	1.050	5.3003	1.0	1.305	0.005
-0.013	0.987	0.4505	2.0	2.370	0.770
-0.500	0.950	7.2004	3.0	3.304	0.050
-0.550	0.920	5.7250	4.0	4.301	0.400
-0.500	0.002	7.3127	5.0	5.359	0.290
1.125	0.007	7.1327			
1.375	1.121	0.9077			
1.625	1.301	0.0717			
1.875	1.604	0.7902			
2.075	2.569	5.7057			
3.125	2.037	5.5872			
4.000	3.707	5.3942			
5.000	4.703	4.6011			
7.000	0.099	0.1090			
9.000	0.097	7.0048			

STATIC PRESSURE, PSIA

RECOVERY TEMPERATURE, R

Y	Z	N	P	Y	Z	N	T
0.5	0.0	0.905	0.9000	-0.5	0.0	0.344	720.
1.5	0.0	1.076	0.0902	-1.5	0.0	1.191	700.
2.5	0.0	2.007	1.0779	-3.5	0.0	3.105	557.
3.5	0.0	3.002	0.9294	4.5	0.0	4.000	571.
0.0	-7.0	7.318	1.2557	-9.0	0.0	0.050	400.

TEST CASE NO. 6

TEST NO. 1.11

CONDITIONS

MJ = 4.0 MA = 2.0 NMA/MJ = 0.47 A/ MJ = 100.

JET PARAMETERS

AM2 = 1.00
M0J = 2.010
T0J = 751. K
P0J = 250.72 PSIA
PJ = 1.526 PSIA
UJ = 9940. FPS

AMBIENT PARAMETERS

T0A = 472. K
P0A = 13.045 PSIA
PA = 1.901 PSIA
UA = 1014. FPS

MIXING SURVEY

PITOT PRESSURE, PSIA

Y = -R	P0
-0.875	5.6089
-1.125	5.6226
-1.375	5.5301
-1.625	5.4053
-1.875	5.3467
-2.625	5.4309
-2.875	5.4611
-3.125	5.2246
-6.000	5.3361
-5.500	5.2109
-5.000	5.2470
-4.000	5.5531
-0.500	5.4060
-7.000	6.0633
-8.000	6.5243

M2 MILE FRACTION

Y	R	AM2
0.0	0.0	0.700
1.0	1.000	0.670
1.5	1.500	0.655
2.0	2.000	0.615
3.5	3.500	0.265

STATIC PRESSURE, PSIA

Y	Z	N	P
0.0	-1.0	1.000	1.2165
0.0	-2.0	2.000	1.2553
0.0	-3.0	3.000	1.2661
0.0	-4.0	4.000	1.2396
0.0	-5.0	5.000	1.2557
0.0	-6.0	6.000	1.2604
0.0	-7.0	7.000	1.3067

RECOVERY TEMPERATURE, R

Y	Z	N	T
0.0	1.0	1.000	666.
0.0	2.0	2.000	670.
0.0	3.0	3.000	597.
0.0	4.0	4.000	625.
0.0	5.0	5.000	603.
0.0	6.0	6.000	572.
0.0	7.0	7.000	553.
0.0	8.0	8.000	529.
0.0	9.0	9.000	507.
0.0	10.0	10.000	530.

TEST CASE NO. 7

TEST NO. 2.53

CONDITIONS

MJ = 3.0 MA = 0.0 RMA/RMJ = 0.00 X/RJ = 60.0

JET PARAMETERS

AM2 = 0.50
M#J = 15.122
TOJ = 520. N
POJ = 91.02 PSIA
PJ = 1.057 PSIA
UJ = 2774. FPS

AMBIENT PARAMETERS

TOA = 528. N
POA = 1.010 PSIA
PA = 1.003 PSIA
UA = 0. FPS

MIXING SURVEY

PITOT PRESSURE, PSIA

Z	R	PO
-2.100	2.587	2.8202
-1.250	1.760	3.2902
-0.950	1.475	3.3295
-0.800	1.335	3.4831
0.075	0.604	3.6777
1.125	0.850	3.6216
1.375	1.002	3.5975
1.625	1.288	3.4324
1.875	1.522	3.4402
2.375	2.000	3.0929
2.625	2.243	3.0624
2.875	2.488	3.0004
3.125	2.733	2.9070
4.000	3.597	2.6100
5.000	4.589	2.2602
6.000	5.584	2.1926
7.000	6.581	1.9831
8.000	7.579	1.8170
9.000	8.577	1.9158

M2 MOLE FRACTION

Y	R	AM2
-7.0	6.515	0.150
-3.0	2.538	0.200
-1.0	0.605	0.295
0.0	0.005	0.294
1.0	1.503	0.265
3.0	3.527	0.245
9.0	9.510	0.075

STATIC PRESSURE, PSIA

Y	Z	R	P
-0.5	0.0	0.438	1.9039
1.5	0.0	2.047	1.8035
2.5	0.0	3.032	1.6058
4.5	0.0	5.019	1.7000
7.0	0.0	7.515	1.7711

RECOVERY TEMPERATURE, N

Y	Z	R	T
0.5	0.0	1.092	537.
-1.5	0.0	1.092	542.
-2.0	0.0	1.503	537.
-2.5	0.0	2.047	533.
3.5	0.0	4.024	524.
4.5	0.0	5.019	524.
7.0	0.0	7.513	528.
11.0	0.0	11.500	528.

TEST CASE NO. 7

TEST NO. 2.50

CONDITIONS

MJ = 3.0 MA = 0.0 RMA/RMJ = 0.66 X/RJ = 80.0

JET PARAMETERS

XM2 = 0.50
MWJ = 15.122
T0J = 523. R
P0J = 87.19 PSIA
PJ = 1.854 PSIA
UJ = 2782. FPS

AMBIENT PARAMETERS

T0A = 528. R
PCA = 1.750 PSIA
PA = 1.739 PSIA
UA = 0. FPS

MIXING SURVEY

PITOT PRESSURE, PSIA

Z	R	P0
-2.100	1.931	2.3421
-1.250	1.127	2.4388
-0.950	0.885	2.4221
-0.800	0.745	2.4580
0.875	1.205	2.4187
1.125	1.438	2.4014
1.375	1.675	2.3839
1.625	1.916	2.3523
1.875	2.159	2.3059
2.375	2.849	2.2890
2.625	2.895	2.3106
3.125	3.389	2.2483
4.000	4.257	2.1500
5.000	5.252	2.0056
6.000	6.248	2.0030
7.000	7.246	1.9203
8.000	8.244	1.8293
9.000	9.242	1.8481

H2 MOLE FRACTION

Y	R	XM2
-5.0	4.528	0.165
-3.0	2.530	0.192
-1.0	0.569	0.194
0.0	0.532	0.194
1.0	1.498	0.195
3.0	3.488	0.182
6.0	6.484	0.145
8.0	8.483	0.120

STATIC PRESSURE, PSIA

Y	Z	R	P
-0.5	0.0	0.231	1.7914
1.5	0.0	1.993	1.7704
2.5	0.0	2.989	1.7597
4.5	0.0	4.985	1.7324
0.0	-7.0	0.787	1.7241

RECOVERY TEMPERATURE, R

Y	Z	R	T
0.5	0.0	1.007	522.
-1.5	0.0	1.046	522.
-2.0	0.0	1.537	523.
-2.5	0.0	2.033	523.
3.5	0.0	3.987	524.
4.5	0.0	4.985	526.
7.0	0.0	7.484	526.
12.0	0.0	12.482	525.

TEST CASE NO. 8

TEST NO. 2.33

CONDITIONS

MJ = 3.0 MA = 0.0 NHA/RMJ = 0.96 X/RJ = 20.0

JET PARAMETERS

XH2 = 0.68
MWJ = 10.285
TUJ = 522. R
POJ = 82.22 PSIA
PJ = 1.791 PSIA
UJ = 3370. FPS

AMBIENT PARAMETERS

TOA = 528. R
POA = 1.790 PSIA
PA = 1.773 PSIA
UA = 0. FPS

MIXING SURVEY

PITOT PRESSURE, PSIA

Z	R	P0
-0.800	0.814	16.2440
-0.950	0.962	14.3530
-1.250	1.259	11.1757
-1.700	1.707	6.3025
-2.100	2.105	4.2642
-0.580	0.599	18.2766
-0.500	0.522	18.7862
1.125	1.135	11.8847
1.375	1.383	9.0830
1.625	1.632	6.7489
1.875	1.881	5.5147
2.125	2.130	3.8288
2.375	2.380	3.1323
2.625	2.629	2.2477
2.875	2.879	2.4620
3.125	3.129	2.2435
5.000	5.002	1.7591
4.000	4.003	1.8159
7.000	7.002	1.8078
8.000	8.001	1.6015
9.000	9.001	1.8037

H2 MOLE FRACTION

Y	R	XH2
-5.0	4.850	0.060
-3.0	2.850	0.310
-2.0	1.850	0.510
-1.0	0.850	0.605
0.0	0.150	0.620
1.0	1.150	0.590
2.0	2.150	0.455
3.0	3.150	0.280
4.0	4.150	0.130

STATIC PRESSURE, PSIA

Y	Z	R	P
0.5	0.0	0.650	1.5295
1.5	0.0	1.650	1.6232
2.5	0.0	2.650	1.6731
3.5	0.0	3.650	1.7392
0.0	-7.0	7.002	1.7969

RECOVERY TEMPERATURE, R

Y	Z	R	T
-3.5	0.0	3.350	525.
0.0	0.0	0.150	530.

TEST CASE NO. 8

TEST NO. 2.19

CONDITIONS

MJ = 3.0 MA = 0.0 RMA/RMJ = 0.97 X/RJ = 40.0

JET PARAMETERS

AM2 = 0.68
MWJ = 10.285
T0J = 526. R
P0J = 83.13 PSIA
PJ = 2.021 PSIA
UJ = 3383. FPS

AMBIENT PARAMETERS

T0A = 528. R
P0A = 1.910 PSIA
PA = 1.887 PSIA
UA = 0. FPS

MIXING SURVEY

PITOT PRESSURE, PSIA

Z	R	P0
-2.100	1.919	5.1862
-1.700	1.522	5.9671
-1.250	1.077	7.6611
-0.950	0.783	7.6079
-0.800	0.639	8.1431
-0.580	0.434	8.2537
0.675	1.082	6.2678
1.125	1.329	5.8305
1.625	1.825	4.6586
1.875	2.074	4.3684
2.125	2.323	3.7205
2.625	2.821	3.2711
2.875	3.071	3.0205
3.125	3.320	2.7357
4.000	4.194	2.3405
5.000	5.193	2.0690
7.000	7.193	1.9263
8.000	8.192	1.9476
9.000	9.192	1.8818

M2 MOLE FRACTION

Y	R	AM2
-5.0	4.814	0.240
-3.0	2.816	0.370
-2.0	1.820	0.455
-1.0	0.832	0.510
0.0	0.269	0.245
1.0	1.205	0.500
2.0	2.198	0.430
3.0	3.196	0.340
5.0	5.193	0.210

STATIC PRESSURE, PSIA

Y	Z	R	P
0.5	0.0	0.716	1.7885
1.5	0.0	1.701	1.8233
2.5	0.0	2.697	1.8331
3.5	0.0	3.695	1.8447
-4.0	0.0	3.815	1.8603
-5.5	0.0	5.313	1.8424
0.0	-7.0	6.813	1.8858

TEST CASE NO. 8

TEST NO. 2.34

CONDITIONS

MJ = 3.0 MA = 0.0 MHA/RMJ = 0.96 X/RJ = 60.0

JET PARAMETERS

AM2 = 0.68
MWJ = 10.265
TOJ = 522. R
POJ = 83.69 PSIA
PJ = 1.804 PSIA
UJ = 3370. FPS

AMBIENT PARAMETERS

TOA = 528. R
POA = 1.820 PSIA
PA = 1.792 PSIA
UA = 0. FPS

MIXING SURVEY

PITOT PRESSURE, PSIA

Z	R	P0
-0.800	0.825	3.4548
-0.950	0.971	3.3986
-1.250	1.266	3.3707
-1.700	1.712	3.0329
-2.100	2.110	2.9363
-0.580	0.814	3.4683
-0.500	0.539	3.3919
1.125	1.143	3.3045
1.375	1.389	3.2762
1.625	1.637	3.1629
1.875	1.886	3.1678
2.125	2.134	2.8502
2.375	2.383	2.8315
2.625	2.633	2.7631
2.875	2.882	2.7825
3.125	3.131	2.6703
4.000	4.005	2.3885
5.000	5.004	2.1470
7.000	7.003	1.9282
8.000	8.002	1.9433
9.000	9.002	1.8923

M2 MOLE FRACTION

Y	R	XM2
-3.0	2.800	0.320
-2.0	1.800	0.310
-1.0	0.800	0.350
0.0	0.200	0.355
1.0	1.200	0.335
2.0	2.200	0.300
3.0	3.200	0.285
4.0	4.200	0.180

STATIC PRESSURE, PSIA

Y	Z	R	P
0.5	0.0	0.700	1.8847
1.5	0.0	1.700	1.8417
2.5	0.0	2.700	1.8070
3.5	0.0	3.700	1.7722
0.0	-7.0	7.003	1.7832

RECOVERY TEMPERATURE, R

Y	Z	R	T
-0.5	0.0	0.300	540
-1.5	0.0	1.300	537
-2.5	0.0	2.300	530
-3.5	0.0	3.300	528
4.5	0.0	4.700	520
6.0	0.0	6.200	515

TEST CASE NO. 8

TEST NO. 2.0

CONDITIONS

MJ = 3.0 MA = 0.0 MMA/MJ = 0.97 A/MJ = 100.

JET PARAMETERS

AM2 = 0.05
M/J = 10.265
TOJ = 325. R
POJ = 89.00 PSIA
PJ = 2.011 PSIA
UJ = 3380. FPS

AMBIENT PARAMETERS

TOA = 320. R
POA = 1.990 PSIA
PA = 1.977 PSIA
UA = 0. FPS

MIXING SURVEY

PITOT PRESSURE, PSIA

Z	R	PO
-4.000	4.250	2.3103
-3.000	3.250	2.3837
-2.000	2.250	2.4606
-1.000	1.250	2.5120
0.075	0.025	2.5119
1.125	0.075	2.5217
1.375	1.125	2.5198
1.625	1.375	2.4838
1.875	1.625	2.4774
2.125	1.875	2.4402
2.375	2.125	2.4073
2.625	2.375	2.4753
2.875	2.625	2.4043
3.125	2.875	2.4299
3.375	3.125	2.3934
3.625	3.375	2.2470
3.875	3.625	2.2101
4.125	3.875	2.1578

M2 MOLE FRACTION

Y	R	AM2
-3.0	3.010	0.196
-2.0	2.010	0.204
-1.0	1.031	0.215
0.0	0.250	0.234
1.0	1.031	0.224
3.0	3.010	0.200
4.0	4.008	0.185
5.0	5.006	0.140

STATIC PRESSURE, PSIA

Y	Z	R	P
0.5	0.0	0.559	2.0122
1.5	0.0	1.521	2.0094
2.5	0.0	2.512	1.9911
3.5	0.0	3.509	1.9893
0.0	-5.0	5.250	1.9500
0.0	-6.0	6.250	1.9534
0.0	-7.0	7.250	1.9505

RECOVERY TEMPERATURE, R

Y	Z	R	T
-0.5	0.0	0.559	330.
-1.5	0.0	1.521	330.
-2.5	0.0	2.512	331.
-3.5	0.0	3.507	329.
0.0	0.0	5.506	329.
0.0	0.0	6.005	329.
7.0	0.0	7.004	329.

TEST CASE NO. 9

TEST NO. 2.51

CONDITIONS

MJ = 3.0 MA = 0.0 RMA/RMJ = 1.84 X/RJ = 60.0

JET PARAMETERS

XM2 = 0.87
MWJ = 5.397
TOJ = 524. R
POJ = 91.56 PSIA
PJ = 1.717 PSIA
UJ = 4662. FPS

AMBIENT PARAMETERS

TOA = 528. R
POA = 1.810 PSIA
PA = 1.809 PSIA
UA = 0. FPS

MIXING SURVEY

PITOT PRESSURE, PSIA

Z	R	PO
-2.100	2.615	2.6069
-1.250	1.811	2.6358
-0.950	1.538	2.6543
0.875	0.835	3.0081
1.125	0.993	3.0181
1.375	1.184	3.0098
1.625	1.394	2.9598
1.875	1.615	2.9584
2.125	1.843	2.7938
2.375	2.077	2.7106
2.625	2.313	2.6756
2.875	2.553	2.6553
3.125	2.794	2.5508
4.000	3.648	2.3600
5.000	4.633	2.1930
6.000	5.624	2.1572
7.000	6.617	2.0410
8.000	7.612	1.8783
9.000	8.609	1.7216

H2 MOLE FRACTION

Y	R	XM2
-7.0	6.314	0.437
-3.0	2.338	0.555
-1.0	0.516	0.566
0.0	0.816	0.554
1.0	1.751	0.553
3.0	5.724	0.487
9.0	9.709	0.255

STATIC PRESSURE, PSIA

Y	Z	R	P
-0.5	0.0	0.465	1.8836
1.5	0.0	2.240	1.8275
2.5	0.0	3.227	1.7979
4.5	0.0	5.217	1.7829
0.0	-7.0	7.453	1.7824

RECOVERY TEMPERATURE, R

Y	Z	R	T
0.5	0.0	1.271	539.
-1.5	0.0	0.904	542.
-2.0	0.0	1.300	540.
-2.5	0.0	1.848	540.
3.5	0.0	4.221	528.
4.5	0.0	5.217	524.
11.0	0.0	11.708	527.

TEST CASE NO. 10

TEST NO. 2.52

CONDITIONS

MJ = 3.0 MA = 0.0 NMA/RMJ = 6.13 X/RJ = 60.0

JET PARAMETERS

XMJ = 1.00
 MWJ = 2.016
 TOJ = 652. R
 POJ = 89.59 PSIA
 PJ = 1.749 PSIA
 UJ = 8508. FPS

AMBIENT PARAMETERS

TOA = 528. R
 PUA = 1.820 PSIA
 PA = 1.842 PSIA
 UA = 0. FPS

MIXING SURVEY

PITOT PRESSURE, PSIA

Z	R	PO
-0.800	1.753	2.4607
-0.950	1.897	2.6388
-1.250	2.188	2.5972
-2.100	3.022	2.6647
0.875	0.500	2.7653
1.125	0.557	2.7537
1.375	0.704	2.7571
1.625	0.897	2.7237
2.025	1.815	2.6357
2.875	2.057	2.6676
3.125	2.300	2.6377
4.000	3.160	2.4533
5.000	4.150	2.2371
6.000	5.144	2.1475
7.000	6.140	2.0525
8.000	7.138	1.9279
9.000	8.135	1.9827

N2 MOLE FRACTION

Y	N	XN2
-7.0	0.559	0.546
-3.0	2.050	0.082
-1.0	1.012	0.715
0.0	1.012	0.720
1.0	1.739	0.716
3.0	3.609	0.656
9.0	9.541	0.426
12.0	12.531	0.295

STATIC PRESSURE, PSIA

Y	Z	R	P
-0.5	0.0	0.860	1.8493
1.5	0.0	2.185	1.8086
2.5	0.0	3.126	1.8430
4.5	0.0	5.077	1.7990
0.0	-7.0	7.096	1.8140

RECOVERY TEMPERATURE, R

Y	Z	R	T
0.5	0.0	1.332	619.
-1.5	0.0	1.332	619.
-2.0	0.0	1.739	622.
-2.5	0.0	2.185	606.
3.5	0.0	4.096	594.
4.5	0.0	5.077	583.
11.0	0.0	11.534	548.

TEST CASE NO. 11

TEST NO. 2.32

CONDITIONS

MJ = 3.0 MA = 2.0 RMA/RMJ = 10.00 X/RJ = 20.0

JET PARAMETERS

XH2 = 1.00
MWJ = 2.016
TOJ = 528. R
POJ = 91.47 PSIA
PJ = 1.855 PSIA
UJ = 7650. FPS

AMBIENT PARAMETERS

TOA = 472. R
POA = 13.043 PSIA
PA = 1.724 PSIA
UA = 1614. FPS

MIXING SURVEY

PITOT PRESSURE, PSIA

Z	R	P0
-2.100	2.107	6.5633
-1.700	1.708	8.0686
-1.250	1.262	12.1325
-0.950	0.965	14.6897
-0.800	0.818	16.0292
-0.580	0.604	17.1266
-0.500	0.528	17.4920
1.125	1.138	11.9535
1.375	1.385	9.6177
1.625	1.634	7.9534
1.875	1.883	7.1436
2.125	2.132	5.2475
2.375	2.381	4.3579
2.625	2.630	4.4766
2.875	2.880	5.4352
3.125	3.130	6.1181
4.000	4.004	8.9793
7.000	7.002	9.2181
8.000	8.002	10.3969
9.000	9.002	9.7902

H2 MOLE FRACTION

Y	R	XH2
-5.0	4.830	0.0
-3.0	2.830	0.450
-2.0	1.830	0.820
-1.0	0.830	0.960
0.0	0.170	0.985
1.0	1.170	0.950
2.0	2.170	0.755
3.0	3.170	0.140
4.0	4.170	0.0

STATIC PRESSURE, PSIA

Y	Z	H	P
0.5	0.0	0.670	1.0166
1.5	0.0	1.670	1.2121
2.5	0.0	2.670	1.5851
3.5	0.0	3.670	1.7749
0.0	-7.0	7.002	1.7825

RECOVERY TEMPERATURE, R

Y	Z	R	T
-0.5	0.0	0.330	525.
-1.5	0.0	1.330	536.
-2.5	0.0	2.330	520.
-3.5	0.0	3.330	487.
6.0	0.0	6.170	595.

TEST CASE NO. 11

TEST NO. 2.20

CONDITIONS

MJ = 3.0 MA = 2.0 RMA/RMJ = 10.00 X/RJ = 40.0

JET PARAMETERS

AMJ = 1.00
 MWJ = 2.016
 TOJ = 528. R
 POJ = 86.46 PSIA
 PJ = 1.831 PSIA
 UJ = 7650. FPS

AMBIENT PARAMETERS

TOA = 472. R
 POA = 13.603 PSIA
 PA = 1.805 PSIA
 UA = 1614. FPS

MIXING SURVEY

PITOT PRESSURE. PSIA

Z	R	PO
-2.100	1.727	7.0093
-1.700	1.365	7.7112
-1.250	0.992	9.3774
-0.950	0.791	9.1426
-0.800	0.716	9.5924
-0.580	0.655	9.4921
0.875	1.521	7.0478
1.125	1.750	6.7377
1.625	2.222	5.9736
1.875	2.462	5.9231
2.125	2.704	5.1369
2.625	3.192	5.3963
3.125	3.683	5.4943
4.000	4.547	6.8313
5.000	5.538	7.9707
7.000	7.528	8.5688
8.000	8.525	8.8272
9.000	9.522	9.0253

M2 MOLE FRACTION

Y	R	XM2
-5.0	4.379	0.200
-3.0	2.403	0.725
-2.0	1.440	0.850
-1.0	0.610	0.910
0.0	0.820	0.580
1.0	1.724	0.840
2.0	2.697	0.670
3.0	3.684	0.385
4.0	4.677	0.080

STATIC PRESSURE. PSIA

Y	Z	R	P
0.5	0.0	1.254	1.1896
1.5	0.0	2.207	1.2459
2.5	0.0	3.189	1.3351
-4.0	0.0	3.387	1.3629
0.0	-7.0	6.532	1.4355

TEST CASE NO. 11

TEST NO. 2.35

CONDITIONS

MJ = 3.0 MA = 2.0 RMA/RMJ = 9.90 X/RJ = 60.0

JET PARAMETERS

XM2 = 1.00
 MWJ = 2.016
 TOJ = 523. R
 POJ = 87.36 PSIA
 PJ = 1.769 PSIA
 UJ = 7620. FPS

AMBIENT PARAMETERS

TOA = 472. R
 POA = 13.016 PSIA
 PA = 1.044 PSIA
 UA = 1014. FPS

MIXING SURVEY

PITOT PRESSURE, PSIA

Z	R	PO
-2.100	2.115	6.0553
-1.700	1.718	6.0776
-1.250	1.275	6.0720
-0.950	0.982	6.0989
-0.800	0.838	6.0731
-0.580	0.632	6.0155
-0.500	0.559	6.7536
1.125	1.152	6.4150
1.375	1.398	6.3884
1.625	1.644	6.1893
1.875	1.892	6.3233
2.125	2.140	5.5000
2.375	2.388	5.4280
2.625	2.637	5.0325
2.875	2.886	5.9422
3.125	3.135	5.8856
4.000	4.008	6.1247
5.000	5.006	6.1362
7.000	7.004	6.0490
9.000	9.003	6.6565

M2 MOLE FRACTION

Y	R	XM2
-3.0	2.750	0.665
-2.0	1.750	0.755
-1.0	0.750	0.830
0.0	0.250	0.825
1.0	1.250	0.800
2.0	2.250	0.680
3.0	3.250	0.570
4.0	4.250	0.365

STATIC PRESSURE, PSIA

Y	Z	R	P
0.5	0.0	0.750	1.4192
1.5	0.0	1.750	1.4308
2.5	0.0	2.750	1.4583
3.5	0.0	3.750	1.3786
0.0	-7.0	7.004	1.3557

RECOVERY TEMPERATURE, R

Y	Z	R	T
-0.5	0.0	0.250	545.
-1.5	0.0	1.250	537.
-2.5	0.0	2.250	520.
-3.5	0.0	3.250	505.
4.5	0.0	4.750	492.
6.0	0.0	6.250	465.

TEST CASE NO. 11

TEST NO. 2.7

CONDITIONS

MJ = 3.0 MA = 2.0 HMA/HMJ = 9.00 K/RJ = 100.

JET PARAMETERS

AM2 = 1.00
MMJ = 2.016
TOJ = 521. R
POJ = 82.89 PSIA
PJ = 1.033 PSIA
UJ = 1005. FPS

AMBIENT PARAMETERS

TOA = 472. R
POA = 13.256 PSIA
PA = 1.790 PSIA
UA = 1014. FPS

MIXING SURVEY

PITOT PRESSURE, PSIA

Z	R	PO
-4.000	4.045	3.7725
-3.000	3.059	3.0635
-2.000	2.088	3.7197
-1.000	1.100	3.0025
0.000	1.001	0.0047
1.000	1.275	0.1011
1.375	1.500	0.1250
1.625	1.732	0.0009
1.875	1.909	0.2245
2.125	2.200	3.0421
2.375	2.450	3.7740
2.625	2.693	0.2520
2.875	2.937	0.3232
3.000	3.045	0.3974
3.000	3.030	7.2711
7.000	7.020	7.4401

H2 MOLE FRACTION

Y	R	AM2
-3.0	4.400	0.320
-3.0	2.400	0.480
-2.0	1.400	0.330
-1.0	0.400	0.340
0.0	0.000	0.340
1.0	1.000	0.315
3.0	3.000	0.340
4.0	4.000	0.260
5.0	5.000	0.220

STATIC PRESSURE, PSIA

Y	Z	R	P
0.5	0.0	1.100	1.3040
1.5	0.0	2.100	1.3824
2.5	0.0	3.100	1.4170
3.5	0.0	4.100	1.4231
0.0	-3.0	3.030	1.3373
0.0	-0.0	3.030	1.3750
0.0	-7.0	7.020	1.2509

RECOVERY TEMPERATURE, R

Y	Z	R	T
-0.5	0.0	0.100	512.
-1.5	0.0	0.700	511.

TEST CASE NO. 12

TEST NO. 2.28

CONDITIONS

MJ = 2.0 MA = 0.0 RMA/RMJ = 0.58 X/RJ = 20.0

JET PARAMETERS

XM2 = 0.08
MWJ = 25.888
TOJ = 505. R
POJ = 21.83 PSIA
PJ = 1.536 PSIA
UJ = 1737. FPS

AMBIENT PARAMETERS

TOA = 528. R
POA = 1.600 PSIA
PA = 1.600 PSIA
UA = 0. FPS

MIXING SURVEY

PITOT PRESSURE, PSIA

Z	R	PO
-2.100	2.201	2.6313
-1.700	1.802	3.6143
-1.250	1.354	7.0315
-0.950	1.057	11.0498
-0.800	0.908	14.5289
-0.580	0.692	18.9116
-0.500	0.615	20.4992
1.125	1.040	10.0951
1.375	1.288	6.9714
1.625	1.536	4.9716
1.875	1.785	4.0302
2.125	2.035	2.8770
2.375	2.284	2.4775
2.625	2.533	2.2356
2.875	2.783	2.0489
3.125	3.033	1.8647
5.000	4.906	1.6020
4.000	3.907	1.3744
7.000	6.906	1.6153
8.000	7.905	1.6439
9.000	8.905	1.6054

M2 MOLE FRACTION

Y	R	XM2
-5.0	4.851	0.0
-3.0	2.852	0.020
-2.0	1.852	0.040
-1.0	0.855	0.070
0.0	0.178	0.080
1.0	1.154	0.060
2.0	2.152	0.030
3.0	3.151	0.010
4.0	4.151	0.0

STATIC PRESSURE, PSIA

Y	Z	R	P
0.5	0.0	0.657	1.5592
1.5	0.0	1.653	1.5210
2.5	0.0	2.652	1.5782
3.5	0.0	3.651	1.5637
0.0	-7.0	7.098	1.6012

RECOVERY TEMPERATURE, R

Y	Z	R	T
-0.5	0.0	0.363	496.
-1.5	0.0	1.353	499.
-2.5	0.0	2.352	510.
-3.5	0.0	3.351	519.
4.5	0.0	4.651	529.
6.0	0.0	6.151	528.

TEST CASE NO. 12

TEST NO. 2.21

CONDITIONS

MJ = 2.0 MA = 0.0 RHA/RMJ = 0.59 X/ RJ = 40.0

JET PARAMETERS

XH2 = 0.08
 MWJ = 25.886
 T0J = 515. R
 P0J = 11.19 PSIA
 PJ = 0.876 PSIA
 UJ = 1754. FPS

AMBIENT PARAMETERS

T0A = 528. R
 P0A = 1.660 PSIA
 PA = 1.659 PSIA
 UA = 0. FPS

MIXING SURVEY

PITOT PRESSURE. PSIA

Z	R	P0
-2.100	1.993	3.3131
-1.700	1.624	3.7171
-1.250	1.231	4.4398
-0.950	0.997	4.5305
-0.800	0.895	4.7674
-0.530	0.774	4.7995
0.875	1.303	4.0041
1.125	1.521	3.9076
1.875	2.215	3.2310
2.125	2.454	2.7985
2.625	2.937	2.5555
2.875	3.181	2.4509
3.125	3.425	2.3025
4.000	4.286	1.9931
5.000	5.275	1.8307
9.000	9.256	1.6029
7.000	7.263	1.6855
0.000	0.259	1.6863

H2 MOLE FRACTION

Y	R	XH2
-5.0	4.316	0.024
-3.0	2.321	0.035
-2.0	1.330	0.042
0.0	0.727	0.045
1.0	1.706	0.040
3.0	3.697	0.020

STATIC PRESSURE. PSIA

Y	Z	R	P
0.5	0.0	1.212	1.6809
1.5	0.0	2.202	1.6410
2.5	0.0	3.198	1.6393
3.5	0.0	4.196	1.6230
-4.0	0.0	3.318	1.6267
0.0	-7.0	0.805	1.6807

TEST CASE NO. 12

TEST NO. 2-41

CONDITIONS

MJ = 2.0 MA = 0.0 MMA/MHJ = 0.58 X/ MJ = 00.0

JET PARAMETERS

AMBIENT PARAMETERS

XM2 = 0.08
MHJ = 25.840
TOJ = 500. R
POJ = 19.03 PSIA
PJ = 1.500 PSIA
UJ = 1742. FPS

TOA = 520. R
POA = 1.020 PSIA
PA = 1.015 PSIA
UA = 0. FPS

MIXING SURVEY

PITOT PRESSURE, PSIA

M2 MOLE FRACTION

Z	R	PO	Y	R	XM2
-2.100	2.274	3.9530	-3.0	2.755	0.015
-1.700	1.877	4.1040	-2.0	1.757	0.010
-0.950	1.138	5.3903	-1.0	0.707	0.027
-0.800	0.992	5.7043	0.0	0.297	0.030
-0.500	0.701	5.8074	1.0	1.200	0.025
-0.500	0.700	5.7022	2.0	2.250	0.015
1.125	0.997	5.2372	3.0	3.254	0.010
1.375	1.240	5.0770	5.0	5.252	0.0
1.625	1.486	4.7991			
1.875	1.733	4.5029			
2.125	1.981	4.1077			
2.375	2.229	3.9740			
2.625	2.478	3.8324			
2.875	2.726	3.7998			
3.125	2.970	3.6627			
5.000	4.840	2.4003			
7.000	6.845	1.0400			
8.000	7.844	1.7190			
9.000	8.844	1.0023			

STATIC PRESSURE, PSIA

RECOVERY TEMPERATURE, R

Y	Z	R	P	Y	Z	R	T
0.5	0.0	0.707	1.0504	-0.5	0.0	0.297	547.
1.5	0.0	1.757	1.0440	-1.5	0.0	1.200	520.
2.5	0.0	2.755	1.0194	-3.5	0.0	3.254	512.
3.5	0.0	3.753	1.0077	4.5	0.0	4.753	514.
0.0	-7.0	7.104	1.5991	-9.0	0.0	0.751	520.

TEST CASE NO. 12

TEST NO. 2.9

CONDITIONS

MJ = 2.0 MA = 0.0 RMA/RMJ = 0.00 A/ RJ = 100.

JET PARAMETERS

AMZ = 0.00
 MJJ = 25.000
 TOJ = 520. R
 POJ = 11.00 PSIA
 PJ = 1.701 PSIA
 UJ = 1776. FPS

AMBIENT PARAMETERS

TOA = 520. R
 POA = 1.720 PSIA
 PA = 1.715 PSIA
 UA = 0. FPS

MIXING SURVEY

PITOT PRESSURE, PSIA

Z	R	PO
-4.000	3.035	1.9017
-3.000	2.648	1.9170
-2.000	1.070	1.9443
-1.000	0.781	1.9350
0.075	1.370	1.9441
1.125	1.005	1.9405
1.375	1.044	1.9372
1.625	2.080	1.9295
1.875	2.329	1.9311
2.125	2.574	1.9039
2.375	2.020	1.9000
2.625	3.000	1.9151
2.875	3.313	1.9003
3.125	3.500	1.8901
4.000	4.420	1.8704
5.000	5.425	1.8247
6.000	6.420	1.8345

M2 MULE FRACTION

Y	R	AMZ
-5.0	4.510	0.025
-3.0	2.532	0.027
-2.0	1.552	0.029
-1.0	0.040	0.030
0.0	0.040	0.030
1.0	1.552	0.020
3.0	3.523	0.025
4.0	4.510	0.025
5.0	5.515	0.020

STATIC PRESSURE, PSIA

Y	Z	M	P
2.5	0.0	3.027	1.7203
0.0	-5.0	4.027	1.7004
0.5	0.0	1.077	1.7334
1.5	0.0	2.040	1.7207
0.0	-0.0	5.022	1.7007
0.0	-7.0	0.019	1.7050

TEST CASE NO. 13

TEST NO. 2.31

CONDITIONS

MJ = 2.0 MA = 2.0 RMA/RMJ = 9.81 X/RJ = 20.0

JET PARAMETERS

XM2 = 0.95
 MWJ = 3.212
 T0J = 531. R
 P0J = 21.60 PSIA
 PJ = 1.379 PSIA
 UJ = 5057. FPS

AMBIENT PARAMETERS

T0A = 472. R
 P0A = 11.573 PSIA
 PA = 1.701 PSIA
 UA = 1614. FPS

MIXING SURVEY

PITOT PRESSURE, PSIA

Z	R	P0
-2.100	2.191	7.0083
-1.700	1.794	9.5360
-1.250	1.350	16.6970
-0.950	1.057	20.4236
-0.800	0.912	22.3305
-0.580	0.703	24.6059
-0.500	0.629	25.3706
1.125	1.077	16.1220
1.375	1.322	12.4543
1.625	1.568	9.4323
1.875	1.815	7.8525
2.125	2.063	5.2879
2.375	2.312	4.6267
2.625	2.560	4.5858
2.875	2.809	5.1086
3.125	3.058	5.0453
4.000	3.931	6.8618
5.000	4.929	6.0518
7.000	6.928	6.6186
8.000	7.927	6.4889
9.000	8.927	6.6966

M2 MOLE FRACTION

Y	R	XM2
-5.0	4.751	0.0
-3.0	2.751	0.370
-2.0	1.752	0.765
-1.0	0.754	0.925
0.0	0.262	0.955
1.0	1.252	0.885
2.0	2.251	0.600
3.0	3.251	0.090
4.0	4.251	0.0

STATIC PRESSURE, PSIA

Y	Z	R	P
0.5	0.0	0.754	0.5500
1.5	0.0	1.752	1.0800
2.5	0.0	2.751	1.1218
3.5	0.0	3.751	1.3256
0.0	-7.0	7.001	1.0264

RECOVERY TEMPERATURE, R

Y	Z	R	T
-0.5	0.0	0.262	514.
-1.5	0.0	1.252	528.
-2.5	0.0	2.251	517.
-3.5	0.0	3.251	490.
4.5	0.0	4.751	479.
6.0	0.0	6.250	465.

TEST CASE NO. 13

TEST NO. 2.40

CONDITIONS

MJ = 2.0 MA = 2.0 MMA/MHJ = 9.00 1/ MJ = 50.0

JET PARAMETERS

AMBIENT PARAMETERS

XM2 = 0.95
MeJ = 3.207
TOJ = 534. R
POJ = 22.30 PSIA
PJ = 1.664 PSIA
UJ = 3075. FPS

TOA = 472. H
POA = 11.453 PSIA
PA = 1.750 PSIA
UA = 1014. FPS

MIXING SURVEY

PITOT PRESSURE, PSIA

N2 MOLE FRACTION

Z	R	PO	Y	N	AME
-2.100	2.338	2.0141	-3.0	2.388	0.875
-1.700	1.940	1.9575	-2.0	1.593	0.900
-0.800	1.085	2.3482	-1.0	0.014	0.915
-0.500	0.886	2.3195	0.0	0.405	0.910
-0.500	0.816	2.3883	1.0	1.434	0.905
1.125	1.016	2.2805	2.0	2.426	0.880
1.375	1.248	2.2910	3.0	3.426	0.845
1.625	1.480	2.1890	4.0	4.425	0.790
1.875	1.727	2.2104	5.0	5.424	0.730
2.125	1.970	1.8398			
2.375	2.215	1.8880			
2.625	2.461	1.8145			
5.000	4.818	1.4085			
7.000	6.813	1.0721			
8.000	7.811	1.0529			
9.000	8.810	1.0192			

STATIC PRESSURE, PSIA

RECOVERY TEMPERATURE, H

Y	Z	R	P	Y	Z	R	T
0.5	0.0	0.941	1.0170	-0.5	0.0	0.215	526.
1.5	0.0	1.940	1.0923	-1.5	0.0	1.098	572.
2.5	0.0	2.927	1.0935	-3.5	0.0	3.000	536.
3.5	0.0	3.925	1.1137	4.5	0.0	4.924	523.
0.0	-7.0	7.212	1.2450	-9.0	0.0	6.582	506.

TEST CASE NO. 13

TEST NO. 2.11

CONDITIONS

MJ = 2.0 MA = 2.0 QMA/RMJ = 9.75 X/RJ = 100.

JET PARAMETERS

AMZ = 0.95
MAJ = 3.212
TOJ = 525. H
POJ = 20.07 PSIA
PJ = 1.099 PSIA
UJ = 5043. FPS

AMBIENT PARAMETERS

TOA = 472. H
POA = 13.307 PSIA
PA = 1.0912 PSIA
UA = 1014. FPS

MIXING SURVEY

PILOT PRESSURE, PSIA

Z	R	P0
-2.000	2.119	0.1020
-1.000	1.221	0.0530
0.075	1.121	0.0090
1.125	1.325	0.9130
1.375	1.543	0.7900
1.625	1.769	0.1100
1.875	2.001	0.0800
2.125	2.237	0.5150
2.375	2.476	0.7050
2.625	2.717	0.1010
2.875	2.959	0.1100
3.125	3.202	0.7420
4.000	4.001	0.9440
6.000	6.041	0.0900

H2 MOLE FRACTION

Y	H	AMZ
-5.0	4.300	0.100
-3.0	2.300	0.325
-2.0	1.300	0.370
-1.0	0.300	0.390
1.0	1.700	0.340
3.0	3.700	0.210
4.0	4.700	0.130
5.0	5.700	0.060

STATIC PRESSURE, PSIA

Y	Z	R	P
2.5	0.0	3.200	1.2079
0.0	-5.0	0.049	1.2343
0.5	0.0	1.200	1.1917
1.5	0.0	2.200	1.2033

RECOVERY TEMPERATURE, R

Y	Z	H	T
-0.5	0.0	0.200	505.
-2.5	0.0	1.000	503.

APPENDIX II
BOUNDARY LAYER MEASUREMENTS

- NOTE:**
- Measurements are presented by increasing Test Number
 - See Table V for the cross-reference of Test Number to Test Conditions

BOUNDARY LAYER MEASUREMENTS

TEST NO. 01.9

CONDITIONS

$M_j = 4.0$ $x_{H_2} = 0.845$ $T_{oj} = 528^\circ R$ $p_{oj} = 381.7 \text{ psia}$

$u_j = 4845 \text{ fps}$

INTERNAL BOUNDARY LAYER SURVEY

Distance from the nozzle wall, in

Normalized pitot pressure, p_o'/p_{oj}

.056	.0489
.080	.0741
.109	.0940
.165	.1149
.248	.1403
.498	.1307
.839	.1344
1.286	.1374
1.736	.1330

TEST NO. 1.12

CONDITIONS

$M_j = 4.0$ $x_{H_2} = 1.0$ $T_{oj} = 529^\circ R$ $p_{oj} = 269.0$ psia

$u_j = 8343$ fps

INTERNAL BOUNDARY LAYER SURVEY

Distance from the nozzle wall, in

Normalized pitot pressure, p_o'/p_{oj}

.084	.0623
.120	.0756
.150	.0938
.183	.1061
.250	.1197
.350	.1282
.520	.1284
.820	.1353
1.270	.1383
1.670	.1406

TEST NO. 1.13

CONDITIONS

$M_j = 4.0$ $x_{H_2} = 1.0$ $T_{oj} = 714^\circ R$ $p_{oj} = 269.1 \text{ psia}$

$u_j = 9692 \text{ fps}$ $M_\infty = 2.0$

INTERNAL BOUNDARY LAYER SURVEY

Distance from the nozzle wall, in Normalized pitot pressure, p_o'/p_{oj}

.084	.0569
.120	.0652
.150	.0896
.183	.0995
.250	.1155
.350	.1273
.520	.1313
.820	.1373
1.670	.1442

TEST NO. 2.42

CONDITIONS

$M_j = 2.0$ $x_{H_2} = .082$ $T_{oj} = 508^\circ R$ $p_{oj} = 19.06$ psia

$u_j = 1742$ fps

INTERNAL BOUNDARY LAYER SURVEY

Distance from the nozzle wall, in

Normalized pitot pressure, p_o'/p_{oj}

.035	.1193
.071	.1859
.101	.2504
.125	.2677
.134	.2913
.201	.3826
.301	.5484
.471	.7295
.625	.7300
.875	.7173

TEST NO. 2.43

CONDITIONS

$M_j = 2.0$ $x_{H_2} = .954$ $T_{oj} = 530^\circ R$ $p_{oj} = 20.83 \text{ psia}$
 $u_j = 5053 \text{ fps}$ $p_{o\infty} = 11.368 \text{ psia}$

INTERNAL BOUNDARY LAYER SURVEY

Distance from the nozzle wall, in	Normalized pitot pressure, p'_o/p_{oj}
.035	.3356
.101	.4422
.125	.4359
.301	.5982
.471	.6362
.625	.6259
.875	.6875

EXTERNAL BOUNDARY LAYER SURVEY

Distance from the nozzle wall, in	Normalized pitot pressure, p'_o/p_o
.401	.2363
.651	.2982
.901	.3955
1.151	.5495
5.276	.6122
7.276	.7238

TEST NO. 2.44

CONDITIONS

$M_j = 3.0$ $x_{H_2} = .682$ $T_{oj} = 524^\circ R$ $p_{oj} = 95.11 \text{ psia}$

$u_j = 3377. \text{ fps}$

INTERNAL BOUNDARY LAYER SURVEY

Distance from the nozzle wall, in Normalized pitot pressure, p_o'/p_{oj}

.029	.0721
.065	.1338
.095	.2004
.128	.2589
.129	.2683
.295	.3348
.379	.3327
.465	.3267
.629	.3266
.879	.3284
1.615	.3321

TEST NO. 2.45

CONDITIONS

$M_j = 3.0$ $x_{H_2} = 1.0$ $T_{oj} = 524^\circ R$ $p_{oj} = 98.23$ psia

$u_j = 7627$ fps $p_{o\infty} = 13.026$ psia

INTERNAL BOUNDARY LAYER SURVEY

Distance from the nozzle wall, in	Normalized pitot pressure, p_o'/p_{oj}
.053	.1424
.089	.1980
.104	.2091
.119	.2851
.152	.3025
.319	.3303
.354	.3267
.489	.3210
.604	.3237
.854	.3305
1.639	.3291

EXTERNAL BOUNDARY LAYER SURVEY

Distance from the nozzle wall, in	Normalized pitot pressure, p_o'/p_o
.333	.2363
.583	.2779
.833	.3660
1.083	.4844
1.333	.5446
3.208	.7444
5.208	.7016
7.208	.6822

TEST NO. 2.46

CONDITIONS

$M_j = 4.0$ $x_{H_2} = .553$ $T_{oj} = 527^\circ R$ $p_{oj} = 273.7$ psia

$u_j = 3201.$ fps $p_{o\infty} = 11.430$ psia

INTERNAL BOUNDARY LAYER SURVEY

Distance from the nozzle wall, in	Normalized pitot pressure, p_o'/p_{oj}
.022	.0451
.058	.0560
.088	.0813
.121	.1004
.129	.1072
.288	.1381
.379	.1415
.458	.1386
.629	.1385
.879	.1395
1.608	.1384

EXTERNAL BOUNDARY LAYER SURVEY

Distance from the nozzle wall, in	Normalized pitot pressure, p_o/p_{oj}
.058	.2603
.308	.3035
.558	.3628
.808	.4380
1.058	.5413
1.308	.6378
5.183	.6925
6.183	.6940
7.183	.7216